Application of cone beam computed tomography in 3D cephalometry

Damstra, Janalt

Application of Cone Beam Computed Tomography in 3D Cephalometry

Janalt Damstra

Application of Cone Beam Computed Tomography in 3D Cephalometry

Janalt Damstra

STELLINGEN
behorende bij het Proefschrift:

APPLICATION OF CONE BEAM COMPUTED TOMOGRAPHY
IN 3D CEPHALOMETRY

Janalt Damstra
Groningen, 26 september 2011

1. The measurement error of most linear and angular two- and three-dimensional cephalometric measurements is clinically relevant. This questions the use of these measurements to detect true treatment effect. *(This thesis)*

2. Cone beam computerized tomography (CBCT) images provide more accurate information regarding the characteristics of mandibular asymmetry (when compared to postero-anterior (PA) cephalograms) and should therefore be used for surgical treatment planning of a chin deviation correction. *(This thesis)*

3. Due to the inherent asymmetry of anatomical landmarks, a morphometric midsagittal plane might be of more value when determining the facial midline. *(This thesis)*

4. The clinician is not only responsible for reading the CBCT scan pertaining to their specialty, but is also responsible for reading the entire image volume. Medicolegal and liability issues related to CBCT imaging should therefore not be taken lightly. *(This thesis)*

5. Considering the rapidly evolving and new advances regarding further radiation reduction and improved image quality, it may be plausible to think that CBCT imaging would eventually become the imaging modality of choice for all orthodontic patients. *(This thesis)*

6. Well done is better than well said. *(Ben Franklin)*

7. The more I examine the universe and the details of its architecture, the more evidence I find that the universe in some sense must have known we are coming. *(Freeman Dyson)*

8. The ultimate authority must always rest with the individual's own reason and critical analysis. *(Dalai Lama)*

9. Sometimes you eat the bear and sometimes the bear eats you. *(American proverb)*

10. For to be free is not merely to cast off one's chains, but to live in a way that respects and enhances the freedom of others. *(Nelson Mandela)*

11. There is no place like home. *(Unknown)*
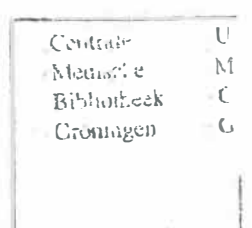
RIJKSUNIVERSITEIT GRONINGEN

Application of Cone Beam Computed Tomography in 3D Cephalometry

Proefschrift

ter verkrijging van het doctoraat in de
Medische Wetenschappen
aan de Rijksuniversiteit Groningen
op gezag van de
Rector Magnificus, dr. E. Sterken,
in het openbaar te verdedigen op
maandag 26 september 2011
om 14.45 uur

door

Janalt Damstra

geboren op 22 september 1973
te Pretoria, Zuid-Afrika
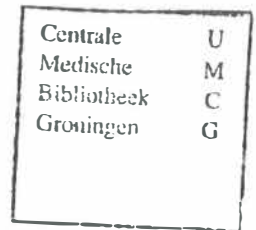
Promotor: Prof. dr. Y. Ren

Beoordelingscommissie: Prof. dr. R.R.M. Bos
                               Prof. dr. A.M. Kuijpers-Jagtman
                               Prof. dr. P.E. Rossouw

Paranimfen: Drs. Floris Pelser
                                   Drs. Katrina Finnema

Table of contents

Chapter 1

Introduction and aims of the study

1.1 Introduction

Cephalometry can be defined as the measurement and study of proportions of the head and face; especially during development and growth.[1] Since Hofrath and Broadbent introduced radiographic cephalometry in 1931, cephalograms have become virtually indispensable in orthodontics.[2-3] Traditionally, lateral cephalograms are used for growth analysis, diagnosis, treatment planning, monitoring of therapy and evaluation of final outcome.[3] Additionally, posteroanterior cephalograms provide valuable mediolateral information which is useful for presurgical and asymmetric growth evaluation.[4] Unfortunately, cephalograms are a two-dimensional (2D) projection of three-dimensional (3D) structures and is therefore subject to projection error, overlapping of anatomical structures, distortion and inaccuracies due to variation of interpretation of landmark data.[5] In 1972 G.N. Hounsfield introduced 3D radiographic imaging by means of computer tomography (CT) which largely solved the problems associated with projections cephalograms.

Modern maxillofacial 3D imaging (characterized by laser scanning, stereophotogrammetry, magnetic resonance imaging or CT techniques) has had a tremendous impact on the practice of orthodontics and craniofacial surgery.[7] The impact has become more evident with the advent of cone-beam computed tomography (CBCT) which has gained wide acceptance during the last 8 years.[8] The first CBCT systems dedicated for imaging of the orthognathic region was developed almost a decade ago.[9] Due to the significant reduction in radiation, CBCT imaging has largely replaced conventional CT in dentistry.[8, 10] With CBCT imaging it is possible to perform a full scan of the head in a few seconds with an effective dose of only 50uSv compared to 2000uSv from conventional CT.[10] Other advantages promoting the use of CBCT are less cost, increased availability, an ability to change the field of view and sub-millimeter spatial resolution.[10, 11] Currently, the most common uses for CBCT images in dentistry are in the fields of endodontics, periodontics, minor oral surgery and implantology, assessment of the TMJ and orthodontics and craniofacial surgery.[7]

Since CBCT imaging will continue to mature rapidly and play an increasingly important role in orthodontics and orthognathic surgery, it must be realized that CBCT imaging is not without limitations and pitfalls. In 1955 Bjork, one of the most eminent contributors to the study of cephalometry, and Palling[12] wrote: "*The value of biometrical methods in clinical diagnosis depends entirely on the user's appreciation of the limitations inherent in the method.*" Keeping these words in mind, it is necessary to

understand the limitations and pitfalls associated with CBCT imaging in order to fully appreciate and correctly apply the possibilities that CBCT imaging offers.

1.2 Inherent Limitations and Pitfalls of CBCT Imaging and Cephalometry: from Utilization to Application

1.2.1 Measurement error in cephalometry

In the nineteenth century, the legendary physicist Lord Kelvin remarked, "to measure is to know" and "when you can measure what you are speaking about, you can express it in numbers, you know something about it; but when you cannot measure it, when you cannot express it in numbers, your knowledge is of a meager and unsatisfactory kind". Ironically, Lord Kelvin certainly did not have cephalometry in mind when he made these statements (Lord Kelvin initially proclaimed x-rays to be a hoax but later accepted the idea after having his hand x-rayed) but they especially hold true for cephalometry because linear and angular measurements are the basis of cephalometric analysis.

Quantification of the measurement error is a critical but often overlooked process in cephalometry.[13] Measurement error in cephalometry is mostly due to random errors associated with anatomical landmark interpretation.[5, 13, 14] With the ideas of Lord Kelvin in mind and the high level of accuracy needed for surgical planning and treatment outcome evaluation, it is therefore important to determine the measurement error at a level which is sensitive enough to detect significant change ($\alpha = 0.05$) if it occurs. A useful way of presenting the measurement error is a repeatability limit.[15] The International Organization of Standardization defines the repeatability limit as the value less or equal to which the absolute difference between two test results obtained under repeatability conditions may be expected to be with a probability of 95%.[15] The smallest detectable difference (SDD) describes the 95% repeatability limit of the measurement error. The SDD is used in all fields of medicine for reliability testing of measurements and is sensitive enough to determine significant changes not caused by measurement error.[13, 16-19] Clinically, this means that if the SDD exceeds the observed difference, one cannot conclude with certainty that the observed change is a result of the treatment instead of a result of the landmark errors.

Few studies have reported the measurement error of 2D cephalometric measurements at a 95% confidence level.[20] In addition, no studies reporting the measurement error of 3D cephalometric measurements at a 95% confidence level could be found. Considering the addition of the third dimension and the fact that there are no

clear operational definitions for specific cephalometric landmarks in the mediolateral direction, it may result in considerable clinical differences of the resulting 3D measurements.[21, 22]

1.2.2 Utilization of CBCT imaging

It is speculated that the use of CBCT images might become routine in orthodontics and orthognathic surgery in the near future.[10, 11, 23] However, CBCT still exposes the patient to more radiation compared to traditional cephalograms which has a significant impact on the indications of CBCT imaging when taking the ALARA (As Low As Reasonably Achievable) principle into account.[7,24] In 2008 the European Academy of Dentomaxillofacial Radiology (EADMFR) devised a set of 20 "Basic Principles" to act as core standards for the use of CBCT imaging.[25] The "SEDENTEXCT' (Safety and Efficacy of a New and Emerging Dental X-ray Modality) project published its provisional guidelines for the use of CBCT maxillofacial imaging in 2009.[26] The House of Delegates of the American Association of Orthodontists adopted a resolution in 2010 that states "RESOLVED, that the AAO recognizes that while there may be clinical situations where a cone-beam computed tomography (CBCT) may be of value, the use of such technology is not routinely required for orthodontic radiography".[27]

According to the SEDENTEXT and AAO guidelines the current evidence does not support the routine use of craniofacial CBCT images for orthodontic treatment.[26, 27] However, the literature remains inconsistent and controversial regarding the orthodontic indications for CBCT with some authors having questioned the definitions of the criteria.[28] They argue that although the radiation is more than conventional radiography, CBCT images offers a unique and new appreciation of the anatomical structures and underlying anomalies and that the benefits of the 3D images often outweighs the risks. Discrepancies in the literature between so-called advantages of CBCT imaging and evidence-based criteria exist. Therefore, there is a need to develop clear, evidence-based selection criteria for obtaining CBCT images in orthodontics and orthognathic surgery.[24]

1.2.3 Acquisition of CBCT images

One of the biggest difficulties of CBCT imaging is the accurate acquisition of patient in the natural head position (NHP). The NHP is stable and reproducible, and represents the true appearance of human beings which gives it a realistic significance. It is therefore used as reference for cephalometry and orthognathic surgery planning.[29-33] During

acquisition of the CBCT scan, the head of the patient is often fixed to avoid distortion and movement artifacts due to the longer scanning times compared to traditional cephalograms. Fixing the head makes capturing of the head in NHP extremely difficult. Therefore, the Frankfort horizontal plane is often used as a reference plane in 3D cephalometry.[6] However, methods to capture the NHP of the patient need to be developed as the Frankfort horizontal might not be reliable as the horizontal reference plane.[33]

A major advantage of most CBCT machines is the ability to collimate the beam to a minimum size needed to image the area of interest in order to limit radiation exposure.[26] In addition the voxel size can be adjusted usually between 0.10 mm and 0.40 mm. A smaller voxel size is associated with better spatial resolution but higher radiation dose. It is therefore very important for a clinician to understand the scanning parameters for each application before acquisition in order to keep radiation exposure as low as possible e.g., for examination of impacted maxillary canines the optimum voxel resolution should be medium sized (0.25mm – 0.30 mm) and only the region of interest should be exposed.[26, 34] The positioning the patient in the CBCT scanner therefore becomes critical and CBCT machine should therefore be equipped with light beams for correct positioning of the patient and an ability to make a "scout" image to confirm that the region of interest is being captured.[25]

1.2.4 Visualization of CBCT-derived surface models

In 2D cephalometry, tracings are made on the cephalogram in order to perform diagnosis and treatment planning. In 3D cephalometry this is not possible due to the addition of the third dimension. 3D cephalometry relies on volume renderings and the surface models derived from the 3D radiographic images. It is therefore important to understand the concept and distinguish between "volume rendering" and "surface models" in 3D cephalometry. 3D surface models are very important for visualization in orthodontics and orthognathic surgery because it allows for actions such as indicating landmarks, performing measurements, moving bone fragments and performing virtual osteotomies which is not possible with the volume rendering.[10] Therefore, the surface models need to be very accurate.[35-37] Generation of surface models is called "segmentation" and the surface models are often referred to as "segmentations". The process of segmentation is critical for the accuracy of the surface models.

In order to fully understand the process of segmentation and the limitations thereof it is necessary to revise the process of visualization of CBCT images after acquisition of the scan. The steps are also illustrated in Figure 1. The first step in the management of the 3D data is provided by the manufactures and consists of converting the 3D data into an exportable DICOM (Digital Imaging and Communications in Medicine) file. In essence the DICOM file consists of a stack of 2D images or slices.[35] The 3D data are composed of voxels, each with its own grey level based on indirect calculation of the radiation absorbed. The voxel can be compared with the pixel of 2D images but with the added dimension of depth. The next step is called the volume rendering. The computer uses the voxel data to "draw" or reconstruct the 3D volume by means of algorithm. In addition; most 3D visualization software can reformat the 3D image allowing the operator to scroll through 2D slice images in sagittal, coronal and axial direction.

Figure 1 A flow chart representing the steps to derive the surface models from a CBCT scan

1. Positioning of patient in the CBCT scanner

2. Scanning of the patient

3. Images of scan converted to DICOM files

4. DICOM file imported into volumetric rendering software

Volume rendering

5. Rendered volumetric images and 2D slices in the sagittal, axial and coronal views

Segmentation

6. Surface models created by means of segmentation

7. Surface models used for surgical treatment planning

Following the volume rendering, 3D surface models of the bone and soft-tissues can be generated. The surface models are constructed from voxel based data, requiring the input of a threshold value which specifies what the structure of interest (e.g. bone or soft-tissue) is.[10] The surface model is created by a triangulated mesh covering the selected surface of interest by applying an algorithm; the most well-known is the marching-cubes algorithm.[10] The user determines the threshold value of visible and invisible voxels. Herein lays the major inherent problem associated with the segmentation process. The accuracy of segmentation therefore relies on the grey-value and the user entered threshold value by the operator.[35] This process is further complicated because CBCT imaging suffers from beam inhomogeneity which results in variation of image quality and accuracy among different manufactures and reconstruction parameters.[38-40] This means that the grey levels of the voxels of the same object imaged by two different scanners are likely to differ, resulting in difference during the segmentation process. The grey-values may also be influenced by the voxel resolution of the CBCT scan. Therefore, the influence of voxel resolution on the linear accuracy of CBCT rendered surface models needs further investigation since a smaller voxel resolution is associated with a significant increase in radiation exposure and longer scanning times.

1.2.5 Application of CBCT for cephalometry

A major difference in the application of 3D cephalometry compared to 2D cephalometry is the addition of the third dimension and use of planes rather than lines to describe geometry of certain anatomical structures. However, the human face is inherently asymmetrical.[41-43] This inherent asymmetry results in differences of plane orientation which may account for clinical differences between 2D and 3D measurements and makes direct comparison between the two modalities difficult. In addition, orthodontists and orthognathic surgeons are used to having "normal' values derived from longitudinal cephalometric growth studies to help in the diagnosis and treatment planning. It is suggested that these problems can also be overcome by deriving lateral cephalograms from the 3D CBCT images since measurements derived lateral cephalograms have been proven to be on average similar to conventional cephalograms.[44-46] Unfortunately, the 3D characteristics are lost when a cephalogram is derived from the CBCT images and additional software is often required to analyze the derived cephalogram. Although direct comparison between 2D and 3D measurements is difficult and inconsistent, it is plausible that it might be possible when references for

quantification are the same and the magnification factors have been corrected. [47-49] Bholsithi et al.[49] found the 3D measurements in the midline to be comparable with 2D measurements. Therefore, to overcome the difficulties of comparison, a 3D cephalometric analysis based on the midsagittal plane may prove to be a valid alternative to analysis of derived cephalograms.

An advantage of 3D surface models is the ability of the software to create a mirror-image of the surface model around an arbitrary plane.[50-52] An interesting application of mirror-imaging is that the mirror-image of the "healthy" side can be superimposed over the "defect" side.[50, 51] The difference between the geometries can be computed and using rapid-prototyping machines, digital templates can be fabricated to produce physical templates to sculpt autogenous bone in order to precisely replace the missing bone.[50, 51] These templates have been reported to increase the accuracy of the operation and reduced total operative time.[51] Superimposition of the healthy side on the defect side might also have an added value in diagnosis of the extent of craniofacial asymmetry because differences of volume can be assessed visually.

CBCT cephalometric analyses usually quantify craniofacial asymmetry by means of subtraction of bilateral measurements or differences of measurements made to a midsagittal plane from laterally positioned landmarks.[53-55] As mentioned, the human face is inherently asymmetrical; therefore the landmarks used to describe the midsagittal plane might have a marked influence on the asymmetry quantification and may result in accuracies. Morphometric methods are used in biology and orthodontics to study object symmetry in living organisms and to determine the true plane of symmetry.[52, 56-64]

Although it is reliable to create a morphometric midsagittal plane using 3D surface models, most 3D cephalometric analyses still rely on a midsagittal planes based on anatomical landmarks which has been questioned in recent literature. Therefore, it is necessary to investigate if there are clinical significant differences between a morphometric midsagittal planes and cephalometric midsagittal planes based on anatomical landmarks since differences between the methods might influence clinical diagnosis and treatment planning of craniofacial asymmetry.

1.3 Aims of the thesis

The general aim of this thesis is to explore some of the potential applications of CBCT in the field of cephalometry and to investigate and define possible solutions for the

limitations and pitfalls associated with CBCT imaging as discussed in Chapter 1.2. In addition to the specific research aims, a simple method to achieve a NHP for CBCT images was developed and the additional value of mirror-imaging in the diagnosis of craniofacial asymmetry was investigated.

The specific research aims were:

1. To investigate the 95% confidence limit of the measuring error of commonly used 2D and 3D cephalometric measurements.
2. To assess the accuracy of linear measurements made on CBCT-derived surface models.
3. To investigate the influence of the voxel sizes on the accuracy of linear measurements made on CBCT-derived surface models.
4. To compare 2D and direct midsagittal 3D cephalometric measurements.
5. To compare postero-anterior cephalograms and cone-beam CT images for the detection of mandibular asymmetry.
6. To perform a 3D comparison of a morphometric midsagittal plane and cephalometric midsagittal planes for assessment of craniofacial asymmetry.

1.4 References

1. http://oxforddictionaries.com/definition/cephalometry
2. Proffit WR, Sarver DM, Ackermann JL. Orthodontic Diagnosis: The Development of a Problem List. In: Proffit WR, Fields HW Jr, Sarver DM eds. Contemporary Orthodontics. 4th ed. Philadelphia, PA: Mosby Elsevier: 2007:201-203
3. Jacobson A. The significance of radiographic cephalometry. In: Jacobson A, Jacobson RL eds. Radiographic Cephalometry: From Basics to Videoimaging. Hanover Park, IL: Quintessence: 1995: 1-16
4. Ghafari GG. Posteroanterior cephalometry: Craniofacial frontal analysis. In: Jacobson A, Jacobson RL eds: Radiographic cephalometry, From Basics to 3-D imaging. Hanover Park. Quintessence Publishing Co, Inc. 2006: 267-292
5. Marci V, Athanasiou AE. Sources of error in lateral cephalometry. In: Athanasiou AE. Orthodontic cephalometry. London, UK: Mosby-Wolfe: 1995: 125-140
6. Swennen GJR, Schutyser F, Hausamen JE. Three-dimensional cephalometry. A color atlas and manual. Heidelberg Springer, Berlin 2005
7. Harrell WE, Jacobson RL, Hatcher DC, Mah J. Cephalometric imaging in 3-D. In: Jacobson A, Jacobson RL eds: Radiographic cephalometry, From Basics to 3-D imaging. Hanover Park. Quintessence Publishing Co, Inc. 2006: 233-246

8. White SC. Cone-beam imaging in dentistry. Health Phys 2008; 95: 628-637

9. Mozzo P, Procacci C, Tacconi A, Martini PT, Andreis IA. A new volumetric CT machine for dental imaging based on the cone-beam technique: preliminary results. Eur Radiol 1998; 8: 1558-1564

10. Halazonetis DJ. From 2-dimensional cephalograms to 3-dimensional computed tomography scans. Am J Orthod Dentofacial Orthop 2005; 127: 627-637

11. Swennen GRJ, Schutyser F. Three-dimensional cephalometry: Spiral multi-slice vs. cone-beam computed tomography. Am J Orthod Dentofacial Orthop 2006; 130: 410-416

12. Bjork A, Palling M. Adolescent age changes in sagittal jaw relation, alveolar prognathy, and incisal inclination. Acta Odontol Scand 1955; 12: 201-231

13. Harris EF, Smith RN. Accounting for measurement error: A critical but often overlooked process. Arch of Oral Biol 2009;54 Suppl 1: S107-117

14. Lou L, Lagravere MO, Compton S, Major PW, Flores-Mir C. Accuracy of measurements and reliability of landmark identification with computed tomography (CT) techniques in the orthognathic area: a systematic review. Oral Surg Oral Med Oral Pathol Oral Radiol Endod 2007; 104: 402-411

15. International Organization of Standardization. Accuracy (trueness and precision) of measurement methods and results. Part 1. General principles and definitions. Geneva, Switzerland: International Organization of Standardization 1994: ISO 5725-1

16. Hopkins WG. Measures of reliability in sports medicine and science. Sports Med 2000;30:1-15

17. Smeulders MJ, Van den Berg S, Odeman J, Nederveen AJ, Kreulen M, Maas M. Reliability of in vivo determination of forearm muscle volume using 3.0 T magnetic resonance imaging. J Magn Reson Imaging 2010; 31: 1252-1255

18. Grunt S, Van Kampen PJ, Van der Krogt MM, Brehm MA, Doorenbosch CAM, Becher JG. Reproducibility and validity of video screen measurements of gait in children with spastic cerebral palsy. Gait Posture 2010; 31: 489-494

19. Kropmans TJ, Dijkstra PU, Stegenga B, Stewart R, de Bont LG. Smallest detectable difference in outcome variables related to painful restriction of the temporomandibular joint. J Dent Res 1999; 78: 784-789

20. Battagel JM. A comparative assessment of cephalometric errors. Eur J Orthod 1993; 15: 305-314

21. Van Vlijmen OJC, Maal T, Berge SJ, Bronkhorst EM, Katsaros AM, Kuipers-Jagtman. A comparison between 2D and 3D cephalometry on CBCT scans of human skulls. Int J Oral Maxillofac Surg 2010; 39: 156-160

22. Ludlow JB, Gubler M, Cevidanes LHS, Mol A. Precision of cephalometric landmark identification: cone-beam tomography vs. conventional cephalometric views. Am J Orthod Dentofacial Orthop 2009; 136: 312e1-10; discussion 312-313

23. Hatcher DC, Aboudara CL. Diagnosis goes digital. Am J Orthod Dentofacial Orthop 2004; 125: 512-515

24. Farman AG, Scarfe WC. Development of imaging selection criteria and procedures should precede cephalometric assessment with cone-beam computed tomography. Am J Orthod Dentofacial Orthop 2006; 130: 257-265

25. EADMFR. Basic principles for the use of dental cone beam CT. www.eadmfr.info 2008

26. EDENTEXCT. Provisional guidelines CBCT for dental and maxillofacial radiology. www.sedentexct.eu/guidelines 2009

27. www.aaomembers.org/Resources/Publications/ebulletin-05-06-10.cfm

28. Mah JK, Hung JC, Choo H. Practical applications of cone-beam computed tomography in orthodontics. J Am Dent Assoc 2010; 141 suppl 3:7S-13S

29. Lundstrom A, Lundstrom F, Lebret LML, Moorrees CFA. Natural head position and natural head position: basic consideration in cephalometric analysis and research. Eur J Orthod 1995; 17: 111-120

30. Cooke MS, Wei SHY. The reproducibility of natural head posture: a methodological study. Am J Orthod Dentofacial Orthop 1988; 93: 20-28

31. Cooke MS. Five-year reproducibility of natural head posture: a longitudinal study. Am J Orthod Dentofacial Orthop 1990; 97: 489-494

32. Peng L, Cooke MS. Fifteen-year reproducibility of natural head posture: a longitudinal study. Am J Orthod Dentofacial Orthop 1999; 116: 82-85

33. Moorrees CFA. Natural head position: the key to cephalometry. In: Jacobson A, Jacobson RL eds: Radiographic cephalometry, From Basics to 3-D imaging. Hanover Park. Quintessence Publishing Co, Inc. 2006: 153-160

34. Liedke GS, Dias da Silviera HE, Dias da Silviera HL, Duntra V, Poli de Figueiredo A. Influence of voxel size in the diagnostic ability of cone beam tomography to evaluate simulated external root resorption. J Endod 2009, 35: 233-235

35. Grauer D, LSH Cevidanes, Profitt WR. Working with DICOM craniofacial images. Am J Orthod Dentofacial Orthop 2009; 136: 460-470

36. Cevidanes LHC, Tucker S, Styner M, Kim H, Chapuis J, Reyes M, Profitt, Turvey T, Jaskolka M. Three-dimensional surgical simulation. Am J Orthod Dentofacial Orthop 2010; 138: 361-371

37. Swennen GRJ, Mollemans W, Schutyser F. Three-dimensional treatment planning of orthognathic surgery in the era of virtual imaging. J Oral Maxillofac Surg 2008; 67: 2080-2092

38. Loubele M, Jacobs R, Maes F, Denis K, White S, Coudyser W et al. Image quality vs radiation dose of four cone-beam computerized scanners. Dentomaxillofac Rad 2008; 37; 309-319

39. Hassan B, Metska ME, Ozok AR, Van der Stelt PF, Wesselink PR. Comparison of five cone beam computed tomography systems for the detection of vertical root fractures. J Endod 2010; 36: 126-129

40. Loubele M, Maes F, Schutyser F, Marchal G, Jacobs R et al. Assessment of bone segmentation quality of cone-beam CT versus multislice spiral CT: a pilot study. Oral Surg Oral Med Oral Pathol Oral Radiol Endod 2006; 102: 255-234

41. Gawilkowska A, Szczurwski J, Czerwinski F, Miklaszwenska D, Adamiec A, Dzieciolowska E. The fluctuating asymmetry of mediaeval and modern human skulls. Homo 2007; 58: 159-172

42. Haraguschi S, Iguchil Y, Takada K. Asymmetry of the face in orthodontic patients. Angle Orthod 2008; 78: 421-426

43. Peck S, Peck L, Kataja M. Skeletal asymmetry in esthetically pleasing faces. Angle Orthod 1991; 61: 43-46

44. Van Vlijmen OJC, Berge J, Swennen GR, Bronkhorst EM, Katsaros C, Kuipers-Jagtman AM. Comparison of cephalometric radiographs obtained from cone-beam computed tomography scans and conventional radiographs. J Oral Maxillofac Surg 2009; 67: 92-97

45. Kumar V, Ludlow JB, Cevidanes LHS. Comparison of conventional and cone beam CT synthesized cephalograms. Dentomaxillofacial Radiology 2007; 36: 263-269

46. Kumar V, Ludlow JB, Cevidanes LHS, Mol A. In vivo comparison of conventional and cone beam CT synthesized cephalograms. Angle Orthod 2008; 78: 873-879

47. Van Vlijmen OJC, Maal T, Berge J, Bronkhorst EM, Katsaros C, Kuipers-Jagtman AM. A comparison between two-dimensional and three-dimensional cephalometry on CBCT scans of human skulls. Int J Oral Maxillofac Surg 2009, doi:10.1016/j.ijoms.2009.11.017

48. Nalçaci R, Öztürk F, Sökücü O. A comparison of two-dimension al radiography and three-dimensional computed tomography in angular cephalometric measurements. Dentomaxillofacial Radiology 2010; 39: 100-106

49. Bholsithi W, Tharanon W, Chintakanon K, Komolpis R, Sinthanayothin C. three-dimensional vs. two-dimensional cephalometric analysis with repeated measurements from 20 Thai males and 20 Thai females. Biomed Imaging Interventional J 2009, 5, e21

50. Gateno J, Xia JJ, Teichgraeber JF, Christensen AM, Lemoine JJ et al. Clinical feasibility of computer-aided surgical stimulation(CASS) in the treatment of complex cranio-maxillofacial deformities. J Oral Maxillofac Surg 2007; 65: 728-734

51. Xia JJ, Gateno J, Teichgraeber JF. Secrets in computer-aided surgical simulation for complex cranio-maxillofacial surgery. In: English JD, Peltomaki T, Pham-Litchel K eds: Mosby's Orthodontic Review. St Loius. Elsevier Inc. 2009: 277-287

52. De Momi E, Chapuis J, Pappas I, Ferrigno G, Hallerman W, Schramm A, Caversaccio M. Automatic extraction of the midfacial plane for cranio orthognathic surgery planning. Int J Oral Maxillofac Surg 2006; 35: 636 - 642

53. Hwang H-S, Hwang CH, Lee K-H, Kang B-C. Orthognathic 3-dimensional image analysis for the diagnosis of facial asymmetry. Am J Orthod Dentofacial Orthop 2006; 130: 779-785

54. Baek S-K, Cho I-S, Chang Y-I, Kim M-J. Skeletodental factors affecting chin point deviation in female patients with class III malocclusion and facial asymmetry: a three dimensional analysis using computed tomography. Oral Surg Oral Med Oral Pathol Oral Radiol Endod 2007; 104: 628-639

55. Jacobson RL. Three-Dimensional Cephalometry. In: Jacobson A, Jacobson RL eds. Radiographic Cephalometry: From Basics to 3-D Imaging. 2nd ed. Hanover Park. Quintessence Publishing Co, Inc. 2006:233-247

56. Klingenberg CP, Barluenga M, Meyer A. Shape analysis of symmetric structures: Quantifying variation among individuals and asymmetry. Evolution 2002; 56: 1909-1920

57. Ferrario VF, Sforsa C, Poggio CE, Tartaglia G. Distance from symmetry: A three-dimensional evaluation of facial asymmetry. J Oral Maxillofac Surg 1994; 52: 1126 – 1132

58. Ferrario VF, Sforsa C, Miani A Jr, Serrao A. A three-dimensional evaluation of facial asymmetry. J Anat 1995; 186: 103-110

59. McIntyre GT, Mossey PA. Asymmetry of the craniofacial skeleton in parents of children with a cleft lip, with or without cleft palate, or an isolated cleft palate. Eur J Orthod 2010 32 : 177-185

60. McIntyre GT, Mossey PA. Size and shape measurement in contemporary cephalometrics. Eur J Orthod 2003; 25: 231-242

61. Hartman J, Meyer-Marcotty P, Hausler G, Stellzig-Eisenhauer A. Reliability of a method for computing facial symmetry plane and degree of asymmetry based on 3D-data. J Orofac Orthop 2007; 68: 477-490

62. Benz M, Laboureux X, Maier T, Nkenke E, Seeger S, Neukam FW et al. The symmetry of faces. In: Greiner G, Niemann H, Ertl T, Girod B, Seidel HP (eds) Vision, modeling and visualization. IOS Press, Amsterdam, 2002; 332-339

63. Meyer-Marcotty P, Alpers GW, Gerdes ABM, Stellzig-Eisenhauer A. Impact of facial asymmetry in visual perception: a 3-dimensional data analysis. Am J Orthod Dentofacial Orthop 2010; 137: 168.e-168.e8

64. Zelditch ML, Donald L, Swiderski H, Sheets D, Fink WL. Geometric morphometrics for biologists: a primer. Elsevier, London, 2004; 1-128

Chapter 2

Measurement error in clinical cephalometry

2.1 Reliability and the smallest detectable differences of lateral cephalometric measurements

Abstract

Introduction: The aim of this study was to determine the reliability and the measuring error (by means of the smallest detectable error or SDD) of 11 angular and 4 linear measurements commonly used for cephalometric analysis. Methods: 25 Digital lateral cephalograms were randomly selected and traced with the Viewbox® Version 3.1.1.13 software. This was repeated three times by two observers during three different sessions. There was at least one week apart between each session. Differences were analyzed with a repeated measurement analysis of variance (ANOVA). Intra- and interobserver reliability was calculated by means of intraclass correlation coefficients (ICC) based on absolute agreement. Measurement error was determined by means of the smallest detectable difference (SDD). Results: The intraobserver agreement of the measurements was good (ICC > 0.82). SNA, SNB, ANB and ANS-Me had the smallest intraobserver measuring for both observers (> 1.86 mm or °). Except for SN-FH (ICC = 0.76), the interobserver agreement was good (ICC > 0.87) Conclusion: Determining the appropriate measuring error of cephalometric measurements by means of the smallest detectable difference (SDD) is necessary to find true difference between the start and the conclusion of active treatment. Depending on the magnitude of clinical significance, the measuring error was possibly clinical significant for all the variables tested and therefore question the use of these variables to detect true treatment effect.

2.1.1 Introduction

Since Hofrath and Broadbent introduced radiographic cephalometry in 1931, it has been an important tool in orthodontic diagnosis, treatment planning and evaluation of treatment results.[1-3] However, landmark identification error is one of the major sources of variability, probably because this step depends the most on human judgment.[3] The reliability of landmark identification has been studied using various experimental and statistical methods.[4-11] Reliability statistics have been reported for landmark identification but the coefficients derived from these reliability statistics are rather abstract and therefore have limited clinical applicability. The clinical applicability is hampered because these coefficients are not expressed in the unit of the cephalometric measurement (mm or degrees).

The effect of the variance of landmark identification on cephalometric measurements may be useful clinically, but this requires that the measurement error be quantified in order to detect true differences. The quantification of the measurement error or technical error of measurement is a critical but often overlooked process.[12] The technical error of measurement can be defined as the variability encountered between dimensions when the same specimens are measured at multiple sessions.[12] The size of the measurement error determines the smallest difference between two measurements that can be considered a true difference. [12-16] The advantage of introducing the calculation of the smallest detectable difference (SDD) in cephalometric analysis is that true treatment effect can be evaluated because the SDD defines the 95% confidence limits of the method error.[12] This means that to be able to detect change during orthodontic treatment, the difference between two observations must be at least equal or larger than the SDD for the specific measurement to be statistically significant. Although the influence of landmark variation on cephalometric measurements has been investigated using different formulas[17-28], to our knowledge, few studies have reported the measuring error at a 95% confidence level.[28, 29] Therefore, the aim of this study was to determine the reliability and the measuring error by means of the SDD of angular and linear measurements commonly used for cephalometric analysis.

2.1.2 Methods and Materials

A group of twenty-five digital lateral cephalograms were randomly selected from the archive of the Orthodontic Department of the University Medical Centre Groningen.

There was no distinction made between sex, age or dentition in the random selection. The average age of the subjects in sample was 14.8 years (95% CI: 12.8 - 16.7 years). Seventeen subjects had a permanent occlusion, whilst eight subjects were still in the mixed dentition but with the first mandibular premolar erupted in occlusion. The digital cephalograms were made (ProMax, DiMax2 Digital Cephalometric Unit, Planmeca, Helsinki, Finland) with a resolution quality of 2272 x 2045 pixels at a 24 bit depth.

Table I	The landmarks used in this study	
Landmark and Abbreviation		**Definition**
1. Sella	S	The midpoint of the pituitary fossa
2. Nasion	N	The most anterior point of the frontonasal suture in the median plane
3. Porion	Po	The superior point of the external auditory meatus
4. Orbitale	Or	The lowest point in the inferior margin of the orbit
5. Anterior nasal spine	ANS	The tip of the bony anterior nasal spine in the median plane
6. Subspinale	Ss or A	The point at the deepest midline concavity on the maxilla between the anterior nasal spine and prosthion
7. Upper incisor incisal tip	Isi	The incisal edge of the most anterior maxillary central incisor (Incision superius incisalis)
8. Upper incisor apex	Isa	The root apex of the most anterior maxillary central incisor (Incision superius apicalis)
9. Lower incisor incisal tip	Iii	The incisal edge of the most anterior mandibular central incisor (Incision inferius incisalis)
10. Lower incisor apex	Iia	The root apex of the most anterior mandibular central incisor (Incision inferius apicalis)
11. Mandibular first molar	L6	The tip of the mesiobuccal cusp of the mandibular first molar
12. Mandibular first premolar	L4	The tip of the cusp of the mandibular first premolar
13. Supramentale	Sm or B	The point at the deepest midline concavity on the mandibular symphysis between infradentale and pogonion
14. Pogonion	Pog	The most anterior point of the bony chin in the median plane
15. Gnathion	Gn	The most anteroinferior point on the symphysis of the chin
16. Menton	Me	The most inferior midline point on the mandibular symphysis
17. Gonion	Go	The constructed point of intersection of the plane tangent to the posterior border of the ramus and a plane tangent to the inferior border of the mandible
18. Condylion	Co	The most superior point on the head of the condyle
19. Glabella	G	The most prominent point in the midsagittal plane of the forehead
20. Subnasale	Sn	The point where the lower border of the nose meets the outer contour of the upper lip
21. Soft tissue Pogonion	Pog'	The most anterior point of the soft tissue contour of the chin

The lateral cephalograms were individually imported into the Viewbox software (vrsion 3.1.1.13, dHal Softwar, Kifassia, Greece) for landmark identification and cephalometric analysis. For each cephalogram, 21 landmarks were identified by a cursor-driven mouse (Table I). The operators were allowed to adjust the digital cephalogram with the

Table II	The measurements used in this study	
Measurement and Unit		**Description**
1. SNA	°	Angle determined by points S, N and A
2. SNB	°	Angle determined by points S, N and B
3. ANB	°	Angle determined by points A, N and B
4. WITS	mm	Distance between the perpendicular line from point A to the occlusal plane and a perpendicular line from point B to the occlusal plane (line passing through L6 and L4)
5. SN-FH	°	Angle between the line SN and the Frankfurt horizontal line (line connecting points Po and Or)
6. FH-NPog	°	Angle between the Frankfurt horizontal line and a line between points N and Pog
7. GoGn-SN	°	Angle between the lines SN and GoGn
8. U1-SN	°	Angle between the line SN and a line connecting points Isa and Isi (U1)
9. L1-GoGn	°	Angle between the line GoGn and a line connecting Iia and Iii (L1)
10. L1-FH	°	Angle between L1 and the Frankfurt horizontal line
11. Co-A	mm	Linear distance between point A and point Co
12. Co-Gn	mm	Linear distance between the point Gn and the point Co
13. ANS-Me	mm	Linear distance between the point ANS and the point Me
14. AFC	°	Angle of Facial Convexity - the angle between a line passing through point G and point Sn and a line connecting Sn and Pog'

software to help with the identification of the landmarks (e.g. increase contrast, adjust the gray levels). Each cephalogram was analyzed three times (at separate sessions at least a week apart) by two examiners.

The 14 cephalometric measurements (11 angular and 4 linear) commonly used in cephalometric analysis were used in this study (Table II).The measurements were calculated from the coordinates of the identified landmarks with the Viewbox® Version 3.1.1.13 software. The result of each analysis was saved and separately imported into a Microsoft Excel (Microsoft Office, Washington, USA).

Statistical analysis

All statistical analysis was performed with a standard statistical software package (SPSS version 16, Chicago, IL). Differences were analyzed using a repeated measurements analysis of variance (ANOVA) with measuring session, observer and session-observer interaction as explaining variables. The ANOVA also included tests for sphericity. P values of less than 0.05 were considered to be significant. To determine size of the measurement error, the standard error of measurement (SEM) of the repeated measurements was calculated as the square root of the variance of the random error from a 2-way random effect ANOVA. The SEM was calculated for each of the angular and linear measurements. The SDD was then calculated with the formula: $1.96 \times \sqrt{2} \times$ SEM. The SDD was used to calculate intraobserver and interobserver measurement error.

As a measure of reliability, the intraclass correlation coefficient (ICC) for absolute agreement based on a 2-way random effects analysis of variance (ANOVA) was calculated to determine the intraobserver and interobserver reliability of the cephalometric measurements. Interobserver reliability was tested by comparison of the means of the repeated measurements.

2.1.3 Results

The data were normally distributed and no violations in sphericity were found. The results are reported in Table III and IV. There were no systematic differences between observers. The factor observer was not significant for any of the variables tested (Table III). There were significant ($P > 0.05$) differences between the measuring sessions for the variables SNA, SNB, GoGn-SN, L1-GoGn and Co-A. The interaction session-observer was significant for the variables of SNA, SNB and L1-GoGn.

The reliability of the cephalometric measurements for both observers was good (ICC > 0.82). The measurement error (SDD) followed the same trends for both observers with the exception for FH-NPog which was smaller for observer 1 and GoGn-SN and AFC which was smaller for observer 2. The intraobserver measurement error of both observers was the smallest for the following variables: SNA, SNB, ANB and ANS-Me. The WITS expressed a measurement error of more than 3.50 mm for both observers at a 95% confidence interval. Interestingly, the measurement error for the dental variables: U1-SN, L1-GoGn, L1-FH was more than 4° even though reliability of the measurements was high (ICC > 0.93) for both observers. The SDD of Co-A was more than 4.00 mm for both observers. The measurement of Co-Gn had a measuring error of more than 3.5mm for both observers.

The measuring error increased when the interobserver error was calculated. The variable ANS-Me expressed measurement error of less than 1 mm or 1° at a 95% confidence interval. Interestingly, even though the interobserver measurement error increased for 12 of the 14 measurements, the interobserver agreement of the measurements remained good (ICC > 0.87), except for SN-FH (ICC = 0.76).

2.1.4 Discussion

Recently, Van der Linden[30] questioned the validity of cephalometric conclusions because of the limitations associated with cephalometric measurements. It is claimed that

| Measurement | Unit | Observer 1 | | | | | | Observer 2 | | | | | | ANOVA, _P_ | | |
| | | M1 | | M2 | | M3 | | M1 | | M2 | | M3 | | Session | Observer | Session x Observer |
		Mean	SD(±)	Mean	SD(±)	Mean	SD(±)	Mean	SD(±)	Mean	SD(±)	Mean	SD(±)			
1. SNA	°	82.48	4.47	82.55	4.23	81.73	4.38	82.70	4.69	82.40	4.37	82.28	4.58	0.01*	0.87	0.01*
2. SNB	°	77.55	3.87	77.62	3.80	77.10	3.76	77.69	4.25	77.44	4.26	77.34	4.24	0.01*	0.36	0.03*
3. ANB	°	4.92	2.88	4.93	2.78	4.63	2.67	5.01	2.68	4.96	2.61	4.93	2.47	0.32	0.85	0.28
4. WITS	mm	-2.29	4.73	-2.88	4.92	-2.91	5.28	-1.81	4.65	-1.72	4.31	-1.74	4.42	0.46	0.48	0.28
5. SN-FH	°	8.11	2.58	7.82	2.43	8.38	2.71	6.73	4.11	6.54	3.78	7.02	4.00	0.97	0.15	0.05
6. FH-NPog	°	93.74	3.65	93.56	3.62	93.84	3.68	94.62	3.56	94.91	3.31	94.85	3.47	0.50	0.28	0.54
7. GoGn-SN	°	33.06	3.85	31.64	4.17	32.36	4.58	33.09	4.20	33.09	4.32	32.96	4.69	0.01*	0.56	0.07
8. U1-SN	°	99.92	9.50	100.49	9.51	100.09	9.10	102.20	9.85	101.88	9.95	102.30	9.78	0.31	0.47	0.45
9. L1-GoGn	°	94.08	7.90	94.94	7.81	94.93	7.70	95.64	6.85	95.14	6.53	95.97	6.66	0.04*	0.65	0.04*
10. L1-FH	°	118.98	9.73	118.94	9.33	118.87	9.34	121.76	9.26	121.22	8.99	121.87	8.85	0.31	0.31	0.50
11. Co-A	mm	88.49	5.30	87.48	4.85	88.14	5.18	87.88	5.42	87.07	4.97	86.84	4.70	0.02*	0.59	0.60
12. Co-Gn	mm	107.26	6.86	107.28	6.31	107.53	6.65	105.42	6.87	105.50	6.43	105.34	6.56	0.60	0.30	0.90
13. ANS-Me	mm	63.52	5.88	63.38	5.99	63.41	5.89	64.03	5.71	63.72	6.08	63.64	5.97	0.18	0.83	0.68
14. AFC	°	16.67	5.12	17.05	4.51	16.75	4.51	16.06	5.00	16.12	5.02	16.22	4.52	0.29	0.61	0.78

Table III   Mean and standard deviations (SD) of the three measurements (M1 – M3) of the two observers. _P_ values of the repeated measures ANOVA with measuring session, observer and session-observer interactions

Table IV	The reliability (ICC), the standard error of measurement (SEM) and size of the measurement error (SDD) of the cephalometric measurements. Interobserver reliability and measurement error was determined by comparison of the means of the three measurements

Measurement		Intraobserver						Interobserver		
		Observer 1			Observer 2			Mean observer 1 vs.2		
		ICC	SEM	SDD	ICC	SEM	SDD	ICC	SEM	SDD
1. SNA	°	0.96	0.67	1.86	0.96	0.59	1.64	0.96	0.76	2.12
2. SNB	°	0.97	0.43	1.20	0.95	0.17	0.46	0.95	0.83	2.31
3. ANB	°	0.94	0.45	1.25	0.87	0.41	1.14	0.87	0.93	2.57
4. WITS	mm	0.95	1.30	3.60	0.86	1.55	4.29	0.89	2.13	5.91
5. SN-FH	°	0.87	0.83	2.31	0.82	1.06	2.93	0.76	1.90	5.26
6. FH-NPog	°	0.96	0.48	1.34	0.89	1.14	3.16	0.91	0.64	1.77
7. GoGn-SN	°	0.92	1.07	2.97	0.89	0.60	1.66	0.87	2.25	6.24
8. U1-SN	°	0.98	1.48	4.09	0.97	1.59	4.40	0.95	2.21	6.12
9. L1-GoGn	°	0.97	1.59	4.40	0.93	1.45	4.02	0.94	2.41	6.68
10. L1-FH	°	0.98	1.72	4.76	0.96	2.09	5.78	0.93	2.49	6.91
11. Co-A	mm	0.93	1.81	5.01	0.90	1.58	4.38	0.94	1.16	3.22
12. Co-Gn	mm	0.97	1.45	4.02	0.95	1.15	3.19	0.92	1.73	4.80
13. ANS-Me	mm	0.99	0.36	1.00	0.99	0.46	1.27	0.99	0.19	0.51
14. AFC	°	0.95	1.21	3.35	0.93	0.62	1.72	0.92	1.57	4.35

clinicians seldom realize the limitations of cephalometric values because to arrive at the conclusion that a measurement has changed significantly between the start and the conclusion of active treatment, the measured change should be at least equal or more than the 95% confidence level of the method error.[30] It is therefore important to introduce the concept of the SDD (also referred to as the smallest real difference or SRD[16]) which measures the smallest statistically significant change in measurement results because it represents 95% confidence level of the method error.[12] When the change in the cephalometric measurement is greater than the value of the SDD, it implies that the change in the measurement is true and not a result of measurement error. In other words, a low SDD indicates adequate sensitivity to detect an actual change.

In cephalometrics Dahlberg's formula has been the accepted method to quantify the measurement error.[28] However, it is important to realize that Dahlberg's formula proved to be equal to the SEM in the present study but detects changes only at a confidence level of around 68%.[12] If the 95% confidence limits of two methods do not overlap, it is suggestive that the methods differ significantly ($\alpha = 0.05$).[12, 31] Therefore, Dahlberg's formula cannot detect significant ($\alpha = 0.05$) change due to orthodontic treatment. In addition, the advantage of determining the SEM with an underlying repeated measures

ANOVA design is that it can be extended to any number of measuring sessions and more complex models can be tested.[12] Battagel[28] found the method error of SNA and SNB to be 1.11 and 0.92 degrees respectively at a 95% confidence level which is comparable to our study. Unfortunately the other measurements tested differed from ours. Because of a lack of literature, further comparison of the SDD values is not possible. However, since the SEM proved to be equal to Dahlberg's formula, we can use these values for comparison. The SEM values of this study were comparable to the Dahlberg's values reported in the literature.[24, 26] The large dental measurement error reported in our study were in the same range as reported by Chen et al.[19] The interobserver errors of the present study were also comparable to the results of Ongkosuwito et al.[27] who used Dahlberg's formula to determine the interobserver error for cephalometric measurements made on digital cephalograms.

The results of the present study show that although reliability of the cephalometric measurements was good, the resulting measurement errors due to the variation of the landmark identification were possibly clinically relevant for almost of the measurements tested. However, the question remains: How big should the difference be to be regarded as clinically relevant? Clinical relevance should be related to the index considered e.g. an error of 1mm for the WITS appraisal could be considered more pronounced than 1° error of the SNA angle. However, we could not find a specific value to determine clinical relevance for each measurement tested. In the literature, the magnitude of the clinical significance for cephalometric measurements varies but is usually regarded as a difference of less than 1 or 2 measuring units. [25, 30] Therefore, although the repeated measurements ANOVA showed that there were statistical differences for SNA and SNB, the clinical significance between the measurement sessions of SNA and SNB is questionable. The differences between measurement sessions of GoGn-SN, L1-GoGn and Co-A were statistically ($P < 0.05$) and clinically significant because the measurement error was more than 2 measuring units.

The magnitude of the measurement error varied amongst the measurements and increased when compared between observers. The increase of the interobserver error confirms previous literature.[19, 27, 32] The following geometric principles offer an explanation why there was significant differences between certain variables and why variation in the measuring error occurs:

Variability in landmark identification is ramified when distances (2 landmarks) and angles (either 3 of 4 landmarks) are determined because the errors are cumulative.[20] The large measuring error of Co-A and Co-Gn of the present study suggests that these

measurements are unsuitable to determine small increases in maxillary or mandibular length. Miethke[4] reported that Co showed the biggest variation (2.88 mm) of all landmarks investigated. The variation of point A and Gn was 1.35 mm and 0.73 respectively.[4] The cumulative effect of the variation of the landmarks of Co, point A and Gn explains the larger measurement error of measurements incorporating these landmarks. The results of the present study also confirm that angular measurement error increases between points with larger variation. For example, the large variation of the landmarks Go (1.44 mm), Gn (0.73 mm) and Iia (1.77 mm)[4] is cumulative and explains the differences and measurement error of L1-GoGn. This also explains the large measurement error associated with the WITS measurement. This possibly resulted from the variation of the construction of the occlusal plane due to variation of the two landmarks used. Both observers commented that L6 and L4 were often difficult to locate due to overlapping of the teeth. Because the WITS value is determined by perpendiculars from points A and B to the occlusal plane, any change in the occlusal plane magnifies the measuring error (Figure 1a).

The variability of landmarks, mostly studied with a Cartesian coordinate system with an x- and y-axis, reveals that some landmarks show a distinct shape of distribution (or envelope of error) which depends on the shape of the curvature on which the landmark is located.[6-9,20] This envelope of error could have an influence on the cephalometric measurement e.g. the variability of point B is mostly scattered along the vertical axis due to the shape of the mandibular symphysis.[6,9,20] A 1mm variation along the vertical axis has less influence on the SNB angle than a 1mm horizontal variation (Figure 1b). This also explains why SNA, SNB and ANB have a relative smaller intraobserver error measuring error.

Nagasaka et al.[32] illustrated that the distances between landmarks also have an influence on the magnitude of measuring error of the linear and angular measurements. They illustrated that the more closely two landmarks are, the greater the angular measurement error tends to be. The large measuring errors of the dental angular measurements were somewhat surprising especially when considering that the landmarks that can be located most exactly are points Iis and Iii.[3, 4] However, there is a larger variation in the landmarks of points Iia and Isa.[3, 4] The increased measurement errors of dental angular measurements were also reported by Chen et al.[19]. This geometric relationship described by Nagasaka et al.[32] explains that the greater error of the dental angular measurements is due to the short distances between the landmarks used to construct the axis of the upper and lower incisors.

Figure 1 *The geometric principles of cephalometric measurement error. (a) The cumulative effect of the occlusal plane canting and the change of the perpendicular lines from points A and B resulted in a significant measuring error of the WITS value. (b) The envelope of error of point B is arranged vertically on the shape of the symphysis. This explains a minor change of SNB although the position of point B varied by 2mm between the measurements. (c) Shorter distances between landmarks results in increased angular measurement error. Although the horizontal variation of point Isa was the same for the short and long incisor, the difference between the first measurement (U1-SN₁ - solid line) and second measurement (U1-SN₂ – dotted line) was significant.*
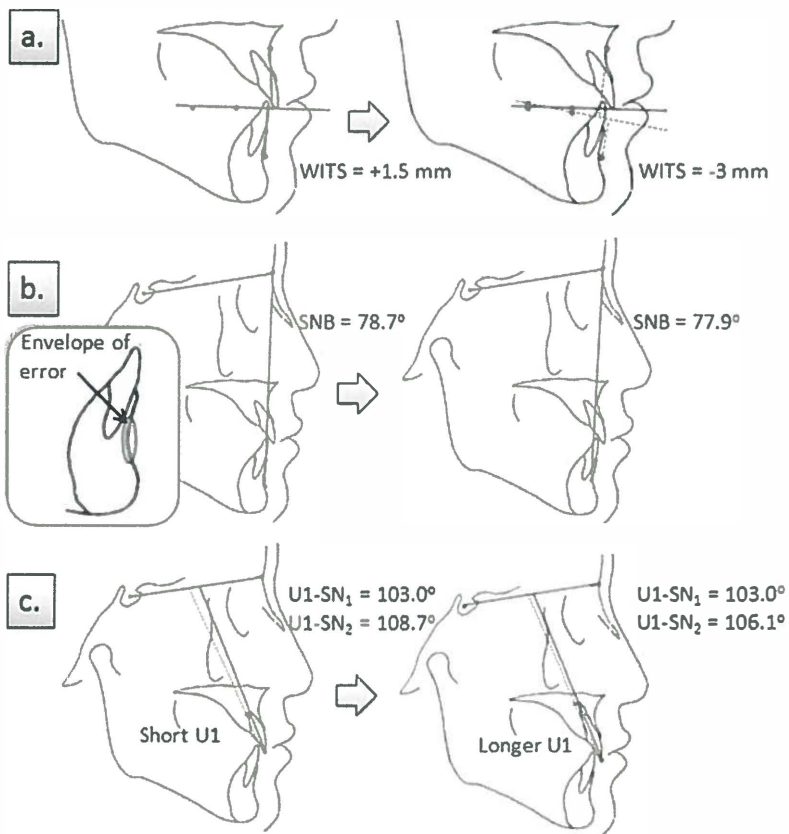
The short distance between the incisor and apex points magnifies the error of the resulting angular measurement (Figure 1c). The large SDD of the dental angular measurements suggests that due to intraobserver measurement error, U1-SN and L1-GoGn are unable to accurately detect changes less than 4° as a result of orthodontic treatment. The importance of quantifying the technical error of measurement for an optimal study design as advocated by Harris and Smith[12] is illustrated in this study. The clinical relevancy becomes more evident when the SDD is used to quantify reliability rather than when the ICC or other correlation coefficients are used.[12]

In the present study, overall intraobserver and interobserver agreement between the measurements was good. However, the SDD illustrated that the measurement error of the most of the cephalometric measurements were considerable and clinically relevant. Therefore, care must be taken when drawing conclusion from studies reporting only correlations coefficients when investigating reproducibility of cephalometric measurements. The results of this study confirm that most cephalometric measurements are possibly not sensitive enough to measure small change between the start and the conclusion of active treatment. This clinical limit of cephalometry should be realized before drawing conclusions from cephalometric data when comparing cephalograms from before and after orthodontic treatment. This SDD questions the use of certain cephalometric measurements to describe small changes due to treatment effects or normal growth.

Measurement errors of cephalometric measurements are cumulative due to the variability of the landmark identification. However, certain geometric principles (e.g. envelope of error and distances between the landmarks) have an influence on the magnitude of the resulting measurement error which makes the error of each variable unique. Therefore, determining the measurement error each of the cephalometric measurements used to describe changes during treatment by means of the SDD is important to detect true differences if they occur during orthodontic treatment or growth.

2.1.5 Conclusion

Determining the appropriate measuring error of cephalometric measurements by means of the SDD is necessary to find a true difference between the start and the conclusion of active treatment. In our study, the measurement error of cephalometric measurements of SNA, SNB, ANB and ANS-Me were the smallest for both observers.

However, depending on the magnitude of clinical significance, the measuring error was possibly clinically significant for all the variables tested and therefore questions the use of these variables to detect true treatment effect.

2.1.6 References

1. Proffit WR, Sarver DM, Ackermann JL. Orthodontic Diagnosis: The Development of a Problem List. In: Proffit WR, Fields HW Jr, Sarver DM eds. Contemporary Orthodontics. 4th ed. Philadelphia, PA: Mosby Elsevier: 2007:201-203
2. Jacobson A. How reliable is cephalometric prediction? In: Jacobson A, Jacobson RL eds. Radiographic Cephalometry: From Basics to Videoimaging. Hanover Park, IL: Quintessence: 1995:233-248
3. Marci V, Athanasiou AE. Sources of error in lateral cephalometry. In: Athanasiou AE. Orthodontic cephalometry. London, UK: Mosby-Wolfe: 1995:125-140
4. Miethke RR. Zur lokalisationsgenauigket kephalometrischer referenzpunkte. Prakt Kieferorthop 1989;3:107-122
5. Sanyinsu K, Isik F, Trakyali G, Arun T. An evaluation of cephalometric measurements on scanned cephalometric image and conventional tracings. Eur J Orthod 2007;29:105-108
6. Chien PC, Parks ET, Eraso F, Hartsfield JK, Ofner S. Comparison of reliability in anatomical landmark identification using two-dimensional digital cephalometrics and three-dimensional cone beam computed tomography in vivo. Dentomaxillofac Radiol 2009;38:262-273
7. Geelen W, Wenzel A, Gotfredsen E, Kruger M, Hansson L-G. Reproducibility of cephalometric landmarks on conventional film, hardcopy, and monitor-displayed images obtained by the storage phosphor technique. Eur J Orthod 1998:20:331-340
8. Yu S-H, Nahm D-S, Baek S-H. Reliability of landmark identification on monitor-displayed lateral cephalometric images. Am J Orthod Dentofacial Orthop 2008;133:790.e1-790.e6
9. Chen Y-J, Chen S-K, Huang H-W, Yao C-C, Chang H-F. Reliability of landmark identification in cephalometric radiography acquired by a storage phosphor imaging system. Dentomaxillofac Radiol 2004;33:301-306
10. Chen Y-J, Chen S-K, Chang H-F, Chen KC. Comparison of landmark identification in traditional versus computer-aided digital cephalometry. Angle Ortho 2000;70:387-92
11. Savage AW. Showfety KJ, Yancey J. Repeated measures analysis of geometric constructed and directly determined cephalometric points. Am J Orthod Dentofacial Orthop 1987;91:295-9
12. Harris EF, Smith RN. Accounting for measurement error: A critical but often overlooked process. Arch of Oral Biol 2009;54 Suppl 1:S107-17
13. Hopkins WG. Measures of reliability in sports medicine and science. Sports Med 2000;30:1-15
14. Kropmans TJ, Dijkstra PU, Stegenga B, Stewart R, de Bont LG. Smallest detectable difference in outcome variables related to painful restriction of the temporomandibular joint. J Dent Res 1999;78-784-89

15. Damstra J, Fourie Z, Huddleston Slater JJR, Ren Y. Accuracy of linear measurements from cone-beam tomography derived surface models of different voxel sizes. Am J Orthod Dentofacial Orthop 2010;137:16.e1-16.e6

16. Beckerman H, Roebroeck ME, Lankhorst GJ, Becher JG, Bezemer PD, Verbeek ALM. Smallest real difference, a link between reproducibility and responsiveness. Qual Life Res 2001;10:571-578

17. Baumrind S, Frantz RC. The reliability of head film measurements. Am J Orthod 1971;60:111-27

18. Baumrind S, Frantz RC. The reliability of head film measurements. 2. Conventional angular and linear measures. Am J Orthod 1971:60:505-517

19. Chen Y-J, Chen S-K, Huang H-W, Yao C-C, Chang H-F. The effects of differences in landmark identification on the cephalometric measurements in traditional versus digitized cephalometry. Angle Orthod 2004;74:155-61

20. Kamoen A Dermaut L, Verbeeck R. The clinical significance of error measurement in the interpretation of treatment results. Eur J Orthod 2001;23:569-578

21. Sommer T, Ciesielski R, Erberdobler J, Orthuber W, Fischer-Brandies H. Precision of cephalometric analysis via semiautomatic evaluation of digital lateral cephalograms. Dentomaxillofac Radiol 2009;38:401-406

22. Santoro M, Jajoura K, Cangialosi TJ. Accuracy of digital and analogue measurements assessed with the sandwich technique. Am J Orthod Dentofacial Orthop 2006;129:345-351

23. Arponen H, Elf H, Evalhari M, Waltimo-Siren J. Reliability of cranial base measurements on lateral skull radiographs.

24. Allen RA, Connolly IH, Richardson A. Early treatment of Class III incisor relationship using the chincap appliance. Eur J Orthod 1993;15:371-376

25. Richardson A. A comparison of traditional and computerized methods of cephalometric analysis. Eur J Orthod 1981;3:15-20

26. Van Vlijmen OJC, Berge SJ, Swennen GRJ, Bronkhorst EM, Katsaros C, Kuipers-Jagtman AM. Comparison of Cephalometric Radiographs obtained from cone-beam computed tomography scans and conventional radiographs. J Oral Maxillofac Surg 2009;67:92-7

27. Ongkosuwito EM, Katsaros C, Van't Hof MA, Bodegom JC, Kuipers-Jagtman AM. The reproducibility of cephalometric measurements: a comparison of analogue and digital methods. Eur J Orthod 2002;24:655-65

28. Battagel JM. A comparative assessment of cephalometric errors. Eur J Orthod 1993; 15: 305-314

29. Gravely JF, Murray Benzies P. The clinical significance of tracing error in cephalometry. Br J Orthod 1984;11:44-48

30. Van der Linden FPGM. Sheldon Friel Memorial Lecture 2007. Myth and Legends in orthodontics. Eur J Orthod 2009;30:449-468

31. Rakosi T. An atlas of cephalometric radiology. London: Wolfe Medical Publications; 1982.

32. Nagasaka S, Fujimora T, Segoshi K. Development of a non-radiographic cephalometric system. Eur J Orthod 2003;25:77-85

2.2 Reliability and the smallest detectable differences of measurements made on three-dimensional cone-beam computed tomography images

Abstract

Introduction: The aim of this study was to determine the reliability and the measurement error (by means of the smallest detectable error or SDD) of 17 commonly used cephalometric measurements made on three-dimensional (3D) cone-beam computed tomography images. Methods: 25 Cone-beam computer tomography (CBCT) scans were randomly selected. 3D images were rendered, segmented and traced with the SimPlant Ortho Pro® 2.1 (Materialise Dental, Leuven, Belgium) software. This was repeated two times by two observers during two sessions with at least one week apart. Measurement error was determined by means of the smallest detectable difference (SDD). Differences were analyzed by means of the Wilcoxon signed-rank tests. Intra- and interobserver reliability was calculated by means of intraclass correlation coefficients (ICC) based on absolute agreement. Results: There was a large variation of measurement error between the angular (range: $0.88° – 6.29°$) and linear (range: 1.33 mm – 3.56 mm) variables. The largest measuring error was associated with the dental measurements U1-FHPL, L1-MdPL and L1-FHPL (range: $3.80° – 6.29°$). The ANB angle was the only variable with a measuring error of one or less measuring unit for both observers. The intraobserver agreement of all measurements was very good (ICC: 0.86 - 0.99). Except for SN-FHPL (ICC = 0.76), the interobserver agreement was very good (ICC > 0.88). Conclusion: The measurement error of 3D cephalometric measurements (except for the ANB angle) can be considered clinically relevant. This questions the use of linear and angular 3D measurements to detect true treatment effect when a high level of accuracy required.

2.2.1 Introduction

Since the introduction of three-dimensional (3D) cone-beam computed tomography (CBCT) for imaging of the maxillofacial region a decade ago, the ability to show spatial relationships in all three planes have expanded the possibilities for diagnosis, craniofacial surgery planning and outcome evaluation in orthodontics and oral maxillofacial surgery.[1-3] The main advantage of CBCT technology is the significant reduction of radiation exposure compared to conventional CT.[3,4] With CBCT it is possible to perform a full scan of the head in a few seconds with an effective dose of only 50uSv compared to 2000uSv from conventional CT.[3-6] Other advantages promoting the use of CBCT are less cost, increased accessibility to orthodontic practices, flexibility in the field of view and sub-millimeter spatial resolution.[3,4,6] In fact, it can be argued that the routine use of CBCT images in orthodontics and craniofacial surgery might not be far away.[3,4,7]

Due to their absolute accuracy [8-13], CBCT images have become powerful tools for evaluation of craniofacial morphology and treatment outcome.[3] Accuracy is of utmost importance when the data from CBCT are used for pre-surgical planning to assure correct jaw repositioning.[14-16] However, accurate CBCT images or precise location of landmarks do not guarantee accurate measurements as geometric factors may have a significant influence on 3D measurements.[17] Moreover, each 3D landmark has its own unique configuration and envelope of error which contributes to measurement error.[14] Recent studies showed the reliability of 3D landmark identification to be very good and even more precise than conventional cephalograms when it is done by trained and experienced operators using the renderings and the cross sectional slices in all three planes of space. [15, 16] In contrast to 2D cephalometry where lines are used for measurements, 3D measurements are often made to planes which may have a different orientation to each other from the frontal view. This means that the measurement between the planes might differ depending on the location of the measurement and can therefore be an additional source of error (Figure 1).

Reliability of 3D measurements reported as correlation coefficients may have limited clinical value as very good correlation does not imply a small measuring error.[18, 19] Unfortunately, only few articles have reported the intra- and interobserver measurement errors associated with 3D measurements. However, It is difficult to draw conclusions from these articles because they used different methods and variables to describe 3D measurement error.[20-24] Nevertheless, the reported 3D measurement errors seem to be clinically relevant (> 1.00 mm or degree) considering the absolute level of

accuracy required for surgical planning and outcome evaluation. Recently, we introduced the concept of the smallest detectable difference (SDD) in cephalometry to describe the measurement error.[18] The SDD implies that in order to be able to detect real change, the difference between two observations must be at least equal or larger than the SDD for the specific measurement.[18, 19]

Since CBCT images are accurate, it is necessary to determine if the numerical data of 3D cephalometric variables derived from the images are sufficiently accurate and reliable for surgical planning and outcome evaluation. The aim of this study was to determine the reliability and the measuring error by means of the SDD of angular and linear measurements commonly used in 3D cephalometric analysis.

Figure 1 *An illustration to show that due to the variation in orientation of the mandibular plane (MdPL) and the Frankfort horizontal plane (FHPL) from the frontal view, the angle between the planes may differ depending on where the measurement is made.*
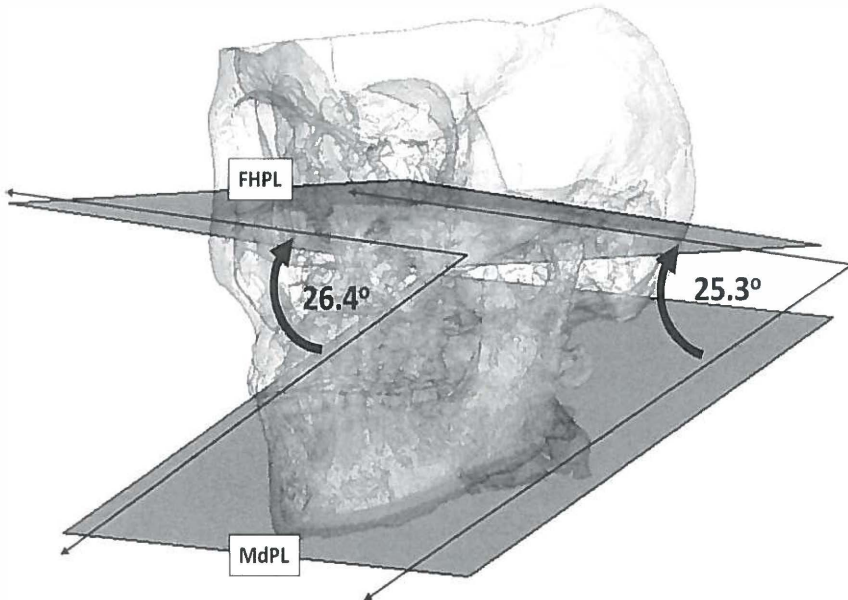
2.2.2 Methods and Materials

The sample consisted of 25 (13 male, 12 female) CBCT scans randomly selected at the Department of Orthodontics of the University Medical Center Groningen (UMCG). The average age of the subjects in the sample was 25.8 years (range: 11.7-49.5 years). Informed consent was obtained from the patients and no identifying marks were used after selection of the CBCT scans. Cleft patients and patients with visible asymmetry (defined by 4.00 mm deviation of point Menton from the midsagittal plane[25]) were not considered. The CBCT images were acquired with the KaVo 3D eXam scanner (KaVo Dental GmbH, Bismarckring, Germany) at a 0.30 voxel resolution. The CBCT data was exported from the eXamVisionQ (Imaging Sciences International LCC, Hatfield, Pennsylvania, USA) software in DICOM multi-file format and imported into SimPlant Ortho Pro® 2.1 (Materialise Dental, Leuven, Belgium) software on an Acer Aspire 7730G laptop (Acer, s'Hertogenbosch, the Netherlands) with a dedicated 512 MB video card (Nvidia® Geforce ® 9600M-GT, NVIDIA, Santa Clara, California, USA).

The 3D surface models of all of the CBCT images were generated by means of a threshold based method performed by one operator (ZF). The surface model was saved and the same surface model was used for each measuring session. All measurements were performed on a 17-inch Acer CrystalBrite™ LCD flat panel color screen with a maximum resolution of 1440 x 900 pixels. The SimPlant Ortho Pro® 2.1 software provides various views using the rotation and translation of the rendered image. Prior to measurement, two experienced observers (with more than 3 years' experience in 3D cephalometry) discussed and reviewed the definitions of the anatomical landmarks (Table I) during a consensus meeting. The definitions of the landmarks and planes as defined by Swennen et al.26 were used for this study. The two observers performed the measurements separately. The same patient was measured two times (T1 and T2) by each observer during two different sessions with at least two weeks apart. The anatomical landmarks were identified by using a cursor-driven pointer on the volume renderings and the cross sectional slices in all three planes of the CBCT images.[14] After landmark identification, a preprogrammed analysis provided the distances to the nearest one-hundredth of a millimeter of the measurements described in Table II. The values were then exported and saved as Excel® file format.

Statistical analysis
The standard error of measurement (SEM) of the repeated measurements was calculated as the square root of the variance of the random error from a 2-way

Table I	The 3D landmarks and planes used in this study

Landmark and Abbreviation		Definition
Unilateral landmarks		
1. Sella	S	Sella is the center of the fossa hypophysialis
2. Nasion	N	Nasion is the midpoint of the frontonasal suture
3. Anterior nasal spine	ANS	Anterior Nasal Spine is the most anterior midpoint of the anterior nasal spine of the maxilla
4. A-point	A	A-Point is the point of maximum concavity in the midline of the alveolar process of the maxilla
5. Upper incisor tip	Isi	Upper incisor tip is the middle point of the tip of the crown of the most prominent upper central incisor
6. Upper incisor apex	Isa	The middle point of the tip of the apex of the most prominent upper central incisor
7. Lower incisor incisal tip	Iii	Lower incisor tip is the middle point of the tip of the crown of the most prominent lower central incisor
8. Lower incisor apex	Iia	The middle point of the tip of the apex of the most prominent lower central incisor
9. B-point	B	B-Point is the point of maximum concavity in the midline of the alveolar process of the mandible
10. Pogonion	Pog	Pogonion is the most anterior midpoint of the chin on the outline of the mandibular symphysis
11. Gnathion	Gn	Gnathion is the midpoint between points Pog and Me on the outline of the mandibular symphysis
12. Menton	Me	Menton is the most inferior midpoint of the chin on the outline of the mandibular symphysis
13. Basion	Ba	Basion is the most anterior point of the foramen magnum
*Bilateral landmarks**		
14. Gonion	Go	Gonion is the point at each mandibular angle that is defined by dropping a perpendicular from the intersection point of the tangent lines to the posterior margin of the mandibular vertical ramus and inferior margin of the mandibular body or horizontal ramus.
15. Condylion	Co	Condylion is the most posterior-superior point of each mandibular condyle in the sagittal plane
16. Orbitale	Or	Orbitale (Or) is the most inferior point of each infra-orbital rim
17. Porion	Po	Porion is the most superior point of each external acoustic meatus
18. Posterior maxillary point	PMP	Posterior Maxillary Point is the point of maximum concavity of the posterior border of the palatine bone in the horizontal plane

Planes and Abbreviation		Definition
1. Frankfort horizontal	FHPL	The Frankfort horizontal plane is defined by a plane that passes both Orbital (Or left and Or right) landmarks and the mean of the two Porion (Po left and Po right) landmarks
2. Palatal plane	PPL	The palatal plane is defined by a plane that passes the Anterior Nasal Spine (ANS) and both Posterior Maxillary Point (PMP left and PMP right) landmarks
3. Mandibular plane	MdPL	The mandibular plane is defined by a plane that passes the Menton and both Gonion (Go left and Go right la

*, left and right landmarks used

random effect ANOVA. The SEM was calculated for each of the angular and linear measurements. The SDD was then calculated with the formula: 1.96 x √2 x SEM.[18, 19] The SDD was used to calculate intraobserver and interobserver measurement error. As a measure of intraobserver and interobserver reliability, the intraclass correlation coefficient (ICC) for absolute agreement based on a 2-way random effects analysis of variance (ANOVA) was

Table II	The 3D measurements used in this study
Measurement	**Description**
Angular measurements	
1. SNA	Angle between points S and A with its vertex at point N
2. SNB	Angle between points S and B with its vertex at point N
3. ANB	Angle between points A and B with its vertex at point N
4. SN-FHPL	Angle between a line through the points S and N and the FHPL in the sagittal plane
5. SN-PPL	Angle between a line through the points S and N and the PPL in the sagittal plane
6. SN-MdPL	Angle between a line connection the points S and N and the MdPL in the sagittal plane
7. PPL-MdPL	Angle between the PPL and the MdPL in the sagittal plane
8. Y-Axis	Angle between points N and Gn with its vertex at point S
9. U1-FHPL	Angle between a line through the points Isi and Isa and the FHPL in the sagittal plane
10. L1-MdPL	Angle between a line through the points Iii and Iia and the MdPL in the sagittal plane
11. L1-FHPL	Angle between a line through the points Iii and Iia and the FHPL in the sagittal plane
12. BaSN	Angle between points and Ba with its vertex at point S
Linear measurements	
13. ANS-Me	Distance in mm between the point ANS and point Me
14. Co-A	Distance in mm between the right point Co and point A
15. Co-Gn	Distance in mm between the right point Co and point Gn
16. AFH	Distance in mm between point Me and point N
17. PFH	Distance in mm between point S and the mean point between the left and right points Go

calculated. Interobserver reliability was tested by comparison of the first measuring sessions. Interobserver reliability was tested by comparison of the first measuring sessions. Because not all variables were normally distributed (Shapiro-Wilk tests), non-parametric tests were performed. The Wilcoxon signed-rank sum tests were performed to compare the repeated measurements of each observer. In addition, Wilcoxon signed-rank sum tests were performed to compare first measuring sessions by between the observers. P values less than 0.05 were considered significant. All statistical analyses were performed with a standard statistical software package (SPSS version 16, Chicago, IL).

2.2.3 Results

The results are reported in Table III. There were no significant statistical differences ($P < 0.05$) between the measuring sessions or observers. The intraobserver reliability of the cephalometric measurements was very good (ICC: 0.86 – 0.99). The interobserver reliability of the 3D measurements was also very good. Except for PPL-MdPL (ICC = 0.76) the interobserver ICCs were all higher than 0.88. The measurement error (SDD) followed the same trends for both observers. The largest angular SDDs for both observers (3.80° – 6.29°) were all dental measurements (U1-FHPL, L1-MdPL, and L1-FHPL). The smallest angular SDD for both observers was the ANB angle (0.88° and 0.98° respectively). Only the ANB angle had an intraobserver measuring error of less than 1.00 mm which is usually regarded as clinically relevant in

Measurement	Intra-observer													Interobserver		
	Observer 1							Observer 2								
	T1		T2		Comparison (T1-T2)			T1		T2		Comparison (T1-T2)			Comparison (T1-T1)		
	Mean	SD(±)	Mean	SD(±)	ICC	P	SDD	Mean	SD(±)	Mean	SD(±)	ICC	P	SDD	ICC	P	SDD
Angular measurements																	
1. SNA	81.73	3.72	82.18	3.77	0.96	0.79	2.08	82.98	3.70	82.32	3.91	0.95	0.48	2.34	0.88	0.26	3.63
2. SNB	78.13	4.15	78.41	4.29	0.98	0.82	1.74	79.04	4.26	78.38	4.27	0.95	0.52	2.75	0.93	0.41	3.28
3. ANB	3.60	3.21	3.77	3.16	0.99	0.69	0.88	4.11	3.22	3.87	3.16	0.99	0.70	0.98	0.97	0.57	1.47
4. SN-FHPL	10.36	2.46	10.36	2.05	0.91	0.66	1.86	9.64	2.39	10.10	2.35	0.86	0.32	2.46	0.76	0.21	3.38
5. SN-PPL	7.20	3.37	6.73	3.52	0.90	0.68	3.06	6.65	3.61	6.94	3.67	0.92	0.95	2.91	0.86	0.67	3.60
6. SN-MdPL	31.59	8.07	31.70	8.19	0.98	0.95	3.39	31.17	8.32	31.85	8.44	0.98	0.87	3.31	0.97	0.80	3.64
7. PPL-MdPL	24.46	7.92	25.04	8.02	0.98	0.82	3.25	24.73	7.94	25.02	8.17	0.97	0.85	3.66	0.98	0.93	2.77
8. Y-Axis	67.59	4.91	67.54	4.87	0.98	0.99	2.11	67.29	5.14	67.97	4.98	0.95	0.50	2.87	0.96	0.71	2.96
9. U1-FHPL	67.32	8.69	66.35	8.47	0.96	0.68	4.81	66.38	9.27	67.22	8.32	0.98	0.63	3.80	0.97	0.55	4.57
10. L1-MdPL	80.44	6.47	80.21	6.95	0.89	0.93	6.29	80.73	6.57	81.21	6.30	0.93	0.76	5.77	0.89	0.91	6.11
11. L1-FHPL	63.63	8.10	64.21	8.25	0.95	0.82	4.93	64.05	7.90	64.11	7.48	0.96	0.89	4.46	0.96	0.85	4.56
12. BaSN	132.21	5.60	131.97	5.74	0.96	0.82	3.17	131.75	5.95	132.53	5.46	0.96	0.46	3.27	0.93	0.63	4.22
Linear measurements																	
13. ANS-Me	66.95	8.66	67.38	8.67	0.99	0.82	2.00	67.34	8.68	67.06	8.79	0.99	0.86	1.33	0.99	0.84	2.12
14. Co-A	96.08	5.62	95.87	5.75	0.99	0.88	1.52	95.87	5.76	95.69	5.49	0.98	0.95	2.33	0.99	0.79	1.42
15. Co-Gn	122.21	8.13	122.08	8.34	0.99	0.98	1.80	121.97	8.36	122.58	8.34	0.99	0.74	2.85	0.99	0.90	2.20
16. AFH	116.72	10.66	116.73	10.85	0.99	0.97	1.89	116.59	10.99	116.85	11.04	0.99	0.90	2.13	0.99	0.96	2.68
17. PFH	75.78	6.51	75.88	6.02	0.97	0.94	2.79	76.21	6.30	76.00	6.37	0.96	0.85	3.56	0.96	0.66	3.60

Statistically significant at $P < 0.05$
ICC Intraclass correlation coefficient
SDD Smallest detectable difference

cephalometry.[27] The linear variable with the smallest SDD for observer 1 was the Co-A (1.52 mm) whilst ANS-Me (1.33 mm) was the linear variable with the smallest SDD for observer 2. The interobserver measuring error did not increase as expected and were in the same range as the interobserver measuring errors and followed the same trend as the intra-observer measuring errors.

2.2.4 Discussion

The clinical relevance of the SDD implies that if the SDD exceeds the observed difference, one cannot conclude with certainty that the observed change is a result of the treatment instead of a result of the landmark errors. In cephalometry it means that if the measured difference between pre- and post-treatment cephalograms does not exceed the SDD, the measured change is not due to treatment effect but most likely due to measurement error. The SDD is used in all fields of medicine for reliability testing of measurements because it is sensitive enough to determine significant ($\alpha=0.05$) changes not caused by measurement error.[18, 19, 28-33] This is not the case with Dahlberg's formula (the current accepted method for determining measuring error in cephalometry) which may not set limits strict enough to detect real change.[18]

No studies reporting the 95% confidence level of the 3D measuring error could be found in literature. In the present study we used 3D measurements commonly used in 2D and 3D cephalometry. This might serve as reference for other studies but it also allows for comparison between 2D and 3D of the corresponding variables. Conversely, the SDD of linear measurements Co-A and Co-Gn were smaller in 3D (average: 1.92 mm and 2.33 mm) than in 2D (average: 4.70 mm and 3.61 mm).[18] The differences in the range of the SDD of the dental angular measurements between 2D (4.21° – 5.27°) and 3D (3.80° – 6.29°) were small.[18] In the present study, the magnitude of the 3D measuring error did not increase as much as the 2D measuring error between two observers.[18] The same geometric principles that have an effect on 2D measurements also apply to 3D measurements.[18] However, the effects differ for certain variables. The following discussion offers an explanation why variation of 3D measurement error occurs and why it may differ from the corresponding 2D measurement error.

In 2D and 3D cephalometry, landmarks have a district shape of distribution (envelope of error) depending on the clarity of the definition, the quality of the image and the geometry of the object.[14,15] Importantly, differences existed between the envelopes of error of corresponding landmarks of 2D and 3D images. This is due to the

fact that certain landmarks can be more accurately identified on 3D views.[16] The bilateral landmarks of Co, Go and Or show greater variations in 2D cephalometry due to overlapping of structures and is therefore associated with large measurement error.[34] These bilateral landmarks can be more precisely located on 3D images probably due to better visualization in all three planes of space.[16]

Variation of landmark identification increases the measurement error because the errors in location are cumulative.[18,35] In 3D cephalometry, the addition of an extra dimension introduces an additional source of error in the mediolateral direction. This offers an explanation why certain angular measurements show greater measurement error in 3D than 2D. For example, the larger SDD of SNB in 3D is due to the added variability in the mediolateral direction. Although the anteroposterior variability of point B was only 0.69 mm, mediolateral variation was 1.32 mm in 3D.[16] Therefore, when constructing an angle between the three points of S, N and point B, the added mediolateral variability of point B resulted in a greater measurement error. The mediolateral variation is also one of the contributing factors to the larger measurement error of the 3D dental measurements. Although the variability of the Isi is very small in the anteroposterior (0.63 mm) and cranial-caudal (0.76 mm) direction, the variability in the mediolateral direction is significantly larger (1.99 mm).[16] Greater variability of certain landmarks in the mediolateral direction in 3D was probably related to inadequate definition of the landmarks.[16] The addition of the extra dimension also means that 3D cephalometry relies on planes rather than lines for reference. Because the human face is inherently asymmetric and the planes are often constructed by connection of two bilateral structures, the orientation of the planes might differ when assessing the patient from the frontal view (Figure 1). This could be an additional source of error because the 3D software automatically calculates the smallest value between the planes. Therefore, the reference for the angular measurement is not standardized and can vary depending on the plane orientation. Although this effect is likely to be small in a symmetric sample, the effect is clinically significant in asymmetric cases. A possible solution to overcome this problem is to select an anteroposterior plane (e.g. midsagittal plane) to serve as reference for angular measurements between planes to allow for more accurate comparison.

Nagasaka et al.[36] illustrated that the more closely two landmarks are, the greater the linear and angular measurement error tends to be. This geometric principal plays a significant role in 3D cephalometry. For example; due to the short distance of the landmarks used to construct the axis of the maxillary incisor, a small variation in the

anteroposterior location of the apex will result in a significantly larger measuring error.[18] In 3D cephalometry this effect also becomes more apparent when two landmarks in close proximity are used to construct reference planes e.g. PMP left and right to construct the PPL. If one of the landmarks varies by a minor amount, the resulting change in the orientation of the plane is significant (Figure 2). Therefore, constructing 3D planes through two landmarks in close relation to each other could result in larger measuring errors and should be avoided.

Another source of measurement error in 3D cephalometry, not investigated in the present study, is the possible effects of the segmentation process. The surface models are constructed from voxel based data, requiring the input of a threshold value which specifies what the structure of interest (e.g. bone or soft-tissue) is or is not. The accuracy of segmentation therefore relies on the gray-value and the user entered threshold value by the operator. This process is further complicated because CBCT imaging suffers from beam inhomogeneity which results in variation of image quality and accuracy among different manufactures and reconstruction parameters.[37-39] This means that the grey levels of the voxels of the same object imaged at two different times are likely to differ, resulting in differences during the segmentation process. We eliminated this problem by using the same surface model for all the measurements. However, in practice the differences between pre- and post-treatment CBCT segmentations might introduce additional measuring error. A possible solution to minimize this problem is to verify the location of each landmark on the axial, coronal and sagittal slices of each CBCT scan rather that to rely on the surface model alone for landmark identification. However, this may not always be possible. Due to geometry, certain landmarks like Gonion (Go) are better visualized and located on the 3D model than on the cross sectional slices.

The clinical significance of the measurement error depends on the level of accuracy required. If the goal is to assess growth changes or to perform surgical planning, a very high degree of accuracy is required.[1-3] In the present study, the overall intraobserver agreement was good. However, the SDD illustrated that the measurement errors of most measurements were considerable and clinically relevant (more than one measuring unit [27]). The 3D measurement error can be a result of accuracy of the landmarks but is influenced by the geometric principles as discussed above. Interplay between the variations in landmark identification and geometric principles exist which explains the variability of the measurement error.

Figure 2.a: The PPL constructed through 3 points as described by Swennen et al.26 (ANS, PMP left and PMP right). Note the close proximity of PMP left and right to each other. b: Minor cranial-caudal variation of point PMP left (< 0.05 mm) results in a significant change in the orientation of the FHPL and PPL from the frontal view.
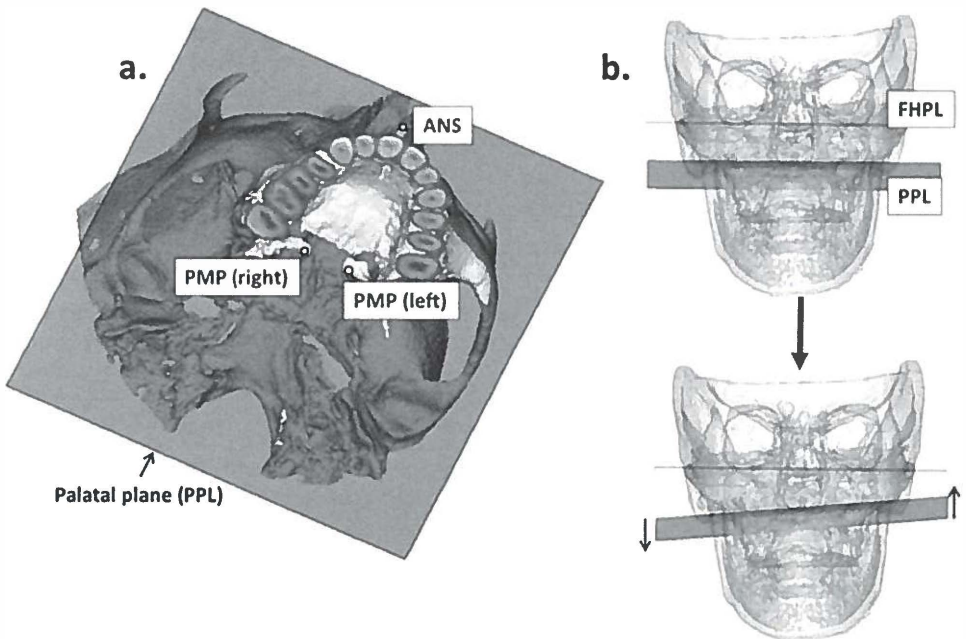
Our results confirm that most 3D cephalometric measurements are possibly not sensitive enough for small changes between the start and end of an active treatment. Reducing the measurement error by repeated measurement is arduous and unrealistic in daily practice because 3D landmark identification can be time consuming. Superimposition of 3D surface models is an alternative method to evaluate growth or treatment outcome and quantifies change by means of color maps.[40] Future research need to assess if superimposition of surface models is a more reliable method than linear and angular measurements to quantify 3D change. Unfortunately it is currently very time-consuming and computer-intensive to perform 3D superimposition. However, new advances will undoubtedly make a simplified analysis available in the future.[40] In addition; more accurate 3D measurements might be obtained when future image

segmentation procedures, based on both intensity and gradient magnitude of the signals, will be implemented rather than the current threshold based methods.

2.2.5 Conclusion

The measurement error of 3D cephalometric measurements (except for the ANB angle) can be considered clinically relevant. This questions the use of linear and angular 3D measurements to detect true treatment effect when a high level of accuracy is required.

2.2.6 References

1. Cevidanes LHC, Tucker S, Styner M, Kim H, Chapuis J, Reyes M, Profitt, Turvey T, Jaskolka M. Three-dimensional surgical simulation. Am J Orthod Dentofacial Orthop 2010; 138: 361-71
2. Swennen GRJ, Mollemans W, Schutyser F. Three-dimensional treatment planning of orthognathic surgery in the era of virtual imaging. J Oral Maxillofac Surg 2008; 67: 2080-92
3. Swennen GRJ, Schutyser F. Three-dimensional cephalometry: Spiral multi-slice vs. cone-beam computed tomography. Am J Orthod Dentofacial Orthop 2006; 130: 410-6
4. Halazonetis DJ. From 2-dimensional cephalograms to 3-dimensional computed tomography scans. Am J Orthod Dentofacial Orthop 2005; 127: 627-37
5. Ngan DC, Kharbanda OP, Geenty JP, Darendeliler MA. Comparison of radiation levels from computed tomography and conventional dental radiographs. Aust Orthod J 2003; 19: 67-75
6. Mah JK, Danforth RA, Bumann A, Hatcher D. Radiation absorbed in maxillofacial imaging with a new dental computed device. Oral Surg Oral Med Oral Pathol Oral Radiol Endod 2003; 96:508-13
7. Hatcher DC, Aboudara CL. Diagnosis goes digital. Am J Orthod Dentofacial Orthop 2004; 125: 512-5
8. Brown AA, Scarfe WC, Scheetz JP, Silveira AM, Farman AG. Linear accuracy of cone beam CT 3D images. Angle Orthod 2009; 79: 150-7
9. Damstra J, Fourie Z, Huddleston Slater JJR, Ren Y. Accuracy of linear measurements from cone-beam computed tomography-derived surface models of different voxel sizes. Am J Orthod Dentofacial Orthop 2010;137:16.e1-16.e6)
10. Lagravere MO, Carey J, Toogood RW, Major PW. Three-dimensional accuracy of measurements made with software on cone-beam computed tomography images. Am J Orthod Dentofacial Orthop 2008;134:112-16
11. Hassan B, van der Stelt P, Sanderink G. Accuracy of three-dimensional measurements obtained from cone beam computed tomography surface-rendered images for cephalometric analysis: influence of patient scanning position. Eur J Orthod 2008;31:129-34
12. Mischkowski RA, Pulsfort R, Ritter L, Neugebauer J, Brochhagen HG, Keeve E, Zoller JE. Geometric accuracy of a newly developed cone-beam device for maxillofacial imaging. Oral Surg Oral Med Oral Pathol Oral Radiol Endod 2007;104:551-9
13. Grauer D, Cevidanes LSH, Profitt WR. Working with DICOM craniofacial images. Am J Orthod Dentofacial Orthop 2009; 136:460-70
14. Lou L, Lagravere MO, Compton S, Major PW, Flores-Mir C. Accuracy of measurements and reliability of landmark identification with computed tomography (CT) techniques in the

maxillofacial area: a systematic review. Oral Surg Oral Med Oral Pathol Oral Radiol Endod 2007; 104: 402-11

15. De Oliviera AEF, Cevidanes LHS, Phillips C Motta A, Burke B, Tyndall D. Observer reliability of three-dimensional cephalometric identification on cone-beam computerized tomography. Oral Surg Oral Med Oral Pathol Oral Radiol Endod 2009; 107: 256-265.

16. Ludlow JB, Gubler M, Cevidanes LHS, Mol A. Precision of cephalometric landmark identification: cone-beam tomography vs. conventional cephalometric views. Am J Orthod Dentofacial Orthop 2009; 136: 312e1-10; discussion 312-3

17. Lagravere MO, Major PW, Carey J. Sensitivity analysis for plane orientation in three-dimensional cephalometric analysis based on superposition of serial cone beam computed tomography images. Dentomaxillofac Radiol 2010: 39: 400-408

18. Damstra J, Huddleston Slater JJR, Fourie Z, Ren Y. Reliability and the smallest detectable difference of lateral cephalometric measurements. Am J Orthod Dentofacial Orthop 2010: 138; 546e1-8; discussion 546-547

19. Harris EF, Smith RN. Accounting for measurement error: A critical but often overlooked process. Arch of Oral Biol 2009;54 Suppl 1:S107-17

20. Van Vlijmen OJC, Maal T, Berge SJ, Bronkhorst EM, Katsaros AM, Kuipers-Jagtman. A comparison between 2D and 3D cephalometry on CBCT scans of human skulls. Int J Oral Maxillofac Surg 2010; 39: 156-160

21. Olszewski R, Zech F, Cosnard G, Nicolas V, Macq B, Reychler H. Three-dimensional computed tomography cephalometric craniofacial analysis: experimental validation in vitro. Int J Maxillofac Surg 2007; 36: 828-33

22. Swennen GRJ, Schutyser F, Barth EL, De Groeve P, De Mey A. A new method of 3-D cephalometry Part I: the anatomic Cartesian 3-D reference system. J Craniofac Surg 2006; 17: 314-25

23. Moerenhout BAMML, Gelaude F, Swennen GRJ, Casselman JW, Van der Sloten J, Mommaerts MY. Accuracy and repeatability of cone-beam computed tomography (CBCT) measurements used in the determination of facial indices in the laboratory setup. J Craniomaxillofac Surg 2009; 37:18-23

24. Suomalainen A, Vehmas T, Kortesniemi M, Robinson S, Peltola J. Accuracy of linear measurements using dental cone beam and conventional multislice computed tomography. Dentomaxillofac Radiol 2008; 37: 10-17

25. Haraguschi S, Takada K, Yasuda Y. Facial asymmetry in patients with skeletal class III deformity. Angle Orthod 2002; 72: 28-35.

26. Swennen GJR, Schutyser F, Hausamne JE. Three-dimensional cephalometry. A color atlas and manual. Heidelberg Springer, Berlin 2005

27. Richardson A. A comparison of traditional and computerized methods of cephalometric analysis. Eur J Orthod 1981;3:15-20

28. Lagerros YT. Physical activity – the more we measure, the more we know how to measure. Eur J Epidemiol 2009; 24: 119-122

29. Hopkins WG. Measures of reliability in sports medicine and science. Sports Med 2000;30:1-15

30. Smeulders MJ, Van den Berg S, Odeman J, Nederveen AJ, Kreulen M, Maas M. Reliability of in vivo determination of forearm muscle volume using 3.0 T magnetic resonance imaging. J Magn Reson Imaging 2010; 31: 1252-5

31. Grunt S, Van Kampen PJ, Van der Krogt MM, Brehm MA, Doorenbosch CAM, Becher JG. Reproducibility and validity of video screen measurements of gait in children with spastic cerebral palsy. Gait Posture 2010; 31: 489-94

32. Kropmans TJ, Dijkstra PU, Stegenga B, Stewart R, de Bont LG. Smallest detectable difference in outcome variables related to painful restriction of the temporomandibular joint. J Dent Res 1999;78-784-89

33. Beckerman H, Roebroeck ME, Lankhorst GJ, Becher JG, Bezemer PD, Verbeek ALM. Smallest real difference, a link between reproducibility and responsiveness. Qual Life Res 2001;10:571-578

34. Marci V, Athanasiou AE. Sources of error in lateral cephalometry. In: Athanasiou AE. Orthodontic cephalometry. London, UK: Mosby-Wolfe: 1995: 125-140

35. Kamoen A Dermaut L, Verbeeck R. The clinical significance of error measurement in the interpretation of treatment results. Eur J Orthod 2001; 23: 569-578

36. Nagasaka S, Fujimora T, Segoshi K. Development of a non-radiographic cephalometric system. Eur J Orthod 2003;25:77-85

37. Loubele M, Jacobs R, Maes F, Denis K, White S, Coudyser W et al. Image quality vs radiation dose of four cone-beam computerized scanners. Dentomaxillofac Rad 2008; 37; 309-319

38. Hassan B, Metska ME, Ozok AR, Van der Stelt PF, Wesselink PR. Comparison of five cone beam computed tomography systems for the detection of vertical root fractures. J Endod 2010; 36: 126-129

39. Loubele M, Maes F, Schutyser F, Marchal G, Jacobs R et al. Assessment of bone segmentation quality of cone-beam CT versus multislice spiral CT: a pilot study. Oral Surg Oral Med Oral Pathol Oral Radiol Endod 2006; 102: 255-234

40. Cevidanes LHS, Styner M, Profitt WR. Three-dimensional superimposition for quantification of treatment outcomes. In: Nanda R, Kapila S. Current therapy in Orthodontics. London, UK: Mosby-Wolfe: 2010: 36-45

Chapter 3

Aspects regarding acquisition, visualization and interpretation of CBCT images

3.1 Simple technique to achieve a natural position of the head for cone beam computed tomography

Abstract

We developed a modified laser level technique to record the natural head position (NHP) in all three planes of space. This is a simple method for use with three-dimensional images and may be valuable in routine craniofacial assessment.

3.1.1 Introduction

The natural head position or NHP is stable and reproducible, and indicates the true appearance of humans.[1-4]. New cephalometric analyses rely on it, rather than on intra-cranial reference lines for diagnosis and treatment planning.[5-7]

Positioning of the head is difficult in cone beam computer tomography (CBCT), because the scanning time is relatively long (20-40s) and this requires the patient's head to be fixed to avoid movement. Because the images derived from CBCT are three-dimensional, the position of the head must be recorded in all three planes of space, as the pitch, roll and yaw of the head to accurately orientate the three-dimensional image (Fig. 1).

Figure 1 *The pitch, roll and yaw of the head must be recorded so that the three-dimensional image may be recorded accurately with the head in the natural position*
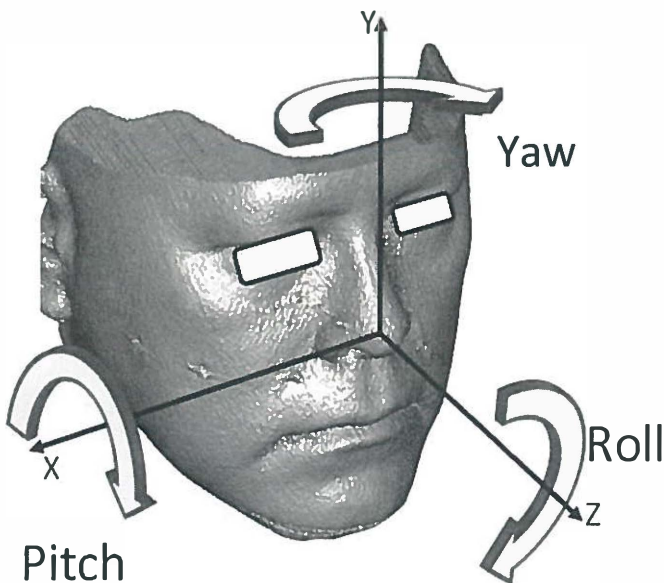
3.1.2 Technique

A standard set was made with a two levels of a laser. The patient stood on two markers on the floor, 1.5 meters in front of a wall-mounted mirror. The horizontally leveled laser was positioned on a tripod, the height of which was adjustable, next to the mirror (Fig. 2a). The vertically leveled laser was attached on a slide directly above the markers on the floor. The slide was adjustable anteriorly and posteriorly. The head was positioned using the standard technique.[1-4] The lasers were turned on and the horizontal laser was adjusted so that it was just above the lip (Fig. 2a). The vertical laser was positioned at the broadest part of the nose (Fig. 2a).

Figure 2 (a) Recording the natural head position. Soft-tissue marks are made with a washable marker on the laser lines. Two marks are made on the horizontal laser line from the lateral view (blue dots) and two are made from the frontal view (yellow dots). Two marks are made on the side of the nose on the vertical laser line (green dots). (b) Glass reference markers (painted black for illustration) are placed on the soft-tissue marks with clear tape prior to making the CBCT scan.
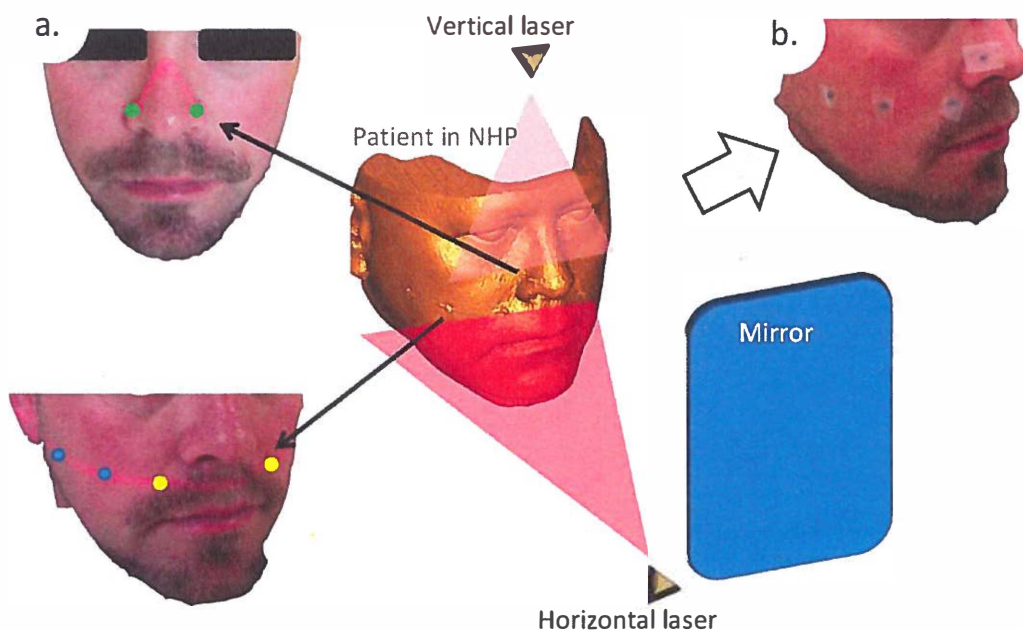
The patient was asked to relax for a minute and the process was repeated with the lasers in the correct positions. Figure 2a and b shows how the laser lines were used as reference lines to place six soft-tissue reference markers: two markers from the lateral view, two from the frontal view and two from the superior view. Glass spheres were used as reference markers because they cause less scattering compared to metal markers when rendered into three-dimensional images.[8] A CBCT scan was made of the patient and the three-dimensional image rendered with the SimPlant Ortho Pro 2.00 software (SimPlant, Leuven, Belgium) (Fig. 3a). The glass markers were used as reference marks to orientate the image in the three planes of space, by aligning the reference marks to the horizontal references lines of the screen using the "Set Natural Head Position" function of the software (Fig 3b-d).

Figure 3 (a) Rendered 3D image with soft-tissue markers. (b-d) Correcting the pitch, roll and yaw by aligning the software horizontal reference lines (red lines) with a line connecting the center of the soft-tissue markers from the lateral, frontal and superior views (blue lines). The image is orientated by grabbing the circle and rotating the image until the lines are parallel.
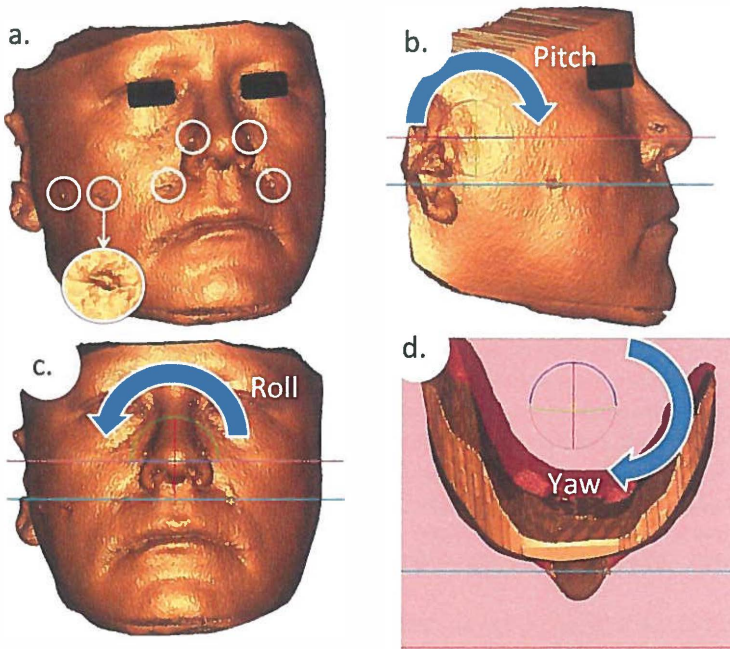
3.1.3 Discussion

With the increasing popularity of CBCT scans in orthodontics and maxillofacial surgery, three-dimensional cephalometry has become a very useful tool for craniofacial assessment and treatment planning. It is therefore necessary to develop a simple and reasonable method to record the natural position of the head in all three planes of space and orientate the three-dimensional images accordingly.

The laser level is an electronic instrument that can project a perfect leveled horizontal or vertical solid line. It is inexpensive (less than $US 50), easy to use and can be mounted on a standard tripod. Chen et al[9] described the use of laser levels to achieve NHP of traditional cephalograms. After an initial learning curve, we were able to record the natural position of the head in about 15 min. Orientating the 3D mages with the software took less than 3 min. With the focus more on improvement of the facial esthetics in orthodontics and craniofacial surgery, the method described may be of value for craniofacial assessment of 3D images.

3.1.4 References

1. Lundstrom A, Lundstrom F, Lebret LML, Moorrees CFA. Natural head position and natural head position: basic consideration in cephalometric analysis and research. Eur J Orthod 1995; 17:111-120.
2. Cooke MS, Wei SHY. The reproducibility of natural head posture: a methodological study. Am J Orthod Dentofacial Orthop 1988; 93:20-28.
3. Cooke MS. Five-year reproducibility of natural head posture: a longitudinal study. Am J Orthod Dentofacial Orthop 1990; 97:489-494.
4. Peng L, Cooke MS. Fifteen-year reproducibility of natural head posture: a longitudinal study. Am J Orthod Dentofacial Orthop 1999; 116:82-85.
5. Jacobson RL. Facial analysis in two and three dimensions. In: Jacobson A. ed. Radiographic cephalometry: From basics to videoimaging. Chicago, Ill: Quintessence; 1995:273-294.
6. Arnett GW. Diagnosing the case. In: Arnett GW, McLaughlin RP. ed. Facial and dental planning for orthodontists and oral surgeons. London, UK : Elsevier Limited; 2004: 135-197.
7. Arnett GW, Gunson MJ. Facial planning for orthodontists and oral surgeons. Am J Orthod Dentofacial Orthop 2004; 126: 290-295.
8. Damstra J, Fourie Z, Huddleston Slater JJR, Ren Y. Accuracy of linear measurements of cone beam CT derived surface models of different voxel sizes. Am J Orthod Dentofacial Orthop In press.
9. Chen C-M, Lai S, Tseng YC, Lee K-T. Simple technique to achieve a natural head position for cephalography. Br J Oral Maxillofac Surg 2008; 46: 677-678.

3.2 Accuracy of linear measurements of cone-beam computed tomography-derived surface models of different voxel sizes

Abstract

Introduction: The aims of the present study were to determine the linear accuracy of 3D surface models derived from a commercially available cone beam computer tomography (CBCT) dental imaging system and volumetric rendering software and to investigate the influence of voxel resolution on the linear accuracy of CBCT surface models. Methods: Glass spheres markers were fixed on 10 dry mandibles. The mandibles were scanned with a 0.40 and 0.25 voxel size resolution during three different sessions. Anatomical truth was established by the mean of six direct digital caliper measurements. The surface models were rendered by a volumetric rendering program and the CBCT measurements were established as the mean of three measurements. Results: The intraclass correlation coefficients (ICC) between the physical measurements and measurements of the CBCT images of 0.4 and 0.25 voxels were all more than 0.99. All CBCT measurements were accurate. There was no difference between the accuracy of the measurements between the 0.40 and 0.25 voxel size groups. The smallest detectable differences of the CBCT measurements were minimal, confirming the accuracy of the CBCT measurement procedure. Conclusion: The measurements on 3D surface models of 0.25 and 0.40 voxel size datasets made with the KaVo 3D eXam CBCT scanner and SimPlant Ortho Pro 2.00 software are very accurate when compared to the direct caliper measurements. An increased voxel resolution did not result in increased accuracy of the surface model measurements.

3.2.1 Introduction

Because of the high cost and relative high radiation exposure of helical computer tomography (CT) imaging methods, cone beam CT (CBCT) is being used more frequently for craniofacial assessment in orthodontics and oral maxillofacial surgery.[1, 2] CBCT captures the craniofacial structures with a single 360° rotation of a tube-detector unit. This is contrary to classical CT where imaging is performed in sections or layers. During the rotational scanning, a series of multiple single projections are produced and these two-dimensional images are churned by the reconstruction algorithm directly into a 3-dimensional (3D) or volumetric dataset.

Drawing an object by a computer is called rendering.[3] The object is given some characteristics to make it appear as a real world object with shadows and transparency. To draw a 3D image, the raw CT data is transformed to vector data by constructing a surface, made up of many triangles, covering the object of interest.[3] Volumetric rendering programs are used to construct the 3D surface models from imported CBCT datasets by implementing an algorithm which is in most cases unique for each program. The 3D surface model allows for actions such as indicating landmarks, performing measurements, moving bone fragments and performing virtual osteotomies. The accuracy of the derived surface models is therefore of utmost importance, not only for diagnostic purposes but also for treatment planning and outcome.

The accuracy of CBCT images have been confirmed in different CBCT scanners.[4-13] However, the accuracy of the CBCT derived surface models seem to vary.[5-8, 13] Some authors illustrated differences that, even though statistically significant it was not considered clinically relevant.[5, 6, 13] These studies used anatomical landmarks on the surface models which is subject to identification error and the segmentation process.[5, 6] It is very likely that these factors might have an influence on the accuracy of the measurement procedure. Therefore, the accuracy of the measurement procedures should be calculated in order to fully determine if a significant difference between surface models and the anatomical truth exists. To overcome the problem of landmark identification, Mischkowski et al[7] used gutta percha markers and concluded that the CBCT device provides satisfactory information about linear distances. Lagravere et al[8] used titanium markers with a hollow cone on a synthetic mandible and concluded that volumetric renderings from the CBCT device produces a 1-to-1 image-to-reality ratio.

A factor which could have a possible influence on the accuracy of the surface models is the voxel resolution. Volume is composed of voxels, which can be considered as tiny cubes arranged next to each other. Each voxel represent a value (brightness or grayscale

color) that represents the x-ray density of the corresponding structure. Reducing the voxel resolution may result in an image with reduced quality, more noise and artifacts and a loss of detailed anatomical information.[2] Spatial resolution is lower at faster scanning times and larger voxel sizes.[4] A greater spatial and voxel resolution results in generally "smoother' images by increasing the signal-to-noise ratio and reduced artifacts from metallic restorations. However, greater voxel resolution is accomplished with an increased scanning time and exposing patients to higher radiation dosages. Moreover, there is also an increased risk of patient movement with longer scanning times. Therefore, the influence of voxel resolution on the linear accuracy of CBCT rendered surface models needs further investigation since the result may be clinically relevant.

Our aims in this study were to determine the linear accuracy of CBCT-derived surface models, to investigate the influence of voxel resolution on the linear accuracy of CBCT derived surface models and to determine the accuracy of the measuring procedures.

3.2.2 Materials and Method

The sample consisted of 10 dry anonymous partially dentate adult human mandibles, selected from the collection of dry skulls at the Department of Orthodontics, University Medical Center Groningen. Mandibles with teeth containing metallic restorations were not considered due to possible scattering and artifact formation. Twelve areas were prepared in the cortical bone of the mandibles with a round surgical bur. Spherical glass markers with a diameter of 2.4mm (KGM Kugelfabrik Gebauer GmbH, Fulda, Germany) was fixed in the prepared areas with cyanoacrylate glue (Pattex, Uni-rapide Gold, Henkel, Nieuwegein, Netherlands). The spherical glass markers were used to minimize inherent differences in landmark identification and to establish fiducial anatomical locations. Twenty five linear distances, representing all three planes of space, were measured between the landmarks (Figure 1a). The midpoint of the outer most part of the sphere from the direct frontal view, opposite where it was glued to the mandible, served as the reference mark. The distances between the reference marks were determined by means of an electronic digital caliper (GAC, Bohemia, NY) on six different occasions, at least three days apart, by two observers (JD and ZF). The mean of the measurements was designated as the reference value, or anatomical truth.

To provide soft tissue equivalent attenuation a latex balloon filled with water was placed in the lingual area of the mandible.[5,6] Prior to imaging in the CBCT scanner, the

mandible was adjusted with the mandibular plane parallel to the floor and the sagittal laser reference coinciding with pogonion. The CBCT images were acquired with the KaVo 3D eXam scanner (KaVo Dental GmbH, Bismarckring, Germany). There were three scanning sessions of the mandibles, each session at least a week apart. Each mandible was scanned twice during each session: once with a 0.40 voxel resolution and once with a 0.25 voxel resolution. Ultimately, each voxel size group consisted out of 30 scanned mandibles. The pre-set parameters of the KAVO 3D eXam scanner are summarized in Table II. The CBCT data was exported from the eXamVisionQ (Imaging Sciences International LCC, Hatfield, Pennsylvania, USA) software in DICOM multi-file format and imported into SimPlant Ortho Pro 2.00 (Materialise Dental, Leuven, Belgium) software on an Acer Aspire 7730G laptop (Acer, s'Hertogenbosch, the Netherlands) with a dedicated 512mb video card (Nvidia® Geforce ® 9600M-GT, NVIDIA, Santa Clara, California, USA). All measurements were performed on the surface models on a 17-inch Acer CrystalBrite™ LCD flat panel color screen with a maximum resolution of 1440 x 900 pixels.

The 3D surface models of all of the mandibular images were generated by the pre-set threshold value for bone (250-3071 HU) as specified by the rendering software. The SimPlant Ortho Pro 2.00 software provides various views using the rotation and translation of the rendered image. The reference points were identified in on the spherical glass markers by using a cursor-driven pointer. After landmark identification, a preprogrammed analysis provided the distances to the nearest one-hundredth of a millimeter of the 25 linear measurements described in Figure 1a. The values were then exported and saved as Excel ® file format. Each of the CBCT images were rendered and measured on three different occasions by one observer (JD). The mean of the three measurements were designated as the CBCT measurement value.

Table I	Pre-set scanning parameters for a field of view of 10cm of the KaVo 3D eXam CBCT scanner			
Voxel size	**Number of projections**	**KV**	**mAs**	**Scanning time (seconds)**
0.40	236	120	18.54	8.9
0.25	400	120	37.07	26.9

Figure 1 a and *b*: 25 linear distances measured between the 12 markers. *C* and *D*: 3D rendered surface models of a mandible with glass markers used in the study. Surface models were made with 0.4 voxel *(c)* and a 0.25 voxel *(d)* sizes.
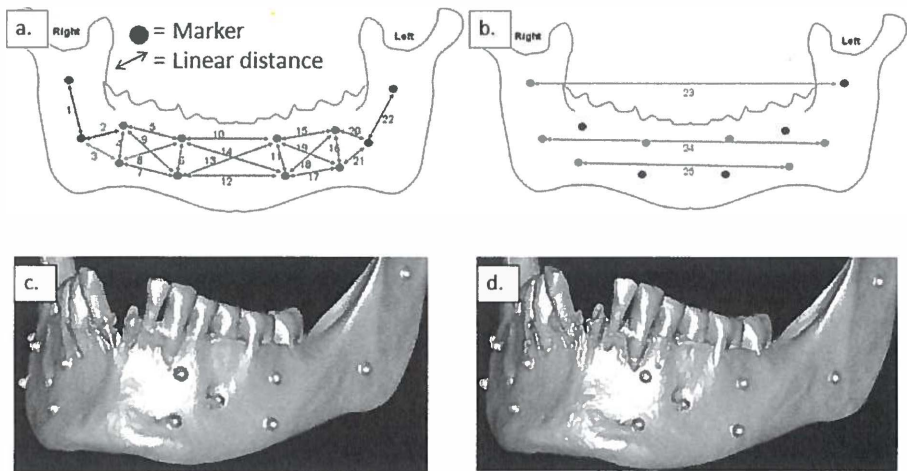
Statistical Analysis

The accuracy of the measurement was expressed by means of the absolute error (AE) and absolute percentage errors (APE). Absolute error was defined as the CBCT measurement value subtracted by the reference value.[7] Absolute percentage error was calculated by means of the following equation: APE= 100 *(AE/Reference value) .[7] Mean values and standard deviations were calculated.

As a measure of reliability, the intraclass correlation coefficient (ICC) for absolute agreement based on a 2-way random effects analysis of variance (ANOVA) was calculated between the three measurement techniques (e.g. digital caliper, 0.40 voxel size and at 0.25 voxel size) used in the study.

To determine the linear accuracy of the measurement procedures (direct caliper and CBCT measurements), the standard error of measurement (SEM) of the three consecutive CBCT sessions was calculated as the variance of the random error (interaction between the locations and the measurement session) from a 2-way random effects ANOVA. The SEM was calculated for each voxel size and for the physical

measurements. The smallest detectable difference (SDD) was then calculated as 1.96 * √2 * SEM. All statistical analysis was performed with a standard statistical software package (SPSS version 14, Chicago, IL).

3.2.3 Results

Accuracy of the measurement was determined by the AE and APE (Table II). The AE was very small for both groups: 0.01-0.15 mm (0.05 ± 0.04 mm) for the 0.4 voxel group and 0.00-0.16 mm (0.07 ±0.05 mm) for the 0.25 voxel group. The APE was 0.25 ± 0.37% and 0.33 ± 0.47% for the 0.40 and 0.25 voxel groups respectively. The ICC between the physical measurements and measurements of the CBCT images of 0.40 and 0.25 voxels were all more than 0.99.

Measurements of the CBCT images and the digital caliper showed excellent intraoperator reliability with ICC values of 1.00. The SDD calculated to determine the accuracy of the CBCT measurement procedure was 0.03 mm for the 0.40 voxel size group compared to the 0.02 mm for the 0.25 voxel size group. The SSD for the direct caliper measurements was 0.03 mm.

The mean values and the standard deviations of the reference values (the anatomical truth) and the CBCT measurements for the 0.40 and 0.25 voxel sizes are summarized in Table II. The CBCT values had a tendency to underestimate the reference values. This occurred in 61.3% of the measurements for the 0.40 voxel size group (0.06 ± 0.05 mm) and in 60% of the measurements for the 0.25 voxel size group (0.08 ± 0.06 mm). However, the measurements were overestimated for 29.3 % of the measurements for the 0.40 voxel size group (0.03 ± 0.02 mm) and in 33.3% of the measurements for the 0.25 voxel size group (0.06 ± 0.03 mm).

3.2.4 Discussion

This study was performed to establish the accuracy of the CBCT derived surface models and to investigate the possible influence of voxel resolution on the accuracy thereof. We used the KaVo 3D eXam CBCT scanner and the SimPlant Ortho Pro 2.00 software to produce the surface models. Our results showed that linear measurements made on CBCT surface renderings of 0.40 and 0.25 voxel resolutions are very accurate and confirmed the accuracy of CBCT surface models reported in previous studies. [5-8, 10] The results of this study justify the use of CBCT derived surface models for orthodontic

Measurement	Physical measurement		CBCT measurements 0.4 voxel								CBCT measurements 0.25 voxel							
			T1		T2		T3		AE		T1		T2		T3		AE	
	Mean	SD	Mean	SD	Mean	SD	Mean	SD	Mean	SD	Mean	SD	Mean	SD	Mean	SD	Mean	SD
1	26.14	5.43	26.09	5.32	26.09	5.33	26.08	5.35	0.09	0.02	26.17	5.43	26.13	5.42	26.13	5.41	0.02	0.01
2	24.52	2.96	24.45	3.02	24.43	3.00	24.42	2.97	0.05	0.05	24.44	2.92	24.39	2.85	24.44	2.88	0.10	0.03
3	23.73	2.84	23.73	2.84	23.63	2.70	23.68	2.82	0.14	0.03	23.72	2.81	23.73	2.77	23.73	2.81	0.00	0.01
4	10.27	0.94	10.15	0.93	10.10	0.96	10.13	0.93	0.06	0.04	10.07	0.96	10.07	0.96	10.07	0.99	0.20	0.00
5	27.41	2.64	27.36	2.59	27.51	2.57	27.43	2.52	0.03	0.04	27.50	2.53	27.50	2.52	27.49	2.49	0.09	0.01
6	10.65	0.64	10.63	0.66	10.58	0.71	10.65	0.71	0.05	0.01	10.62	0.68	10.63	0.71	10.57	0.67	0.04	0.03
7	28.69	2.19	28.64	2.11	28.63	2.09	28.64	2.09	0.13	0.04	28.74	2.05	28.72	2.12	28.71	2.06	0.03	0.02
8	30.61	2.31	30.45	2.13	30.46	2.10	30.52	2.15	0.01	0.01	30.56	2.10	30.51	2.11	30.52	2.09	0.08	0.03
9	29.16	2.51	29.17	2.43	29.15	2.33	29.18	2.38	0.01	0.02	29.25	2.32	29.29	2.35	29.24	2.34	0.10	0.03
10	36.51	3.94	36.55	3.86	36.51	3.84	36.51	3.82	0.01	0.00	36.50	3.85	36.50	3.87	36.47	3.89	0.02	0.02
11	11.10	0.29	11.09	0.30	11.11	0.28	11.09	0.28	0.02	0.01	11.02	0.27	11.09	0.30	11.07	0.31	0.04	0.04
12	37.85	4.06	37.88	4.14	37.86	4.10	37.84	4.16	0.08	0.01	37.73	4.18	37.72	4.10	37.72	4.15	0.13	0.01
13	39.47	3.59	39.39	3.69	39.38	3.66	39.39	3.67	0.05	0.02	39.33	3.66	39.33	3.64	39.32	3.67	0.14	0.01
14	38.04	3.73	38.08	3.69	37.99	3.71	37.97	3.73	0.07	0.03	37.93	3.75	37.94	3.69	37.90	3.74	0.12	0.02
15	28.49	2.38	28.44	2.32	28.42	2.39	28.39	2.42	0.15	0.02	28.45	2.42	28.47	2.40	28.50	2.37	0.02	0.02
16	10.12	1.38	9.98	1.34	9.99	1.36	9.95	1.31	0.06	0.02	9.94	1.36	9.96	1.36	9.97	1.36	0.16	0.02
17	29.45	2.71	29.53	2.62	29.51	2.61	29.50	2.66	0.01	0.01	29.49	2.59	29.53	2.70	29.57	2.64	0.08	0.04
18	31.88	2.43	31.88	2.33	31.86	2.35	31.86	2.37	0.03	0.02	31.88	2.37	31.95	2.40	31.94	2.36	0.04	0.04
19	29.67	2.33	29.71	2.26	29.70	2.28	29.66	2.32	0.04	0.02	29.64	2.23	29.66	2.28	29.68	2.27	0.02	0.01
20	20.67	3.88	20.64	3.90	20.61	3.89	20.65	3.90	0.01	0.01	20.64	3.87	20.56	3.86	20.56	3.87	0.08	0.05
21	22.38	4.56	22.39	4.52	22.40	4.48	22.39	4.51	0.01	0.02	22.48	4.54	22.42	4.54	22.37	4.56	0.05	0.05
22	25.57	4.72	25.60	4.69	25.57	4.73	25.58	4.71	0.04	0.02	25.59	4.77	25.56	4.78	25.60	4.75	0.02	0.01
23	94.53	2.75	94.50	2.76	94.51	2.79	94.47	2.79	0.02	0.01	94.58	2.72	94.56	2.73	94.53	2.73	0.03	0.03
24	86.49	4.88	86.52	4.82	86.50	4.85	86.50	4.88	0.04	0.04	86.56	4.82	86.52	4.80	86.49	4.82	0.03	0.04
25	72.83	3.76	72.79	3.75	72.75	3.69	72.83	3.77	0.09	0.02	72.78	3.74	72.76	3.75	72.74	3.74	0.07	0.02
Mean absolute error									0.05	0.04							0.07	0.05
Mean absolute percentage error									0.25	0.37							0.33	0.46

Table II   Mean, standard deviation (SD), absolute error (AE) and the mean absolute percentage error (APE)

T, Scanning session

and craniofacial treatment planning. There was no difference between the CBCT measurements of the 0.40 mm and 0.25 mm voxel resolution group when compared to the anatomical truth. The results of this study confirm the results of Ballrick et al[4] and suggest that the 0.4mm voxel resolution is adequate for measurement.

The increase in voxel resolution did not lead to a difference in accuracy of the surface models. Therefore, the benefits of a shorter scanning time (namely less radiation exposure and less patient movement) might outweigh the poorer resolution. However, care must be taken when interpreting this result. The diagnostic ability of CBCT images appears to be influenced by voxel size. Liedkte et al[14] investigated simulated external root resorption of tooth roots imaged with a voxel size of 0.40, 0.30 and 0.20 mm respectively. They concluded that even though the results from the different voxel sizes were the same, the diagnosis was made easier at a smaller voxel size of 0.30 or 0.20 mm. While the benefits of a shorter scanning time satisfy the ALARA (*as low as reasonably achievable*) principle, the risks of misdiagnosis and treatment complications must also be weighed. Therefore, a scanning protocol of a 0.40 mm voxel size might not be suitable for every patient and depends on the nature of their problems and treatment plan.

The mean difference between the CBCT measurements and the caliper measurements were very small: 0.05 ± 0.04mm for the 0.4 voxel group and 0.07 ± 0.05mm for the 0.25 voxel group. These values are similar to the values previously reported in the literature for differences between 3D CBCT renderings and direct caliper measurements. Stratemann et al[10] used chromium balls with a 2.4mm diameter as markers and reported very small mean differences (0.00 and 0.07mm). However, the standard deviations of the mean differences were significantly larger (0.41 and 0.22mm) compared to our results. Mischkowski et al[7] used prepared holes filled with gutta percha as markers and reported a mean absolute difference of 0.26mm. In a pilot study, we found that metal and chromium markers caused significant artifact formation when rendering the surface models due to scattering whilst the prepared gutta perch markers was not clearly visible on our surface models. These markers were therefore not considered for this study. Hassan et al[13] used anatomical landmarks which resulted a slightly larger differences of 0.10-0.39mm between the 3D renderings and caliper

measurements. The mean difference between the rendered 3D surface models and caliper measurements is less than the relevant error of 0.5mm postulated by Marmulla et al[19] and less than the voxel size of the image and can therefore not be regarded as clinically relevant for craniofacial measurements.

The results show the CBCT values had a tendency to underestimate the reference values; however it was not as severe as previously reported. The CBCT values were underestimated for 60.7% of the total measurements in this study but this is significantly less compared to the 94.4% reported by Ballrick et al[4]. Lascala et al[12] also reported smaller computer based linear measurements than direct digital caliper measurements of dry skulls. However, the CBCT measurements in these studies were made on axial, coronal, and sagittal cuts of the 3D image rather than 3D surface renderings which probably accounts for the difference of underestimation.[8]

In this study, the smallest detectable difference (SDD) was used to determine the accuracy of the measurement procedures. The SDD has been proposed as an adequate measure for quantitative and statistically significant difference between measurements.[15, 16] The SDD is expressed in the same unity as the measurement device used and is generalizable to all facets included (observers, techniques, measurement times, repeated measures). The SDD for the CBCT measurements was very small; 0.03mm for the 0.40 voxel size group and 0.02mm for the 0.25 voxel size group. The small SDD confirmed the accuracy of the measurement procedure used in this study. The SDD values indicate that the measurement procedure for the surface models was just as accurate as the direct caliper measurement procedure. For a statistically significant difference between two separate observations, the difference must be at least the SDD of the measurement procedure. If this is not the case, and the SSD is larger than the reported difference, the difference could be result of inaccuracies of the measurement procedure rather than the true difference between the observations. In this study, the CBCT measurement procedure has the power to detect differences of 0.03mm. If the measurement procedure is less accurate (i.e. influenced by the segmentation process and landmark identification error), the SDD will be larger. A large SDD could have a significant effect on the interpretation of the differences between two observations, especially when the reported differences are small.

The accuracy of the CBCT measurement procedure is due to the fact that the landmark identification error was reduced by using opaque glass spheres as fiducial markers. Additionally, the spherical glass markers are likely to be less affected by the segmentation process due to the uniform density of the markers. The glass spheres used in this study were produced from soda-lime-silica-glass, the most prevalent type of glass which is commonly used for windows or glass containers (bottles and jars).The main advantage of glass versus metallic markers is that glass markers produce no scattering and artifacts when rendered to surface models (Figure 1c and d). This is due to the fact that bone and glass spheres have similar values on the Hounsfield unit scale.[18, 19]

The present study showed the technical limits of the CBCT scanner and rendering software but may not directly apply to patient care. The mandibles used in this study do not move and have fiducial markers for measurement which is not the case with patients. In the present study a latex balloon filled with water was placed in the lingual area of the dry mandible to simulate soft-tissue attenuation, a method also used by Brown et al[5] and Periago et al[6]. An alternative method used to simulate soft tissue attenuation is a water bath,[8, 10, 13] which might be problematic during positioning in the CBCT scanner and might damage the dry skulls. In addition, absorption of water by the dry mandibles can influence measurement accuracy due to expansion of the bone. It must also be kept in mind that neither the balloon filled with water nor the water bath method equates in either quantity or distribution to the soft tissue seen in patients. While the water filled balloon in the lingual provided some degree of soft tissue attenuation, the lack of peripheral attenuation material may have allowed for increased contrast of the landmarks.

3.2.5 Conclusion

Linear measurements on 3D surface models of 0.25 and 0.40 voxel size CBCT datasets made with the KaVo 3D eXam CBCT scanner and the SimPlant Ortho 2.00 software are very accurate when compared to direct caliper measurements. Increasing the voxel resolution from 0.4mm to 0.25mm to construct a 3D surface model did not result in an increased accuracy of the CBCT measurements.

We thank Dr. J Van der Meer of the Department of Orthodontics of the UMCG for his technical input and advice during this research project.

3.2.6 References

1. Harrell WE, Jacobson RL, Hatcher DC, Mah J. Cephalometric Imaging in 3-D. In: Jacobson A, Jacobson RL eds. Radiographic Cephalometry: From Basics to 3-D Imaging. 2nd ed. Hanover Park, IL: Quintessence: 2006: 233-248.
2. Schutyser F, van Cleynenbreugel J. From 3-D Volumetric Computer Tomography to 3-D Cephalometry. In: Swennen GRJ, Schutyser F, Hausamen J-E eds. Three-Dimensional Cephalometry: A Color Atlas and Manual. Heidelberg, Germany: Springer-Verlag: 2006: 2-11.
3. Halazonetis DJ. From 2-dimensional cephalograms to 3-dimensional computed tomography scans. Am J Orthod Dentofacial Orthop 2005; 127: 627-637.
4. Ballrick JW, Palomo JM, Ruch E, Amberman BD, Hans MG. Image distortion and spatial resolution of a commercially available cone-beam computed tomography machine. Am J Orthod Dentofacial Orthop 2008; 134: 573-582.
5. Brown AA, Scarfe WC, Scheetz JP, Silveira AM, Farman AG. Linear accuracy of cone beat CT 3D images. Angle Orthod 2009; 79: 150-157.
6. Periago DR, Scarfe WC, Moshiri M, Scheetz JP, Silveira AM, Farman AG. Linear accuracy and reliability of cone beam CT derived 3-dimensional images using an orthodontic volumetric rendering program. Angle Orthod 2008; 78: 387-395.
7. Mischkowski RA, Pulsfort R, Ritter L, Neugebauer J, Brochhagen HG, Keeve E, Zoller JE. Geometric accuracy of a newly developed cone-beam device for maxillofacial imaging. Oral Surg Oral Med Oral Pathol Oral Radiol Endod 2007; 104: 551-559.
8. Lagravere MO, Carey J, Toogood RW, Major PW. Three-dimensional accuracy of measurements made with software on cone-beam computed tomography images. Am J Orthod Dentofacial Orthop 2008; 134:112-116.
9. Pinsky HM, Dyda S, Pinsky RW, Misch KA, Sarment DP. Accuracy of three-dimensional measurements using cone-beam CT. Dentomaxillofac Radiol 2006; 35: 410-416.
10. Stratemann SA, Huang JC, Maki K, Miller AJ, Hatcher DC. Comparison of cone beam computed tomography imaging with physical measures. Dentomaxillofac Radiol 2008; 37: 80-93.
11. Eggers G, Klein J, Welzel T, Muhling J. Geometric accuracy of digital volume tomography and conventional computed tomography. Br J Oral Maxillofac Surg 2008;
12. Lascala CA, Panella J, Marques MM. Analysis of the accuracy of linear measurements obtained by cone beam computed tomography (CBCT-NewTom). Dentomaxillofac Radiol. 2004; 33: 291-294.
13. Hassan B, van der Stelt P, Sanderink G. Accuracy of three-dimensional measurements obtained from cone beam computed tomography surface-rendered images for cephalometric analysis: influence of patient scanning position. Eur J Orthod 2008; Advance Access, In Press

14. Liedke GS, Dias da Silviera HE, Dias da Silviera HL, Duntra V, Poli de Figueiredo A. Influence of voxel size in the diagnostic ability of cone beam tomography to evaluate simulated external root resorption. J Endod 2009, 35: 233-235.
15. Marmulla R, Wortche R, Muhling J, Hassfeld S. Geometric accuracy of the NewTom 9000 Cone Beam CT. Dentomaxillofac Radiol 2005;34:28-31
16. Kropmans THJB, Dijkstra PU, Stegenga B, Stewart R, De Bont LGM. Smallest detectable difference in outcome variables related to painful restriction of the temporomandibular joint. J Dent Res 1999; 78: 784-789.
17. Kropmans THJB, Dijkstra PU, Stegenga B, Stewart R, De Bont LGM. Smallest detectable difference of maximal mouth opening in patients with painfully restricted temporomandibular joint function. Eur J Oral Sci 2000; 108: 9-13.
18. Enomoto K, Nishimura H, Inohara H, Murata J, Horii A, Doi K, Kubo T. A rare case of a glass foreign body in the parapharyngeal space: pre-operative assessment by contrast-enhanced CT and three dimensional CT images. Dentomaxillofac Radiol 2009; 38: 112-115.
19. Gor DM, Kirch CF, Leen J, Turbin R, Von Hagen S. Radiologic differentiation of intraocular glass: Evaluation of imaging techniques, glass types, size and effect on intraocular hemorrhage. AJR 2001; 177: 1199-1203.

3.3 Comparison between two-dimensional and midsagittal three-dimensional cephalometric measurements of dry human skulls

Abstract

The aim of this study was to compare two-dimensional and three-dimensional cephalometric values by using a three-dimensional analysis based on the midsagittal plane. Spherical metal markers were fixed on the anatomical landmarks of 10 human skulls, which were examined radiographically with conventional lateral cephalograms and with cone-beam computed tomography scans (CBCT) scans. Preprogrammed analyses determined the 18 angular and linear two-dimensional and three-dimensional cephalometric values. An error study was made to determine the accuracy and reliability of the methods used. Both sets of values were compared by means of the Wilcoxon signed-rank tests. Probabilities of less than 0.05 were accepted as significant. Reliability of the measurements was determined by means if intraclass correlation coefficients (ICC) based on absolute agreement. The method error (ME) was tiny (average ME < 0.61 measuring unit) and reliable (ICC > 0.97). Comparison of the two- and three-dimensional measurements showed that they were reliable (ICC > 0.88) and that there were no significant differences (P = 0.41 − 1.00). The values from two-dimensional and three-dimensional cephalometric analysis are comparable and interchangeable when using the midsagittal three-dimensional approach described in this study.

3.3.1 Introduction

As three-dimensional cone beam computed tomography (CBCT) is becoming more popular in orthodontics and maxillofacial surgery, the next step is three-dimensional cephalometry on three-dimensional images. Therefore, it is important to know whether two-dimensional cephalometry is comparable with three-dimensional cephalometry.[1,2] However, direct comparison is difficult because classic cephalometry is a two-dimensional representation of three-dimensional structures and is subjected to systemic errors (e.g. magnification error and projection error).[3] To our knowledge, a few studies have compared two-dimensional and three-dimensional cephalometry and the results of these studies were inconsistant.[2, 4, 5] Nalçaci et al.[4] compared them and found no significant differences except for the angular measurements of the upper incisors. Bholsithi et al.[5] found only the three-dimensional measurements in the midline to be comparable with two-dimensional ones. In contrast, Van Vlijmen et al.[2] found significant differences between almost all groups of measurements. Although they found the differences to be clinically unimportant, they concluded that three-dimensional cephalometry are not suitable for longitudinal research when there are only two-dimensional records from the past.

Alternatively, lateral cephalograms can be derived from three-dimensional CBCT images and the resulting measurements are comparable with traditional cephalograms and suitable for longitudinal research.[6-8] Unfortunately, it is time consuming to derive a lateral cephalogram from CBCT; it requires extra steps and could be costly because it often requires additional software to analyze the derived cephalogram. More importantly, the three-dimensional characteristics are lost when a cephalogram is derived from the CBCT images because a derived cephalogram remains a two-dimensional representation of a three-dimensional structure.

To overcome the difficulties of comparing two-dimensional and direct three-dimensional measurements we use a three-dimensional cephalometric analysis based on the midsagittal plane of the skull. In our three-dimensional analysis the position of the bilateral structures of gonion (Go), porion (Po), condylion (Co) and orbital (Or) are indicated by a point on the midsagittal plane where it coincides with a line joining the left and right anatomical points of these structures (Fig. 1 and Table I). The resulting measurements are therefore based on lines in the midsagittal plane (Fig. 1). The aim of this study was to compare two-dimensional and three-dimensional cephalometric values by using our midsagittal three-dimensional approach. We hypothesised that

there will be no difference between two-dimensional and midsagittal three-dimensional cephalometric values.

Figure 1 *Gonion, porion, condylion and orbital are indicated by a point (white dot) on the midsagittal plane (pink) where it intersects with a line (black) joining the left and right anatomical points of the structures. The three-dimensional (3D) analysis is based on the lines (red) in the midsagittal plane (the 3D surface model was removed so that it can be seen better)*
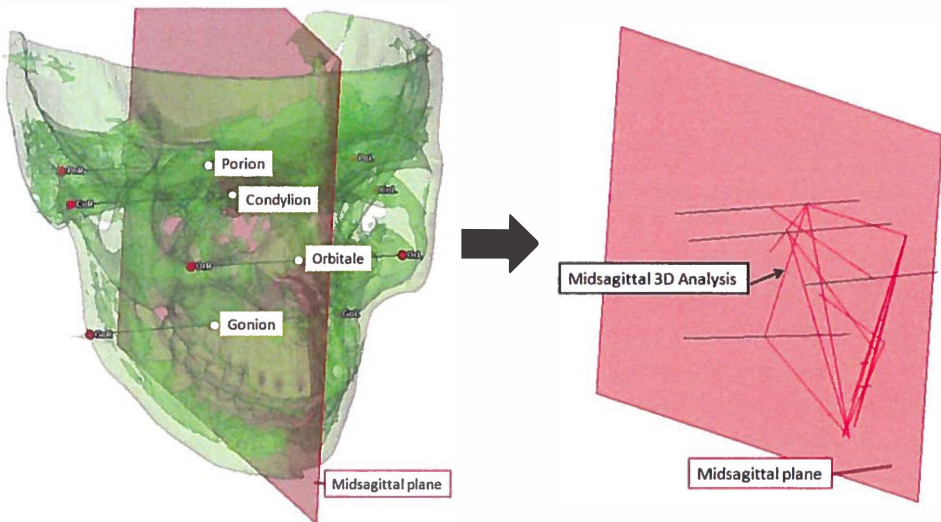
3.3.2 Materials and Methods

The sample consisted of 10 human skulls obtained from the collection of the Department of Orthodontics. The skulls were selected from a larger sample according to the following criteria: presence of maxillary and mandibular incisors, presence of a stable occlusion, no visible asymmetries and the roof of the skull had to be removable to allow for visualization of the sella turcica. The mandible was related to the skull with the teeth in maximal occlusal interdigitation and the condyle in the fossa by means of two metal springs. To eliminate errors in the identification of landmarks, spherical metal

markers 1.5mm in diameter were glued onto the selected landmarks (Table I) with cyanoacrylate glue (Pattex, Uni-rapide Gold, Henkel, Nieuwegein, Netherlands). It was impossible to fix a metal marker in the center of the sella turcica, so the metal marker representing sella was placed in the center of the floor of the sella turcica.

Table I		The two-dimensional (2D) and three –dimensional (3D) landmarks used
Landmarks and abbreviation		**Description**
Sella	S	Centre of sella turcica
Nasion	N	Most anterior limit of the frontonasal suture in the facial midline
A -point	A	Deepest bony point on the contour of the premaxilla below ANS
B -point	B	Deepest bony point on the contour of the mandibula above pogonion
Anterior nasal spine	ANS	Tip of the anterior nasal spine
Posterior nasal spine	PNS	The most posterior point on the bony hard palate
Pogonion	Pog	The most anterior part of the symphysis of the mandible
Gnathion	Gn	The most anterior inferior part of the bony chin
Menton	Me	The most inferior point of the bony chin
Gonion right (3D)	Go_R	The most posterior inferior point of the right angle of the mandible
Gonion left (3D)	Go_L	The most posterior inferior point of the left angle of the mandible
Gonion	Go	2D : The most posterior inferior point of the angle of the mandible in
		3D : The point on a line connecting left and right gonion where it intersects the midsagittal plane
Porion left (3D)	Po_L	The most superior point of the left external auditory meatus
Porion right (3D)	Po_R	The most superior point of the right external auditory meatus
Porion	Po	2D : The most superior point of the external auditory meatus
		3D : The point on a line connecting left and right porion where it intersects the midsagittal plane
Orbital left (3D)	Or_L	The lowest point of the inferior margin of the left orbit
Orbitale right (3D)	Or_R	The lowest point of the inferior margin of the right orbit
Orbitale	Or	2D : The lowest point of the inferior margin of the orbit
		3D : The point on a line connecting left and right orbitale where it intersects the midsagittal plane
Condylion left (3D)	Co_L	The most superior midpoint of the left head of the condyle
Condylion right (3D)	Co_R	The most superior midpoint of the right head of the condyle
Condylion	Co	2D : The most superior point of the head of the condyle
		3D : The point on a line connecting left and right condylion where it intersects the midsagittal plane
Incision superius	Is	2D : The incisal tip of the most prominent upper incisor
		3D : A point where a perpendicular from the most incisal tip of the most prominent upper incisor intersects with the midsagittal plane
Incision inferius	Ii	2D : The incisal tip of the most prominent lower incisor
		3D : A point where a perpendicular from the most incisal tip of the most prominent lower incisor intersects with the midsagittal plane
Basion	Ba	Median point of the anterior margin of the foramen magnum

Table II	The planes, lines and measurements used (3D = 3-dimensional)
Planes and lines	**Description**
Midsagittal plane (3D)	A vertical plane through points S, N perpendicular to the Frankfort horizontal plane
SN	A line between S and N
FH line / plane (Frankfort horizontal)	A line connecting Po and Or (2D) / a plane passing through the bilateral points of Or and Po (3D)
PL (Palatal line)	A line connecting ANS and PNS
ML (Mandibular line)	A line connecting Gn and Go
NA	A line connecting A-point and N
NB	A line connecting B-point and N
APo	A line connecting A-point and pogonion
Measurements	**Description**
Sagittal	
1. SNA	Angle between S, N and A
2. SNB	Angle between S, N and B
3. ANB	Angle between A, N and B
4. Co-A	Distance between condylion and A-point representing the maxillary length
5. Co-Gn	Distance between condylion and gnathion representing the mandibular length
Vertical	
6. ANS-Me	Distance between ANS and Me representing the anterior lower facial height
7. SN-FH	Angle between lines SN and FH
8. SN-PL	Angle between SN and the palatal line
9. SN-ML	Angle between SN and the mandibular line
10. PL-ML	Angle between the palatal line and the mandibular line
11. AFH	Distance between N and Me representing the anterior facial height
12. PFH	Distance between S and Go representing the posterior facial height
13. PFH:AFH	The ratio of the PFH to the AFH
14. Y-Axis	Angle between N, S and Gn
Dental	
15. Is-NA	Distance from Is to the NA line
16. Ii-NB	Distance from Ii to the NB line
17. Ii-APo	Distance from Ii to the line connecting A-point and pogonion
Cranial base	
18. Ba-S-N	Angle between Ba, S and N

Radiographic examination consisted of conventional lateral cephalograms and CBCT scans. The lateral cephalograms were made (ProMax, DiMax2 Digital Cephalometric Unit, Planmeca, Helsinki, Finland) with a resolution quality of 2272 x 2045 pixels 24-bits depth. Each skull was placed with the midline laser-beam of the cephalostat passing through nasion (N) and the anterior nasal spine (ANS).

The ear rods were used to orientate the skull but were carefully removed prior to radiographing the skull. This was done to allow for visualization of anatomical porion markers. The lateral cephalograms were individually imported into the Viewbox® Version 3.1.1.13 (Halazonetis, Athens, Greece) software. The magnification error was corrected and the centers of the metal markers were identified by a cursor-driven

mouse. In two-dimensional cephalometry, the midpoint between bilateral structures is used for analysis,[3] so when both of the markers of bilateral structures were visible the midpoint on a line connecting these two markers indicated the anatomical position of the landmark (Fig. 1)

The CBCT images were acquired with the KaVo 3D eXam scanner (KaVo Dental GmbH, Bismarckring, Germany). The laser-beam of the CBCT scanner was used to position the skull with light passing through N and ANS. The skulls were scanned at a 0.40 voxel size resolution (120KV, 18.57mAs and 8.9s). The CBCT datasets were exported from the eXamVisionQ (Imaging Sciences International LCC, Hatfield, Pennsylvania, USA) software in DICOM multi-file format and imported into SimPlant Ortho Pro 2.00 (Materialise Dental, Leuven, Belgium) software. The centers of the metal markers were identified by a cursor-driven mouse in the axial, coronal and sagittal slices because of scattering in the three-dimensional reconstruction. Importantly, lines were constructed between bilateral points (e.g. left and right gonion) and the intersection of these lines with the midsagittal plane was regarded as the representative point of the respective anatomical position (Table I and Fig. 1). Preprogrammed analyses in the two-dimensional and three-dimensional software calculated the measurements (Table II) for each lateral cephalogram and CBCT scan.

We made an error study whereby the method was repeated and the 10 skulls were captured radiographically for a second time. The measurements were repeated on the second radiographs and the two-dimensional and three-dimensional method errors were determined by means of Dahlberg's formula.[9] The intraclass correlation coefficient (ICC) for absolute agreement was calculated to determine the reliability of the methods. Mean values for both groups were determined by the average of the measurements from the first and second radiograph or CBCT scan.

Wilcoxon signed-rank sum test was used to help in the calculation of the significance of differences between the two- and three-dimensional measurements. Probabilities of less than 0.05 were considered to be significant. The ICC for absolute agreement was calculated to determine the reliability of the three-dimensional, compared to the two-dimensional, measurements. The mean differences between the two sets of measurements were also calculated to determine clinical relevance. All statistical analyses were made with the help of the Statistical Package for the Social Sciences (SPSS Inc., version 16, Chicago, IL).

3.3.3 Results

The results of the error study are illustrated in Table III and results of the comparison between the two-dimensional and three-dimensional measurements are illustrated in Table IV. Because of the standardized organization, and the use of metal markers, the method error for the two-dimensional and three-dimensional methods proved to be both small and reliable, the mean method errors for the two- and three-dimensional techniques being 0.61 and 0.52 mm or degrees respectively. The ICC (0.97 -1.00) confirmed the excellent reliability of the two-dimensional and three-dimensional methods. Wilcoxon signed-rank sum test confirmed that there were no significant differences (P = 0.41 – 1.00) between the two types of measurement (Table 3). Except for Is-NA (mean 1.13 mm), the average clinical differences were less than one measuring unit which is clinically acceptable. The reliability of all the three-dimensional measurements compared with that of the two-dimensional ones was excellent (ICCs; 0.88 – 1.00).

Table III	The results of the error study. The reliability (ICCs) and the method error (ME)				
Measurement	**Unit**	**2D group**		**3D group**	
		ICC	ME	ICC	ME
Sagittal					
1. SNA	degree	1.00	0.63	1.00	0.82
2. SNB	degree	1.00	0.63	1.00	0.54
3. ANB	degree	1.00	0.27	1.00	0.56
4. Co-A	mm	1.00	0.94	1.00	0.31
5. Co-Gn	mm	1.00	0.72	1.00	0.41
Vertical					
6. ANS-Me	mm	1.00	0.49	1.00	0.07
7. SN-FH	degree	0.97	0.94	0.99	0.49
8. SN-PL	degree	0.99	0.65	0.99	0.64
9. SN-ML	degree	1.00	0.65	1.00	0.66
10. PL-ML	degree	1.00	0.45	1.00	0.74
11. AFH	mm	1.00	0.69	1.00	0.62
12. PFH	mm	1.00	0.58	1.00	0.62
13. PFH:AFH	ratio (%)	0.99	0.63	1.00	0.00
14. Y-Axis	degree	1.00	0.40	1.00	0.56
Dental					
15. Is-NA	mm	1.00	0.54	0.99	0.68
16. Ii-NB	mm	1.00	0.65	1.00	0.52
17. Ii-APo	mm	1.00	0.49	1.00	0.36
Cranial base					
18. Ba-S-N	degree	1.00	0.63	1.00	0.69

Table IV	Mean values, standard deviation (SD), average differences with confidence intervals (CI) at 95%, reliability (ICC) and comparison of the 2D and 3D cephalometric measurements								
Measurement	Unit	2D group		3D group		Differences		2D vs. 3D	
		Mean	SD	Mean	SD	2D – 3D	95% CI	ICC	P
Sagittal									
1. SNA	degree	81.58	5.40	81.78	5.01	0.48	0.18 - 0.78	0.99	0.82
2. SNB	degree	75.12	3.92	75.30	3.86	0.25	0.10 - 0.41	1.00	0.71
3. ANB	degree	6.45	4.15	6.46	4.09	0.26	0.10 - 0.42	1.00	0.85
4. Co-A	mm	76.77	5.59	76.40	5.48	0.41	0.16 - 0.67	1.00	0.71
5. Co-Gn	mm	97.19	8.49	97.03	8.39	0.41	0.16 - 0.67	1.00	0.76
Vertical									
6. ANS-Me	mm	61.48	7.71	61.21	7.97	0.52	0.20 - 0.84	1.00	0.76
7. SN-FH	degree	12.24	1.53	12.33	1.62	0.20	0.08 - 0.33	0.99	1.00
8. SN-PL	degree	9.04	3.12	9.79	3.00	0.80	0.30 - 1.29	0.94	0.41
9. SN-ML	degree	35.98	5.11	36.16	5.45	0.61	0.23 - 0.99	0.99	1.00
10. PL-ML	degree	26.95	7.36	27.36	7.89	0.82	0.31 - 1.33	0.99	0.94
11. AFH	mm	106.34	9.44	106.59	9.79	0.48	0.18 - 0.78	1.00	0.91
12. PFH	mm	63.64	7.10	64.15	7.45	0.68	0.26 - 1.10	1.00	0.76
13. PFH:AFH	ratio	59.76	2.96	60.10	3.21	0.51	0.19 - 0.83	0.98	0.71
14. Y-Axis	degree	69.48	3.57	69.66	3.64	0.28	0.11 - 0.45	1.00	0.79
Dental									
15. Is-NA	mm	3.67	2.46	4.38	2.85	1.13	0.43 - 1.83	0.88	0.55
16. Ii-NB	mm	7.45	3.99	7.19	3.79	0.80	0.30 - 1.29	0.97	0.94
17. Ii-APo	mm	4.38	2.22	4.66	2.55	0.72	0.28 - 1.17	0.94	0.88
Cranial base									
18. Ba-S-N	degree	136.21	6.70	135.40	6.81	0.89	0.34 - 1.44	0.99	0.65

3.3.4 Discussion

We compared two-dimensional cephalometric values with midsagittal three-dimensional cephalometric values derived from a three-dimensional analysis on the three-dimensional images of CBCT scans. We used dry skulls with metallic markers to eliminate possible landmark identification error. The method of the present study was reliable, and the method error was small, which was necessary to detect true differences. Dry skulls were used because it would be unethical to expose patients to additional radiation of a CBCT scan after a lateral cephalogram has been made.

The three-dimensional analysis was modified so that the measurements were based on lines in the midsagittal plane. The comparison showed that with this approach the resulting values from the analysis were reliable, and comparable with those from two-dimensional cephalometry. Our findings are in agreement with Bholsithi et al.[5] but in contrast to the results of Van Vlijmen et al.[2]. It must be kept in mind, however, that they used a three-dimensional approach based on planes that could cause differences in

measurements as a result of orientation differences. By using the three-dimensional analysis described in this study, the values from direct three-dimensional cephalometry are interchangeable with two-dimensional cephalometry, and can be used for comparison with longitudinal research. This is clinically important, because although CBCT has become popular, it is unlikely that three-dimensional reference values will become available from growth studies as they have for two-dimensional cephalometry. The radiation dose of CBCT is still appreciably higher than that of conventional cephalometric radiographs, and ethical reasons prohibit longitudinal studies using CBCT. Another clinical advantage of our approach is that the presentation of the three-dimensional measurements is very similar to conventional two-dimensional measurements that are routinely used by orthodontists and maxillofacial surgeons, so a steep learning curve is not needed to enable an orthodontist or maxillofacial surgeon to make a diagnosis from the three-dimensional measurements.

The cephalometric measurements compared in this study allow for diagnosis of anteroposterior and vertical problems, and do not allow for diagnosis in the transverse plane. However, the analysis is made on three-dimensional images and therefore the characteristics are not lost, as with a derived cephalogram. In a three-dimensional analysis the actual anatomical structures can be identified rather than their two-dimensional projections, as with derived cephalograms. In addition, our approach does not require extra steps or additional software as the analysis is made directly in the three-dimensional software. It is not recommended for use in patients with asymmetric features because measurements will deviate from the midsagittal plane and could therefore differ from two-dimensional measurements.[5] To establish the midsagittal plane in asymmetric cases is problematic; where the midface is affected, a midsagittal plane constructed using the landmark ANS or the Frankfurt horizontal plane would be inaccurate. A possible solution for this problem might be to establish the midsagittal plane according to the method described by Hajeer et al.[10] They created an "individual symmetrical configuration" by calculating the mean of the original and the mirrored version of the configuration after alignment. The symmetrical configuration indicated the midline and was superimposed over the original configuration to determine the magnitude of the asymmetry. However, it must be kept in mind that CBCT images are useful for the detection of craniofacial asymmetry, which can be calculated as the measurement of the left side subtracted by that of the right side.[11, 12] A result of zero indicates perfect asymmetry, and a negative or positive result indicates a larger measurement on the right or left side.

3.3.5 References

1. Cevidanes LHS, Styner MA, Profitt WR. Image analysis and superimposition of 3-dimensional cone-beam computed tomography models. Am J Orthod Dentofacial Orthop 2006; 129: 611-18.
2. Van Vlijmen OJC, Maal T, Berge J, Bronkhorst EM, Katsaros C, Kuipers-Jagtman AM. A comparison between two-dimensional and three-dimensional cephalometry on CBCT scans of human skulls. Int J Oral Maxillofac Surg 2009, doi:10.1016/j.ijoms.2009.11.017.
3. Marci V, Athanasiou AE. Sources of error in lateral cephalometry. In: Athanasiou AE. Orthodontic cephalometry. London, UK: Mosby-Wolfe; 1995: 125-40.
4. Nalçaci R, Öztürk F, Sökücü O. A comparison of two-dimension al radiography and three-dimensional computed tomography in angular cephalometric measurements. Dentomaxillofacial Radiology 2010; 39: 100-6.
5. Bholsithi W, Tharanon W, Chintakanon K, Komolpis R, Sinthanayothin C. three-dimensional vs. two-dimensional cephalometric analysis with repeated measurements from 20 Thai males and 20 Thai females. Biomed Imaging Interventional J 2009, 5, e21.
6. Van Vlijmen OJC, Berge J, Swennen GR, Bronkhorst EM, Katsaros C, Kuipers-Jagtman AM. Comparison of cephalometric radiographs obtained from cone-beam computed tomography scans and conventional radiographs. J Oral Maxillofac Surg 2009; 67: 92-7
7. Kumar V, Ludlow JB, Cevidanes LHS. Comparison of conventional and cone beam CT synthesized cephalograms. Dentomaxillofacial Radiology 2007; 36: 263-9.
8. Kumar V, Ludlow JB, Cevidanes LHS, Mol A. In vivo comparison of conventional and cone beam CT synthesized cephalograms. Angle Orthod 2008; 78: 873-79.
9. Houston WJ. The analysis of errors in orthodontic measurements. Am J Orthod 1983; 83: 382-90
10. Hajeer MY, Ayoub AF, Millet DT. Three-dimensional assessment of facial soft-tissue asymmetry before and after orthognathic surgery. Br J Oral Maxillofac Surg 2004; 42: 396-404.
11. Hwang H-S, Hwang CH, Lee K-H, Kang B-C. Maxillofacial 3-dimensional analysis for the diagnosis of facial asymmetry. Am J Orthod Dentofacial Orthop 2006; 130: 779-785.
12. Baek S-K, Cho I-S, Chang Y-I, Kim M-J. Skeletodental factors affecting chin point deviation in female patients with class III malocclusion and facial asymmetry: a three dimensional analysis using computed tomography. Oral Surg Oral Med Oral Pathol Oral Radiol Endod 2007; 104: 628-39.

Chapter 4

Application of CBCT in craniofacial asymmetry

4.1 Evaluation and comparison of postero-anterior cephalograms and cone-beam computed tomography images for the detection of mandibular asymmetry

Abstract

The aim of this study was to evaluate and compare postero-anterior (PA) cephalograms and cone-beam computed tomography (CBCT) images for the detection of mandibular asymmetry. Six asymmetric anonymous dry human skulls with visible chin deviation were available for this study. Metallic markers were glued on the anatomical landmarks to avoid identification error. PA cephalograms and CBCT scans were made by means of a standardized set-up. Each scan and cephalogram was measured three times by a single observer and the means used for analysis. Asymmetry was defined by the subtraction of the left side and right side measurements. CBCT was reliable [intraclass reliability coefficient (ICC > 0.957)] and very accurate (within 0.5mm) in detection of all asymmetry. PA cephalograms were not accurate in detection of asymmetry of the mandibular ramus length, the mandibular body length and the total mandibular length. PA cephalograms were the least reliable in determining the mandibular body length asymmetry (ICC = 0.686). The use of CBCT to detect mandibular asymmetry was validated with this study. CBCT images are very reliable and accurate for the detection of asymmetry and should be considered over conventional PA cephalometry when a chin deviation is present.

4.1.1 Introduction

Radiographic investigation is essential when a visible chin deviation is diagnosed which requires surgery to correct the mandibular asymmetry. The aims of the radiographic examination are to correctly diagnose the cause of the resulting asymmetry and chin deviation, and to enable accurate pre-surgical planning. Currently, two imaging modalities e.g., PA cephalograms and CBCT imaging can be utilized to determine the cause of chin deviation, plan the surgical correction, and to determine outcome assessment after orthognathic surgery. (Reyneke, 2003; Ghafari, 2006; Hwang et al., 2006; Ko et al., 2009; Kokich, 2010).

Since the introduction of conventional postero-anterior (PA) cephalogram in the 1930's, the PA cephalogram has been used in orthodontic and orthognathic diagnosis and surgery planning for the treatment of asymmetry (Bishara et al., 1994; Athanasiou and Van der Meij, 1995; Reyneke, 2003; Ghafari, 2006). The PA cephalogram provides valuable mediolateral information which is not only useful for facial asymmetric evaluation but is essential for transverse evaluation of the craniofacial skeleton and dentoalveolar structures (Ghafari, 2006). Therefore, PA cephalometric projections and relevant analyses constitute an important adjunct for qualitative and quantitative evaluation of the dentofacial region. However, the PA cephalogram is a projection of a three-dimensional (3-D) object onto a two-dimensional (2-D) surface and is therefore subject to distortion and projection error. This differences between actual linear measurements and measurements derived from the PA cephalograms have been well documented in the literature (Athanasiou and Van der Meij, 1995; Pirttiniemi et al., 1996; Athanasiou et al., 1999; Yoon et al., 2002; Ghafari, 2006; Van Vlijmen et al., 2009a and b). Furthermore, the PA cephalogram can be used to compare the right and left structures since they are located at relatively equal distances from the film and x-ray source (Bishara et al., 1994). As a result the effects of unequal enlargement by diverging rays are minimized and distortion is reduced. This principle allows for valid comparison between two sides of the face in order to evaluate asymmetry (Bishara et al., 1994).

Due to the significant reduction in radiation, CBCT imaging has largely replaced spiral CT in dentistry and has made 3-D imaging routinely accessible to the orthodontist office (Halazonetis, 2005). CBCT has been shown to produce very accurate 3-D images of the craniofacial region and produces a 1-to-1 image-to-reality ratio which is necessary for accurate detection of the underlying deformities (Hassan et al., 2008; Lagravere et al., 2008; Brown et al., 2009; Damstra et al., 2010a). In addition, the advantages of CBCT

imaging for the evaluation of asymmetry is suggested in the literature (Hwang et al., 2006; Kokich, 2010)

However, it is important to realize that despite the radiation reduction of CBCT compared to spiral CT, CBCT still exposes the patient to more radiation compared to a PA cephalogram (Harrell et al., 2006; SEDENTEXCT, 2009). CBCT imaging is generally also more costly than conventional radiographs. Since the long-term effects of CBCT imaging are unknown, there is a need for evidence-based selection criteria for CBCT imaging to guarantee responsible use of the modality (Farman and Scarfe, 2006; EADMFR, 2008; SEDENTEXCT, 2009). Therefore, since comparison of the left and right sides of the PA cephalogram might be accurate in evaluating asymmetry (Bishara et al., 1994), the added benefits of the 3-D images in evaluating mandibular asymmetry should be carefully weighed against the higher radiation dose before CBCT imaging can be justified. We could not find any studies comparing the accuracy of CBCT images and PA cephalograms for the detection of mandibular asymmetry. Therefore, the aim of this study was to evaluate and compare PA cephalograms and CBCT images for the detection of mandibular asymmetry by comparison of left and right side structures.

4.1.2 Materials and Methods

The sample was selected from the collection of anonymous dry skulls from the Department of Orthodontics of the University Medical Center Groningen (UMCG). Before the study sample was selected, the anatomical landmarks described in Table 1 were marked on the skulls with a pencil by means of consensus of two observers (JD and ZF). An inclusion criterion for the selection of skulls was visible chin deviation, defined as at least 4mm deviation of pogonion (Pog) from the midsagittal line (Haraguschi et al., 2002). The midsagittal line was constructed with a laser level beam which connected nasion (N) and the anterior nasal spine (ANS) of the dry skulls (Figure 1a). This was based on Harvold (1954) who reported that a line through N and ANS represented the midsagittal line in more than 90 per cent of patients. The distance from the laser line to the respective points was measured to Pog by means of a digital caliper. The skulls also had to have a fixed occlusion, with the mandible fixed to the skull by means of two metal springs. Six asymmetric skulls met the selection criteria were included for this study (Figure 1b). Prior to the radiographic examination, metal markers with a diameter of 1.5mm were glued onto the selected landmarks with cyanoacrylate glue. The metal markers were used to eliminate landmark identification error which is common in

frontal 2-D (Major et al., 1994; Pirttiniemi et al.,, 1996; Athanasiou et al., 1999) and 3-D cephalometry (Lou et al., 2007; De Oliviera et al., 2009; Ludlow et al., 2009).

Table 1	Landmarks used in this study	
Landmark	**Abbreviation**	**Definition**
Unilateral		
1. Nasion	N	The most anterior of the frontonasal suture in the median plane
2. Anterior nasal spine	ANS	The tip of the bony anterior nasal spine in the median plane
3. Pogonion	Pog	The most anterior point of the bony chin in the median plane
4. Menton	Me	The most inferior midline point on the mandibular symphysis
Bilateral		
1. Orbitale	Or	The lowest point in the inferior margin of the orbit
2. Condylion lateral	CoL	The most lateral point on the condylar head
3. Jugulare	J	The intersection of the outline of the maxillary tuberosity and the zygomatic buttress
4. First upper molar	U6	The tip of the mesiobuccal cusp of the maxillary first permanent molar
5. Gonion	Go	The constructed point of intersection of the plane tangent to the posterior border of the ramus and a plane tangent to the inferior border of the mandible
6. Antegonion	AG/GA	The lateral inferior margin of the antegonial protuberances

Figure 1. (a) A midsagittal line constructed by a laser beam through nasion (N) and the anterior nasal spine (ANS) used to determine chin deviation. *(b)* Surface models (with the midsagittal plane) derived from the CBCT scans of the 6 skulls used in this study
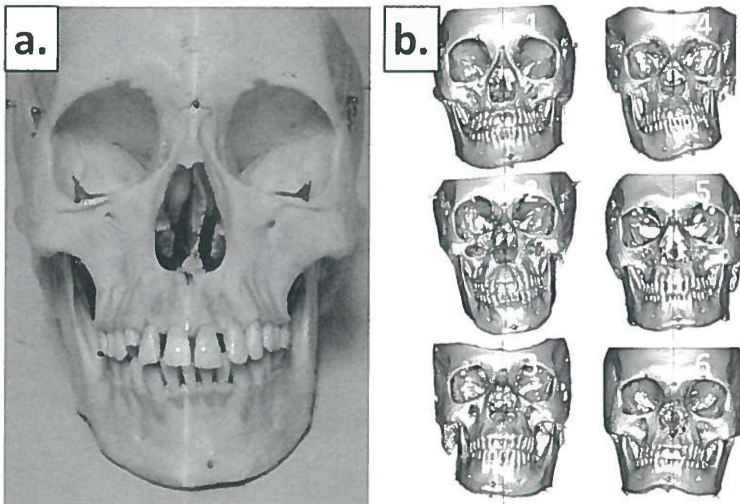
The 14 linear distances illustrated in figure 2 were measured directly on the skull by means of a digital caliper by one operator. The centers of the metal markers were used as the reference points. Asymmetry was then calculated as the left side measurement subtracted by the right side measurement (Ghafari, 2006; Hwang et al., 2006). A result of zero indicates perfect asymmetry, a negative or positive result indicates a larger measurement on the right or left side. The direct caliper measurements were repeated 5 times and the mean values were regarded as the reference values.

Figure 2 *The 14 measurements used in this study. 1, 2: Mandibular ramus length (CoL – Go); 3, 4: Mandibular body length (Go – Me); 5, 6: Total mandibular length (Co – Me); 7, 8: Maxillary height (Or – J); 9, 10: Maxillary dental height (Or – U6); 11, 12: Maxillary height by means of the triangulation approach (N – J); 13, 14: Mandibular ramus height by means of the triangulation approach (N – AG).*
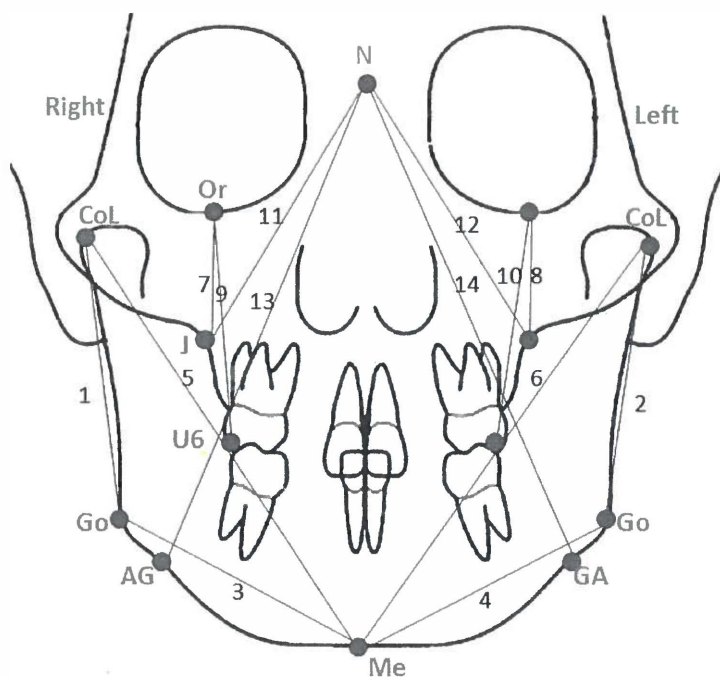
Radiographic examination consisted out of conventional PA cephalograms and CBCT scans. The PA cephalograms were made (ProMax, DiMax2 Digital Cephalometric Unit, Planmeca, Helsinki, Finland) with a resolution quality of 2272 x 2045 pixels at a 24 bit depth. Each skull was carefully placed in the cephalostat with the Frankfurt horizontal plane orientated parallel to the floor and the midsagittal plane parallel to the x-ray beam. The orientation of the skull in the cephalostat was checked with laser levels. The PA cephalograms were individually imported into the Viewbox® Version 3.1.1.13 (Halazonetis, Athens, Greece) software. The PA cephalograms were then scaled and the magnification error of 12% corrected using the software. For each PA cephalogram, the centers of the metal markers were identified by a cursor-driven mouse.

The CBCT images were acquired with the KaVo 3-D eXam scanner (KaVo Dental GmbH, Biberach/Riß, Germany). The light beams of the CBCT scanner were used to position the skull with the Frankfurt horizontal parallel to the floor. The skulls were scanned at a 0.30 voxel size resolution (120KV, 37.07mAs and 26.9s). The CBCT datasets were exported from the eXamVisionQ (Imaging Sciences International LCC, Hatfield, Pennsylvania, USA) software in DICOM multi-file format and imported into SimPlant Ortho Pro 2.00 (Materialise Dental, Leuven, Belgium) software. Importantly, due to scattering in the 3-D reconstruction, the centers of the metal markers were accurately identified by a cursor-driven mouse in the axial, coronal and sagittal slices and not on the volume renderings and surface models (figure 3).

Preprogrammed analyses in the Viewbox and SimPlant Ortho Pro 2.00 software calculated the asymmetry for each CBCT scan and PA cephalogram. Each PA cephalogram and CBCT scan was measured 3 times (each time during a different session, at least two weeks apart) and the mean values were regarded as the true values for the respective group.

Statistical analysis

The mean and standard deviation of the three measuring techniques (direct caliper, PA cephalogram and CBCT imaging) were calculated. The accuracy of the asymmetry evaluation was expressed by means of the absolute error (AE). Absolute error was defined as the CBCT or PA cephalogram value subtracted by the reference value.

As a measure of reliability, the intraclass correlation coefficient (ICC) for absolute agreement based on a 2-way random effects analysis of variance (ANOVA) was calculated between reference values and the two imaging techniques (e.g. PA cephalogram and CBCT). The smallest detectable difference (SDD) was used to determine the error of the three measurement procedures (Damstra et al., 2010b). The

standard error of measurement (SEM) of the three measurement sessions was calculated as the square root of the variance of the random error from 2-way random effects ANOVA. The SDD was then calculated as 1.96 x √2 x SEM. The SDD defines the 95% confidence limits of the method error (Damstra et al., 2010b). All statistical analysis was performed with a standard statistical software package (SPSS version 14, Chicago, IL).

Figure 3 *A screen shot of the CBCT images in the 3-D software illustrating accurate identification in the center of the metal marker of nasion (N) in the axial, coronal and sagittal slices. The 3-D image was not used for location of the reference points in the middle of the metal markers.*
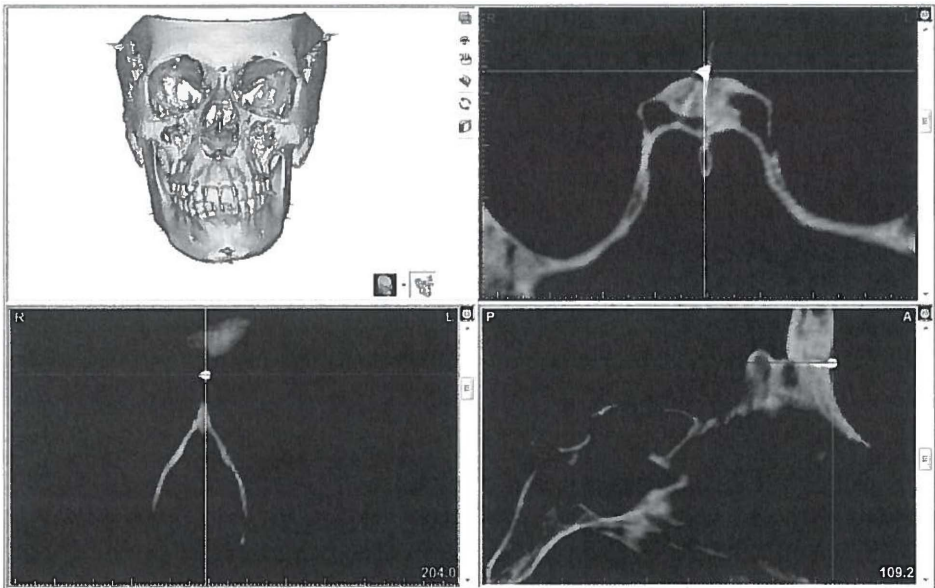
4.1.3 Results

The results of this study are summarized in Tables 2 and 3. Table 2 illustrates the mean and standard deviations of the three measuring techniques. There was less than 1 mm difference between all the mean CBCT measurements compared to the reference (direct caliper) measurements. However, major differences (> 3 mm) existed between the

mean reference and PA cephalogram values for the mandibular ramus length (triangulation approach), the mandibular body length and the total mandibular length measurements.

Table 3 describes the accuracy of the evaluation of the asymmetry. The CBCT scans were very accurate (< 0.50 mm) in the detection of all asymmetry. The PA cephalograms were fairly accurate (0.50 mm – 1.00 mm) in detection of the asymmetry for the following measurements: the mandibular ramus length, the maxillary height, the maxillary dental height and the maxillary height (triangulation approach). The PA cephalograms were not accurate (> 1.00 mm) in detection of asymmetry of the total mandibular length and the mandibular ramus length (triangulation approach).

The method errors for the direct caliper, CBCT scans and PA cephalograms were very small (0.05 mm, 0.11 mm and 0.02 mm respectively) confirming the absolute accuracy of the methods. The CBCT measurements were very reliable compared to the reference values (ICC > 0.957). The reliability of the PA cephalometric measurements varied when compared to the reference values. The reliability of the total mandibular length difference, maxillary height difference and maxillary dental height difference was very good (ICC > 0.900). The maxillary height difference and mandibular ramus difference (triangulation approach) was slightly less reliable (ICC = 0.873 and 0.819 respectively). The mandibular body length difference was the least reliable (ICC = 0.686).

Table 2	Mean and standard deviation (SD) of the physical (reference), CBCT and PA cephalometric measurements (mm).					
Measurement	**Reference**		**CBCT**		**PA Cephalogram**	
	Mean	SD	Mean	SD	Mean	SD
1. Right mandibular ramus length	52.77	2.10	52.48	2.10	52.85	2.34
2. Left mandibular ramus length	51.33	6.92	50.92	6.95	51.09	6.75
3. Right mandibular body length	80.26	6.25	79.51	6.22	59.13	11.78
4. Left mandibular body length	78.77	1.59	78.22	1.79	54.13	14.01
5. Right mandibular length	114.63	8.01	113.74	7.95	101.64	8.89
6. Left mandibular length	111.43	6.75	110.57	6.81	95.75	13.70
7. Right maxillary height	23.12	2.07	22.70	2.24	20.64	1.76
8. Left maxillary height	23.90	2.45	23.72	2.28	21.41	2.68
9. Right maxillary dental height	46.59	4.06	46.10	3.68	47.60	4.65
10. Left maxillary dental height	45.09	4.65	44.89	4.60	45.77	4.41
11. Right maxillary height (TA)	64.97	1.26	64.73	1.17	62.91	2.62
12. Left maxillary height (TA)	64.06	2.21	63.83	2.41	62.32	3.37
13. Right mandibular ramus length (TA)	115.43	3.38	114.69	3.27	106.21	6.98
14. Left mandibular ramus length (TA)	113.99	4.85	113.33	4.57	104.34	8.34

All measurements = mm

TA, Triangulation approach

Table 3   Accuracy determined by means of the absolute error or AE of the CBCT images and the PA cephalograms (PAC). Reliability (ICC) of the CBCT and PA cephalograms values when compared to the reference values.

Asymmetry measurement	AE – CBCT vs. Reference			AE - PAC vs. Reference			ICC	
	Mean	SD	CI (95%)	Mean	SD	CI (95%)	CBCT	PA
1. Mandibular ramus length difference	0.34	0.28	0.25 - 0.44	0.67	0.39	0.49 – 0.85	0.999	0.994
2. Mandibular body length difference	0.35	0.16	0.23 - 0.46	5.38	5.96	2.63 – 8.13	0.998	0.686
3. Total mandibular length difference	0.32	0.01	0.21 - 0.43	2.60	2.72	1.34 – 3.86	0.999	0.934
4. Maxillary height difference	0.30	0.35	0.21 - 0.40	0.51	0.29	0.35 – 0.61	0.980	0.957
5. Maxillary dental height difference	0.47	0.09	0.32 - 0.62	0.99	0.58	0.72 – 1.26	0.979	0.923
6. Maxillary difference (TA)	0.31	0.04	0.16 - 0.46	0.63	0.57	0.37 – 0.90	0.957	0.873
7. Mandibular ramus difference (TA)	0.29	0.16	0.18 - 0.41	2.58	1.51	1.89 – 3.28	0.995	0.819

All measurements = mm
TA, Triangulation approach

4.1.4 Discussion

The aim of this study was to evaluate and compare PA cephalograms and CBCT images for the detection of mandibular asymmetry by comparison of left and right side structures. The results confirmed the absolute accuracy of CBCT images previously reported in the literature (Mischkowski et al., 2007; Hassan et al., 2008; Lagravere et al., 2008; Brown et al., 2009; Damstra et al., 2010a) and validate the use of CBCT imaging to evaluate the cause of mandibular asymmetry. The accuracy of CBCT imaging in determining the characteristics of asymmetry is not only important for diagnosis and evaluating treatment outcomes, but it may also enable more precise planning of surgical treatment.

In contrast to the CBCT images, the PA cephalograms were inaccurate in detection of the characteristics of the mandibular asymmetry of this study. This is important because differences of mandibular ramus and body length differences are important factors in detection of chin deviation (Hwang et al., 2006; Baek et al., 2007). The results confirm previous findings that suggest that conventional PA cephalograms might not be reliable for asymmetry analysis (Peck et al., 1991; Hwang et al., 2006). In PA cephalometry, landmarks have their own magnification error since the structures are located at different distances from the film. However, due to the positioning of the head in the cephalostat, the magnification error of bilateral landmarks should be the same since the bilateral structures are located at relatively equal distances from the film and x-ray source (Bishara et al.,1994). This suggests that the comparison of left and right side structures is possible with PA cephalograms. The results of this study suggest that

left and right side measurements cannot be compared when evaluating asymmetry. Simple geometry might offer an explanation. By nature, when mandibular asymmetry is present, point Menton (Me) is most likely to deviate across the facial midline. Therefore, in such cases the structures will not be located at relatively equal distances making left and right side comparisons unreliable.

It is ethically questionable to expose a patient to radiation from both a conventional PA cephalogram and a CBCT scan for comparative studies. We therefore decided to use dry skulls in combination with metal markers aiming to reduce the measurement error. The absolute accuracy of the methods used in this study was confirmed by the small method error. Although the sample size can be regarded as small, it can be justified because the method error was very small (the SDD means that differences of more than 0.11 mm could be regarded as significant). In addition, it must be noted that the sample is unique and that asymmetric dry skulls are difficult to acquire for comparative study.

The present study investigated the differences between the two imaging modalities by evaluating mandibular asymmetry using dry skulls. It must be kept in mind that this method differs from direct patient care. In the clinical setting, the process of detection of the asymmetry with PA cephalometry or CBCT imaging might be more problematic. The dry skulls used in this study do not move and have fiducial markers for measurement which is not the case with patients. In addition, the lack of soft-tissues and peripheral attenuation material may have allowed for increased contrast of the landmarks. Landmark identification error is a major source of PA cephalometric measurement error (Major et al., 1994; Pirttiniemi, 1996; Athanasiou et al., 1999). Although we eliminated this problem by using metal markers, in practice the inaccuracy of the asymmetry might be magnified or hidden by the measurement error resulting from identification error. Landmark identification is possibly more accurate on 3-D CBCT images than 2-D cephalograms (Ludlow et al., 2009; De Oliviera et al., 2009). The positioning of the patient is very critical when making a PA cephalogram because rotation of the head results in measurement differences (Yoon et al., 2002; Ghafari, 2006; Van Vlijmen et al., 2009a). We used a standardized set up which is difficult to reproduce in practice. Hassan et al. (2008) reported that small variation of the head position when making a CBCT does not influence measurement accuracy which makes positioning of the patient in CBCT scanner less critical compared to PA cephalograms.

The measurements we used to detect the contributing factors of the chin deviation were previously described (Bishara et al., 1994; Athanasiou and Van der Meij, 1995; Reyneke, 2003; Hwang et al., 2006; Baek et al., 2007). We used the most lateral point of

the condyle (CoL) as reference mark instead of condylion (Co) in order to make direct caliper measurements possible while the teeth are fixed in occlusion. Although the ramus length difference (CoL – Go) was accurate on the PA cephalograms, it is very important to realize that the points of gonion (Go) are not identifiable on PA cephalograms. Instead, the points antegonion (AG/GA) is used in PA cephalometry. We found that determining the ramus length with antegonion was not accurate. This confirms the observation by Hwang et al. (2006) that different vertical positions of antegonion are not always evident with conventional PA cephalogram analysis.

It was not the intention to establish CBCT imaging as routine imaging modality for all mandibular asymmetry cases. However, the results show that the CBCT imaging was more accurate in determining the difference of the mandibular dimensions (ramus length, body length and total length) than conventional PA cephalometry. Therefore, a CBCT scan should be considered in order to determine the characteristics of the asymmetry of a visible chin requiring surgical correction. In such cases, the risk of misdiagnosis and inappropriate surgical treatment planning using a PA cephalogram possibly outweighs the risk of a higher radiation dose of a CBCT scan.

4.1.5 Conclusion

CBCT imaging provides more accurate information regarding the characteristics of mandibular asymmetry than conventional PA cephalograms. Therefore, a CBCT scan should be considered when a visible chin deviation is present which requires surgical correction.

4.1.6 References

Athanasiou AE, Van der Meij AJW 1995 Posteroanterior (frontal) cephalometry. In: Athanasiou AE. Orthodontic cephalometry. London, UK: Mosby-Wolfe: 125-140

Athanasiou AE, Miethke RR, Van der Meij AJW 1999 Radom errors in location of landmarks in postero-anterior cephalograms. Br J Orthod 26: 273-283

Baek S-K, Cho I-S, Chang Y-I, Kim M-J 2007 Skeletodental factors affecting chin point deviation in female patients with class III malocclusion and facial asymmetry: a three dimensional analysis using computed tomography. Oral Surg Oral Med Oral Pathol Oral Radiol Endod 104: 628-39

Brown AA, Scarfe WC, Scheetz JP, Silviera JP, Farman AG 2009 Linear accuracy of cone beat CT 3-D images. Angle Orthod 79: 150-157

Bishara SE, Burkey PS, Kharouf JG 1994 Dental and facial asymmetries: a review. Angle Orthod 64: 89-98

Damstra J, Fourie Z, Huddleston Slater JJR, Ren Y 2010a Accuracy of linear measurements from cone-beam computed tomography-derived surface models of different voxel sizes. Am J Orthod Dentofacial Orthop 2010; 137: 16.e1-16.e6.

Damstra J, Huddleston Slater JJR, Fourie Z, Ren Y 2010b Reliability and the smallest detectable difference of lateral cephalometric measurements. Am J Orthod Dentofacial Orthop 138: 546.e1-e8

EADMFR 2008 Basic principles for the use of dental cone beam CT (www.eadmfr.info) (23 September 2010, date last accessed)

De Oliviera AEF, Cevidanes LHS, Phillips C, Motta A Burke B, Tyndall D 2009 Observer reliability of three-dimensional cephalometric identification on cone-beam computerized tomography. Oral Surg Oral Med Oral Pathol Oral Radiol Endod ; 107: 256-265

Farman AG, Scarfe WC 2006 Development of imaging selection criteria and procedures should precede cephalometric assessment with cone-beam computed tomography. Am J Orthod Dentofacial Orthop 130: 257-265

Ghafari GG 2006 Posteroanterior cephalometry: Craniofacial frontal analysis. In: Jacobson A, Jacobson RL, eds: Radiographic cephalometry, From Basics to 3-D imaging. Hanover Park. Quintessence Publishing Co, Inc: 267-292

Halazonetis DJ 2005 From 2-dimensional cephalograms to 3-dimensional computed tomography scans. Am J Orthod Dentofacial Orthop 127: 627-637

Haraguschi S, Takada K, Yasuda Y 2002 Facial asymmetry in patients with skeletal class III deformity. Angle Orthod 72: 28-35

Harrell WE, Jacobson RL, Hatcher DC, Mah J 2006 Cephalometric imaging in 3-D. In: Jacobson A, Jacobson RL, eds: Radiographic cephalometry, From Basics to 3-D imaging. Hanover Park. Quintessence Publishing Co: 233-247

Hassan B, Van der Stelt P, Sanderink G 2008 Accuracy of three-dimensional measurements obtained from cone beam computed tomography surface-rendered images for cephalometric analysis: influence of patient scanning position. Eur J Orthod 31: 129-134

Harvold E 1954 Cleft lip and palate: Morphological studies of the facial skeleton. Am J Orthod 40: 493-506

Hwang H-S, Hwang CH, Lee K-H, Kang B-C 2006 Maxillofacial 3-dimensional image analysis for the diagnosis of facial asymmetry. Am J Orthod Dentofacial Orthop 130: 779-785

Ko EW, Huang CS, Chen YR 2009 Characteristics and corrective outcome of face asymmetry by orthognathic surgery. J Oral Maxillofac Surg 67: 2201-2209

Kokich VG 2010 Cone-beam computed tomography: have we identified the orthodontic benefits? Am J Orthod Dentofacial Orthop 137, S16

Lagravere MO, Carey J, Toogood RW, Major PW 2008 Three-dimensional accuracy of measurements made with software on cone-beam computed tomography images. Am J Orthod Dentofacial Orthop 134: 112-116

Lou L, Lagravere MO, Compton S, Major PW, Flores-Mir C 2007 Accuracy of measurements and reliability of landmark identification with computed tomography (CT) techniques in the maxillofacial area: a systematic review. Oral Surg Oral Med Oral Pathol Oral Radiol Endod 104: 402-411

Ludlow JB, Gubler M, Cevidanes LHS, Mol A 2009 Precision of cephalometric landmark identification: cone-beam tomography vs. conventional cephalometric views. Am J Orthod Dentofacial Orthop; 136: 312e1-10; discussion 312-3

Major PW, Johnson DE, Hesse KL, Glover KE 1994 Landmark identification error in posterior anterior cephalometrics. Angle Orthod 64: 447-454

Mischkowski RA, Pulsfort R, Ritter L, Neugebauer J, Brochhagen HG, et al. 2007 Geometric accuracy of a newly developed cone-beam device for maxillofacial imaging. Oral Surg Oral Med Oral Pathol Oral Radiol Endod 104: 551-559

Peck S, Peck L, Kataja M 1991 Skeletal asymmetry in esthetically pleasing faces. Angle Orthod 61: 43-46

Pirttiniemi P, Miettinen J, Kantomaa T 1996 Combined effects of errors in frontal-view asymmetry diagnosis. Eur J Orthod 18: 629-636.

Reyneke JP 2003 Systematic patient evaluation. In Reyneke JP ed. Essentials of Orthognathic Surgery. Hanover Park. Quintessence Publishing Co, Inc: 13-68

SEDENTEXCT 2009 Provisional guidelines CBCT for dental and maxillofacial radiology (www.sedentexct.eu/guidelines) (23 September 2010, date last accessed)

Van Vlijmen OJC, Berge SJ, Bronkhorst EM, Swennen GRJ, Katsaros C, Kuipers-Jagtman AM 2009a A comparison of frontal radiographs obtained from cone-beam CT and conventional frontal radiographs from human skulls. In J Oral Maxillofac Surg 38: 773-778

Van Vlijmen OJ, Maal TJJ, Berge SJ, Bronkhorst EM, Katsaros C, Kuipers-Jagtman AM 2009b A comparison between two-dimensional and three-dimensional cephalometry on frontal radiographs and on cone beam computed tomography scans of human skulls. Eur J Oral Sci 117: 300-305

Yoon YJ, Kim DH , Yu PS, Kim HJ, Choi EH, Kim KW 2002 Effect of head rotation on posteroanterior cephalometric photographs. Angle Orthod 72: 36-42.

4.2 Combined 3-dimensional and mirror-image analysis for the diagnosis of asymmetry

Abstract

The advent of 3-dimensional (3D) imaging techniques has greatly improved our ability to assess asymmetry by means of linear and angular measurements. However, visualizing deformities enables a unique appreciation of the underlying deformity which may not be possible by looking at quantitive numbers alone. This article describes the method of a mirror-image analysis technique to visualize the asymmetry in order to assist in diagnosis and treatment planning. Other advantages of performing a mirror-image analysis in addition to the quantitive analysis are also discussed.

4.2.1 Introduction

The development of computer tomography (CT) has greatly reduced errors of frontal cephalometry and improved our ability to diagnose asymmetry and other craniofacial deformities.[1,2] Cone-beam computed tomography (CBCT) was developed for 3-dimensional (3D) imaging of the maxillofacial area and has become popular in dentistry, orthodontics and maxillofacial surgery.[3] Advantages of CBCT include less radiation exposure (when compared to a conventional CT), less artifact formation and sub-millimeter spatial resolution.[3] CBCT has been shown to produce very accurate 3D images of the craniofacial region and produces a 1-to-1 image-to-reality ratio which is necessary for accurate detection of the underlying deformities and asymmetry.[4-8]

Recent literature has described new quantitive analyses to diagnose asymmetries on 3D CT or CBCT images.[1-3, 9-14] Because quantitive measurement is a key element in diagnosis of asymmetry, 3D images are best suited for accurate diagnosis. Quantitive measurements provide important information regarding the treatment planning e.g. it determines the target area for operation and the surgical method to be followed. However, by looking at quantitive numbers alone, it may not be possible to appreciate the extent of the underlying deformity. To overcome this limitation, Terajima et al.[14] described a visual 3D method for analyzing the morphology of patients with maxillofacial deformities. They superimposed a standard 3D Japanese skeletal model on the patient's 3D CT images to show the underlying deformities.[14] However, these 3D templates only satisfy the Japanese norms which limit their clinical application. We use a mirror-image for visual analysis of the asymmetry. The mirror-image analysis does not rely on population norms and can therefore be used for the detection of asymmetries in all populations.

A mirror-image is a reflected duplication that appears identical but in reverse. By superimposition of the mirror-image of the anatomical correct part of the anatomy over the deformity, the differences become visual and can also be quantified. The use of mirror-images is not new in craniofacial imaging techniques. In maxillofacial surgery, the reverse models of 3D mirror-image templates have been described to correct and reconstruct various craniofacial abnormalities.[15, 16]

The aim of this study is to illustrate and discuss the method of performing a mirror-image analysis in addition to the quantitive 3D analysis of asymmetry by means of a case report. The advantages of the mirror-image analysis will also be discussed.

4.2.2 Method

A male patient, aged 14, was referred to the Department of Orthodontics of the University Medical Center Groningen as part of the multidisciplinary approach for treatment of the Parry-Romberg syndrome. A medical history revealed that noticeable asymmetry began at the age of 6 years indicating early onset of the disease. The diagnosis of Parry-Romberg disease was made at the age of 7 years. Extra-oral examination revealed a marked asymmetry due to atrophy of the right side of the face. The chin was deviated to the right and a deviation of nose to the affected side was noticeable. Intra-oral examination revealed that the mandibular dental midline was rotated to the right. Delayed eruption of the mandibular premolars and molars was noted on the right side.

A CBCT image of the patient was acquired using a KaVo 3D eXam scanner (KaVo Dental GmbH, Bismarckring, Germany). The image was made with a 17 cm field of view at a voxel resolution of 0.4 mm. The CBCT dataset was exported in DICOM file format and imported into SimPlant Ortho Pro 2.00 (Materialise Dental, Leuven, Belgium) software. The 3D image was rendered and surface models of the hard tissues were created with the software (Figure 1). To quantify the osseous changes, a 3D analysis was developed combining linear and angular measurements previously described.[1-3] The measurements used for the quantitive 3D analysis are illustrated in Figure 2 and described in Table 1. Asymmetry was described by the left side measurement subtracted by the right side.[1, 2]
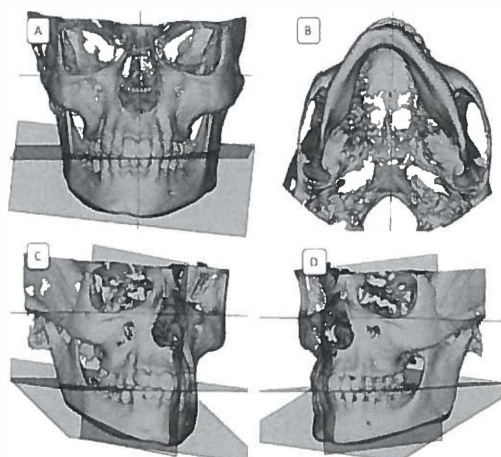

Figure 1 *3D surface model of the patient with early onset Parry-Romberg syndrome.* *A:* *Fontal view.* *B:* *Inferior view.* *C:* *Right lateral view.* *D:* *Left lateral view.*

Figure 2 *Measurements used for the quantitive analysis of the asymmetry.* *(1)* *Maxillary rotation,* *(2)* *Maxilla height,* *(3)* *Maxilla dental height,* *(4)* *Maxilla width,* *(5)* *Maxilla dental width,* *(6)* *Mandibular rotation,* *(7)* *Ramus length,* *(8)* *Mandibular body length,* *(9)* *Total mandibular length,* *(10)* *Mandibular width,* *(11)* *Mandibular dental width,* *(12)* *Mandibular dental height,* *(13)* *Gonion angle,* *(14)* *Lateral ramus inclination,* *(15)* *Frontal ramus inclination,* *(16)* *Facial width,* *(17)* *Occlusal cant,* *(18)* *Mandibular cant,* *(19)* *Total maxilla width and the total mandibular width,* *(20)* *Condylar width.*
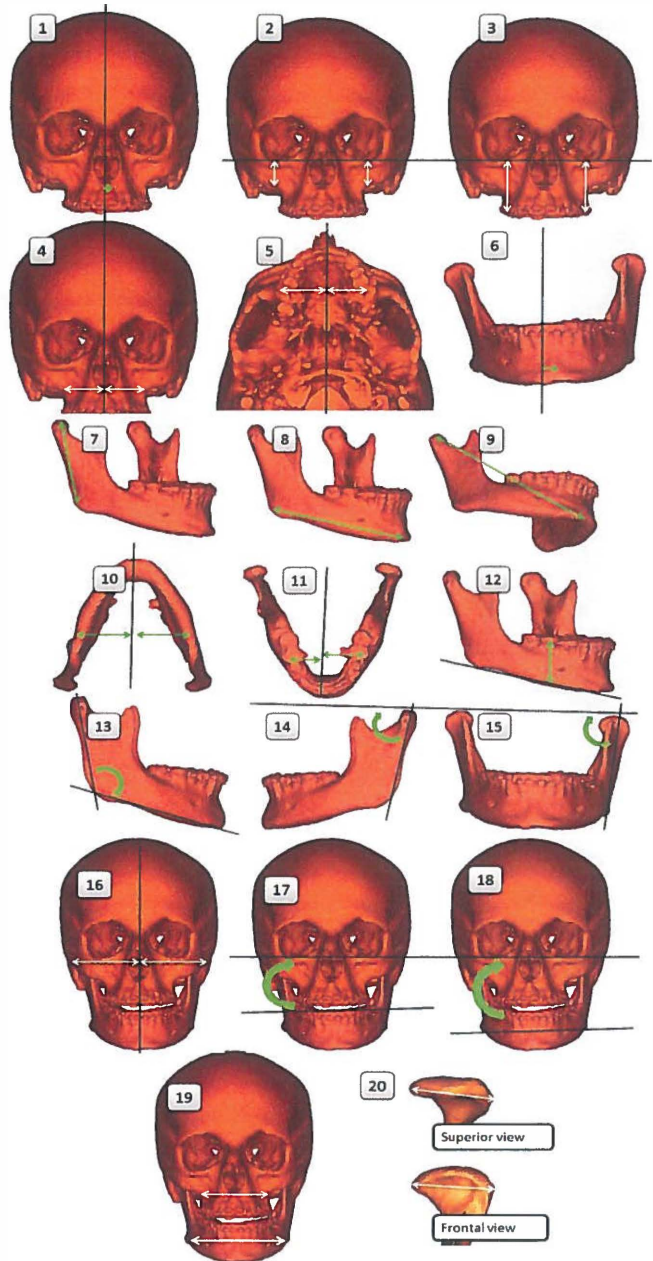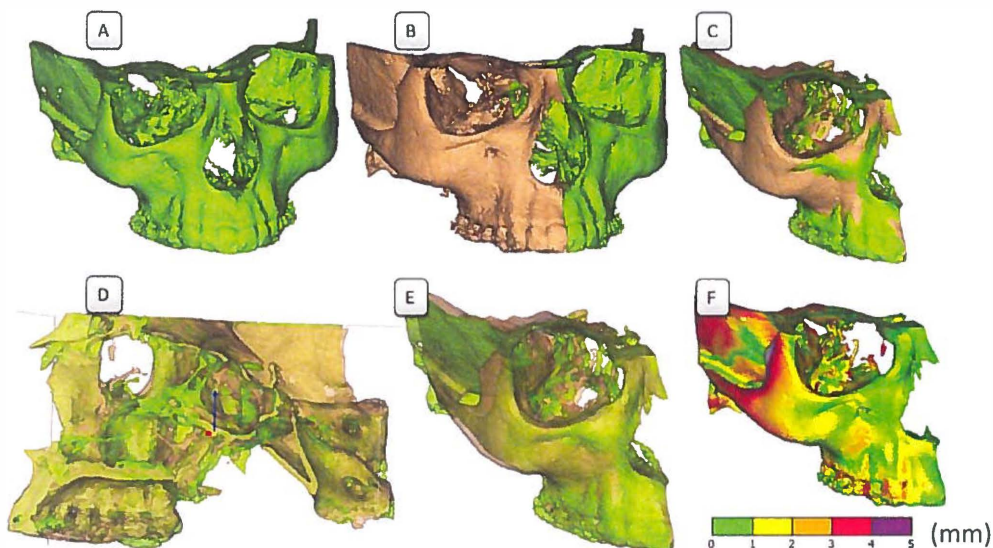
Figure 3 *Mirror-image analysis of the maxilla. (**A-C**) The left side of the maxilla is mirrored (brown) over the original right surface model (green) along the midsagittal plane. (**D**) The superimposition is adjusted to best fit along the cranial base if necessary. (**E**) Final superimposition with the surface models semi-transparent to visualize the differences. (**F**) The differences of the mirror-image and original surface model calculated and expressed by means of a customized color scale (in mm)*

In addition to the quantitive 3D analysis, a mirror-image analysis was performed to visually analyze the extent of the atrophy and confirm the diagnosis. The method for the mirror-image of the maxilla was as follows: the left unaffected side was mirrored along the midsagittal plane. The mirror-image was then superimposed over the right affected side (Figure 3A-C). The software allows for the surface models to become semi-transparent and allows for movement of the models in all three planes of space. Visual inspection of the anterior and posterior cranial base confirmed the superimposition (Figure 3D). For the mandible, a vertical plane through the Spina mentalis, parallel to the midsagittal plane was used because of the chin deviation (Figure 4A). The left side was mirrored and superimposed over the right side (Figure 4A-C). Visual inspection of the inner contour of the cortical plates of the inferior border of the symphysis confirmed the

superimposition (Figure 4D). For both maxilla and mandibula, the difference in volume was visualized with the software by means of a customized color scale (Figure 3F and 4F). The measurement differences were used as a guide to determine the parameters of the color scales

*Figure 4 Mirror-image analysis of the mandibula. (**A-C**): The left side of the mandibula is mirrored (blue) over the right original surface model (pink) along the vertical plane through Menton. (**D**): The superimposition is adjusted to best fit along the inner contour of the cortical plates of the inferior border of the symphysis if necessary. (**E**): Final superimposition with the surface models semi-transparent to visualize the differences. (**F**): The differences of the mirror-image and original surface model calculated and expressed by means of a customized color scale (in mm)*
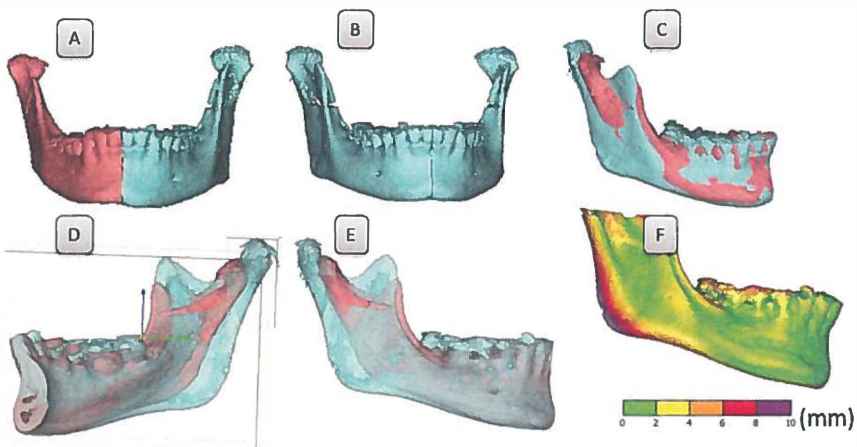
4.2.3 Results

The quantitive results of the 3D cephalometric analysis are described in Table 2. The smaller measurements indicate that the mandible and maxilla were affected on the right side. The facial width was 5mm less on the right side compared to the left side. This indicates the restricted growth of the zygomatic arch due to the soft-tissue atrophy. The maxillary height was decreased on the right side (1.7 mm). However, there was no difference between the maxillary dental heights of the left and right side, possibly as a result of the over-eruption of the maxillary dentition due to delayed eruption of the posterior mandibular dentition. The mandible was rotated 4.88mm to the right. On the affected side, the mandibular body length was 10.3 mm shorter when compared to the

left side. The ramus was also 4.2 mm shorter on the affected side. The difference in the ramus length explains the significant cant of the mandible (13.0 degrees). The restrictive nature of the disease did not only manifest as restriction of the lengths but also the angular development of the mandibula. The most noticeable was the underdevelopment of the gonion angle on the right side. The gonion angle was 113.0 degrees on the left side compared to 125.9 degrees on the right side. The lateral and frontal ramus inclination was smaller on the right side (6.2 and 3.0 degrees).

The delayed eruption caused an underdevelopment of the alveolar process of the mandibula (5.3 mm) and resulted in an occlusal cant. Interestingly, although the lower face of the affected side showed significant osseous changes, the condylar width dimensions were not different from the unaffected side. The mirror-image technique visualized the findings of the quantitive 3D analysis regarding the hypoplasia of the zygomatic region and the mandible. The differences between the mirror-image and the affected side were calculated and illustrated with color scales in Figure 3F and 4F.

| Table II	Results of the quantitive 3D analysis. Asymmetry defined as the left side subtracted by the right side. (All measurements in mm except for measurements no. 13 – 17 in degrees)			
	Maxilla	**Right**	**Left**	**Asymmetry**
1.	Maxillary rotation	0.2		
2.	Maxilla height difference	21.0	22.5	1.5
3.	Maxilla dental height difference	42.4	41.9	-0.5
4.	Maxilla width difference	34.1	33.1	-1.0
5.	Maxilla dental width difference	27.1	26.1	-1
	Mandible			
6.	Mandibular rotation	4.88		
7.	Ramus length difference	47.4	52.3	4.9
8.	Body length difference	73.9	84.2	10.3
9.	Total length difference	108.7	115.2	6.5
10.	Mandibular width difference	42.6	43.7	1.1
11.	Mandibular dental width difference	23.4	22.6	-0.8
12.	Mandibular dental height difference	19.2	24.5	5.3
13.	Gonion angle difference	125.9	113.0	-12.9
14.	Lateral ramus inclination difference	78.0	82.2	6.2
15.	Frontal Ramus inclination difference	85.0	88.0	-3.0
	Other			
16.	Occlusal cant	1.0		1.0
17.	Mandibular cant	13.0		13.0
18.	Mandibular width - Maxillary width	80.0	67.0	13.0
19.	Facial width difference	54.4	59.4	5.0
20.	Condyle width difference	18.27	18.07	-0.20

4.2.4 Discussion

Parry-Romberg syndrome (or Progressive Hemifacial Atrophy) is an uncommon degenerative condition characterized by a slow and progressive atrophy of facial tissues, muscles, bones and skin.[17-26] The progressive atrophy of the facial tissues is often in stark contrasted to the apparently normal contra-lateral side. The extent of the atrophy is usually limited to one side of the face. The osseous lesions described in Parry-Romberg syndrome appear to be related to the age in which the condition appears. With late onset of the condition after the age of 15 years, the lesions are considered to appear exclusively in the soft tissue.[24] The restriction of skeletal growth due to the soft-tissue atrophy of early onset Parry-Romberg syndrome has been previously reported. However, Duymaz et al.[26] reported no osseous changes of the craniofacial region after 3D CT examination of a case of early onset Parry-Romberg syndrome. In our case, early onset of the atrophy resulted in hypoplasia of the fronto-orbitozygomatic region, mandibular rotation and underdevelopment of the mandibula in all dimensions of space. This is in contrast to the finding of Duymaz et al.[26] It would however be incorrect to draw conclusions from one case report because the extent of the osseous changes might be different from individual to individual. This is due to the fact that involvement can stabilize in any stage of growth and development and patients who manifest atrophy in early ages, have bigger repercussions.[24] Future studies will investigate a larger group of patients with early onset Parry-Romberg syndrome by means of 3D analysis to fully determine the characteristics of the early onset soft-tissue atrophy on the middle and lower face.

The mirror-image analysis performed in addition to the quantitive 3D analysis proved to be very valuable. Not only does it confirm the diagnosis derived from quantitive measurements; it helps to reduce diagnostic errors when relying on numbers alone, it does not rely on normative values, it creates new appreciation of osseous changes because the differences could be depicted as volume rather than numbers, it helps in development of treatment strategies and it improves communication between orthodontists and maxillofacial surgeons. Perhaps the most valuable contribution of the visual analysis is that it has been an excellent tool to explain the extent of the osseous changes to the patient to further their understanding of the disease and the possibilities and limitations of the treatment necessary. It is therefore recommended to perform a mirror-image analysis in addition to quantitive analysis in asymmetric cases which will enable a unique appreciation of the underlying deformity which may not be possible by studying quantitive numbers alone.

Importantly, where there is unilateral growth of the mandible, the mandible will have a tendency to rotate toward the area of less growth and cause chin deviation. Therefore, it is debatable if the mandible can be divided in an affected and unaffected side because the unaffected side is always indirectly affected. As a result of rotation, the ramus inclinations on both sides might be affected. The chin deviation also excludes the use of the midsagittal plane and the mandible should be divided and mirrored with a vertical plane through the Spina mentalis.

Figure 5 *The effects of unilateral mandibular growth. **(A):** The maxilla is mirrored along the midsagittal plane, the mandibula through the Spina mentalis. **(B):** The plane through Spina mentalis is aligned with the midsagittal plane to correct the chin deviation. **(C):** With a rotation point on menton (arrow), both the mandibular halves (dark) are rotated to align the condylar heads in the fossa **(D)** (circle). Inferior view **(E)** and frontal view **(F)** to illustrate the ideal position of the mandibula and maxilla (dark) in comparison to the original (light). Unilateral growth of the mandibula affects the left and right side of the mandibula when rotation occurs.*
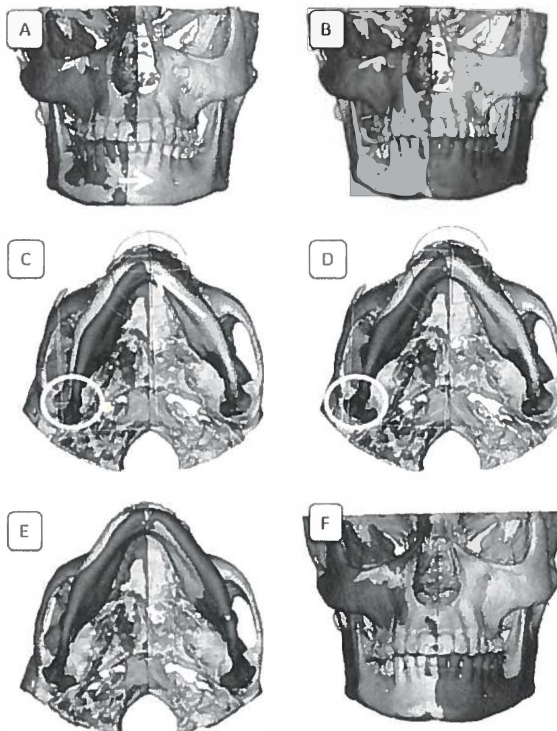
The effect of unilateral growth of the mandibula is illustrated in figure 5 A – F. Therefore, it is important to realize that mirror-image analysis is unlikely to give an accurate representation of the ramus inclinations when a chin deviation exists. However, the differences in mandibular body length, ramus length and gonion angle differences can be accurately determined with a mirror-image analysis (Figure 4E).

In the literature, there seems to be a large variation concerning the vertical axis or midsagittal plane for asymmetry analysis.[2, 3,11, 13, 27] Jacobson defined the midsagittal plane as a midline plane bisecting the head sagittally when viewing the patient from the frontal view.[3] Jacobson used nasion (N), the midpoint of the frontonasal suture, as the reference point. Grummons used a midsagittal line through crista galii (Cg) and the anterior nasal spine (ANS).[27] Tuncer et al. used a plane through N, sella (S), and ANS as the midsagittal plane for their 3D analysis.[13] Harvold[28] reported that a line through N and ANS represented the midsagittal line in more than 90% of patients. Baek et al.[2] used the most superior edge of the Cg and the midpoint between the anterior clinoid processes to construct a midsagittal plane perpendicular to the Frankfort horizontal (FH) plane. However, ANS and the FH plane might not be accurate when asymmetry of the upper and mid-facial regions exists.[14, 29] In addition, we experienced variations in the midsagittal plane due to landmark identification differences of orbitale (Or) and porion (Po) when using the method of Baek et al.[2] The midpoint between the foramina spinosum (ELSA)[30] was considered as reference point but we found that the foramina was not always clear on the CBCT images. To construct the midsagittal plane we used N, the midpoint between the anterior clinoid processes and the midpoint between the most lateral points on the foramen magnum. The possible advantages of this method include: the landmarks are easily identifiable on CBCT images; the accuracy of the midsagittal plane is not reliant on accuracy of other planes e.g. the Frankfurt horizontal plane and the midsagittal plane is not influenced by upper and mid-facial deformities.

4.3.5 Conclusion

We introduced a new method for visualizing asymmetries. The combined 3D and mirror-image analysis were very useful to visualize and better understand the osseous changes that occurred. The mirror-image analysis is useful to confirm the diagnosis derived from the quantitive results and assists in the 3D treatment planning. The combined analysis revealed that early onset Parry-Romberg syndrome caused rotation of the mandible, hypoplasia of all of the dimensions of the mandibula, hypoplasia of the zygomatic region and zygomatic arch.

4.2.5 References

1. Hwang H-S, Hwang CH, Lee K-H, Kang B-C. Maxillofacial 3-dimensional image analysis for the diagnosis of facial asymmetry. Am J Orthod Dentofacial Orthop 2006; **130**: 779-85.

2. Baek S-K, Cho I-S, Chang Y-I, Kim M-J. Skeletodental factors affecting chin point deviation in female patients with class III malocclusion and facial asymmetry: a three dimensional analysis using computed tomography. Oral Surg Oral Med Oral Pathol Oral Radiol Endod 2007;104:628-39

3. Jacobson RL. Three-Dimensional Cephalometry. In: Jacobson A, Jacobson RL eds. Radiographic Cephalometry: From Basics to 3-D Imaging. 2nd ed. Hanover Park. Quintessence Publishing Co, Inc. 2006:233-47

4. Damstra J, Fourie Z, Huddleston Slater JJR, Ren Y. Accuracy of linear measurements from cone-beam computed tomography-derived surface models of different voxel sizes. Am J Orthod Dentofacial Orthop 2010;137:16.e1-16.e6)

5. Lagravere MO, Carey J, Toogood RW, Major PW. Three-dimensional accuracy of measurements made with software on cone-beam computed tomography images. Am J Orthod Dentofacial Orthop 2008;134:112-16

6. Hassan B, van der Stelt P, Sanderink G. Accuracy of three-dimensional measurements obtained from cone beam computed tomography surface-rendered images for cephalometric analysis: influence of patient scanning position. Eur J Orthod 2008;31:129-34

7. Brown AA, Scarfe WC, Scheetz JP, Silveira AM, Farman AG. Linear accuracy of cone beat CT 3D images. Angle Orthod 2009;79:150-7.

8. Mischkowski RA, Pulsfort R, Ritter L, Neugebauer J, Brochhagen HG, Keeve E, Zoller JE. Geometric accuracy of a newly developed cone-beam device for maxillofacial imaging. Oral Surg Oral Med Oral Pathol Oral Radiol Endod 2007;104:551-9.

9. Park S-H, Yu H-S, Kim K-D, Lee K-J, Baik H-S. A proposal for a new analysis of craniofacial morphology by 3-dimensional computed tomography. Am J Orthod Dentofacial Orthop 2006; 129:600.e23-600.e34

10. Haraguschi S, Takada K, Yasuda Y. Facial asymmetry in patients with skeletal class III deformity. Angle Orthod 2002;72:28-35

11. Cho HJ. A three-dimensional cephalometric analysis. J Clin Orthod 2009;43:235-252

12. Maeda M, Katsumata A, Ariji Y, Maramatsu A, Yoshida K, Goto S, Kurita K, Ariji A. 3D-CT evaluation of facial asymmetry in patients with maxillofacial deformities. Oral Surg Oral Med Oral Pathol Oral Radiol Endod 2006;101:652-7

13. Tuncer BB, Atac MS, Yuksel S. A case report comparing 3-D evaluation in the diagnosis and treatment planning of hemimandibular hyperplasia with conventional radiography. J Craniomaxillofac Surg 2009, doi:10.1016/j.jcms.2009.01.004

14. Terajima M, Nakasima A, Aoki Y, Goto TK, Tokumori K, Mori N, Hoshino Y. A 3-dimensional method for analyzing the morphology of patients with maxillofacial deformities. Am J Orthod Dentofacial Orthop 20009;136:857-67

15. Zhou L, He L, Shang H, Lui G, Zhoa J, Lui Y. Correction of hemifacial microsomia with the help of mirror imaging and rapid prototyping technique: a case report. Br J Oral Maxillofacial Surg 2009;47:486-88

16. Lee JW, Fang JJ, Chang LR, Yu CK,. Mandibular defect reconstruction with the help of mirror imaging coupled with laser stereolithographic modeling technique. J Formos Med Assoc 2007;106:244-50

17. Mazzeo N, Fisher JG, Mayer MH, Mathieu GP, Mcade FGG. Progressive Hemifacial atrophy (Parry Romberg Syndrome). Case Report. Oral Surg Oral Med Oral Pathol Oral Radiol Endod.1995; 79: 30-35

18. Lakhani PK, David TJ. Progressive Hemifacial atrophy with scleroderma and ipsilateral limb wasting (Parry-Romberg Syndrome). J R Soc Med 1984; 77: 138-39.

19. Gomez-Diez S, Gallego-Lopez L, Lopez-Escobar M, Junquera-Gutierrez L, Perez-Olivia N. Progressive facial hemiatrophy with associated osseous lesions. Med Oral Patol Oral Cir Bucal 2007; 12: E602-E604.

20. Miller MT, Sloane H, Goldberg MF, Grislolano J, Frenkel M, Mafee MF. Progressive Hemifacial atrophy (Parry Romberg Disease). J Pediatr Oftamol Strabismus 1987; 24: 27-36.

21. Neville BW, Damm DD, Allen CN, Bouquot JE, eds. Patologica oral e Maxilofacial. Rio de Janeiro: Guanabara Koogan; 1998: 85.

22. Moore WH, Wong KS, Proudman TW, David DJ. Progressive Hemifacial atrophy (Romberg's disease): skeletal involvement and treatment. Br J Plast Surg 1993; 46:39-44.

23. da Silva-Pinheiro TP, Camarinha-da Silva C, Limeira-da Silveira CS, Botelho Ereno-PC, Rodrigues-Pinheiro MG, Viana-Pinheiro JJ. Progressive Hemifacial atrophy – Case Report. Med Oral Parol Oral Cir Bucal 2006; 11: E112-E114.

24. Zafarulla MY. Progressive Hemifacial atrophy: a case report. Br J Ophthalmol 1985; 69:669-76.

25. Asher S, Berg BO. Progressive hemifacial atrophy: Report of three cases , including one observed over 43 years and computer tomographic findings. Arch Neurol 1982;39:44-46.

26. Duymaz A, Karabekmez FE, Keskin M, Tosun Z. Parry-Romberg syndrome: facial atrophy and ots relationship with other regions of the body. Ann Plast Surg 2009;63:457-61

27. Grummons DC, Kappeye van de Coppello MA. A frontal asymmetry analysis. J Clin Orthod 1987;21:448-65

28. Harvold E. Cleft lip and palate: Morphological studies of the facial skeleton. Am J Orthod 1954;40:493-506

29. Athanasios A, van der Wij. Posteroantrior (Frontal) cephalometry. In: Athanasios A ed. Orthodontic cephalometry. London. Times Mirror Int. Publishers, Ltd. 1995: 141-62

30. Lagravere MO, Major PW. Proposed reference point for 3-dimensional cephalometric analysis with cone-beam computerized tomography. Am J Orthod Dentofacial Orthop 2005;128:657-60

4.3 A three-dimensional comparison of a morphometric and conventional cephalometric midsagittal planes for craniofacial asymmetry

Abstract

Introduction: Morphometric methods are used in biology to study object symmetry in living organisms and to determine the true plane of symmetry. The aim of this study was to determine if there are clinical differences between three-dimensional (3D) cephalometric midsagittal planes used to describe craniofacial asymmetry and a true symmetry plane derived from a morphometric method based on visible facial features. The sample consisted of 14 dry skulls (9 symmetric and 5 asymmetric) with metallic markers which were imaged with cone-beam computed tomography. An error study and statistical analysis were performed to validate the morphometric method. The morphometric and conventional cephalometric planes were constructed and compared. Results: The 3D cephalometric planes constructed as perpendiculars to the Frankfort horizontal plane resembled the morphometric plane the most in both the symmetric and asymmetric groups with mean differences of less than 1.00 mm for most variables. However, the standard deviations were often large and clinically significant for these variables. There were clinically relevant differences (>1.00 mm) between the different 3D cephalometric midsagittal planes and the true plane of symmetry determined by the visible facial features. Conclusions: The difference between 3D cephalometric midsagittal planes and the true plane of symmetry determined by the visible facial features were clinically relevant. Care has to be taken using cephalometric midsagittal planes for diagnosis and treatment planning of craniofacial asymmetry as they might differ from the true plane of symmetry as determined by morphometrics.

4.3.1 Introduction

In biology, bilateral symmetry is described as matching symmetry or object symmetry [1]. Matching symmetry refers to a structure of interest which is present in two separate copies of a mirror image of one another, each located on either side of the body. With object symmetry, the structure is symmetric within itself and therefore has an internal plane of symmetry so that the left and right halves are mirror images of each other. The human skull is an example of object symmetry. Therefore, clinical diagnosis and treatment planning in orthodontics and maxillofacial surgery of craniofacial asymmetry is reinforced by measurements made to an internal symmetry plane or midsagittal plane [2-7]. The symmetry plane of the skull is also fundamental in other areas of medicine, for example the study of functional and anatomical brain symmetry [8, 9].

In the literature, there is no consensus to which is the best or most accurate cephalometric plane to describe craniofacial asymmetry. Most cephalometric 3D analyses rely on midsagittal planes based on midline structures [4-7, 10, 11]. This has evoked some concerns regarding the validity of these reference planes because living organisms are hardly ever perfectly symmetric and a degree of facial asymmetry is a common phenomenon in nature [1, 12, 13]. The structures that lie in the midsagittal plane of the ideal body plan might also be affected. In other words, the surfaces containing the midline points can deviate from the true plane of symmetry. It has been suggested that internal structures of the skull is irrelevant to the visible facial symmetry i.e., the midline of the cranial base can deviate from the visible facial symmetry [15]. Although this is true for patients with pathological asymmetries for example plagiocephaly or hemifacial microsomia, it may also apply to other asymmetries and even symmetric skulls. Kwon et al. [7] studied a group of noncleft or plagiocephaly patients and found no difference in the cranial base between the symmetric and asymmetric groups and concluded that the cranial base structures were not dominant factors in explaining the degree of facial asymmetry. Provided that the internal structures of the skull are relevant to visual symmetry perception, this result suggests that the cranial base may be used as reference to determine the midsagittal plane for mild or moderate craniofacial asymmetries.

To overcome the possible problems of cephalometric midsagittal planes, shape analysis by means of morphometric methods such as Procrustes analysis and Euclidean distance matrix analysis has been applied to study craniofacial asymmetry [14, 16-20]. Morphometric methods are accepted in all fields of biology to determine the true plane of symmetry in structures with object symmetry [1]. Since the perception of symmetry

of faces is very important [20], the midsagittal plane used for diagnosis and treatment planning should be determined by the external visible facial features [16]. Landmark or surface-based Procrustes analysis uses visible facial features as reference to align original and mirrored images and therefore determines the true plane of symmetry relevant to facial perception. This morphometric approach has been shown to produce very accurate and reliable midsagittal planes that can be used for comparative study [15, 18-20].

Unfortunately, the extraction of the midsagittal plane by means of morphometrics requires additional training, additional software, and could be more costly which limits its clinical use. This might explain why 3D evaluation of craniofacial symmetry is still primarily performed with cephalometric methods [2-7]. However, these cephalometric planes might differ from the true plane of symmetry providing unreliable or even misleading information for the diagnosis and treatment planning.

Therefore, the aim of this study was to investigate if the cephalometric midsagittal planes using internal and midline structures are relevant to visible facial symmetry. Six cephalometric midsagittal planes described in the literature [2-7] were compared to the true plane of symmetry determined by morphometrics using visible facial features rather than internal landmarks as reference.

4.3.2 Materials and Methods

Materials

To reduce random error due to landmark identification, dry human skulls were used with radiopaque metal markers. The sample was selected from a collection of anonymous dry skulls from the Department of Orthodontics of the University Medical Center Groningen. No ethical approval was required. Two groups of skulls were studied: (1) a group with visible asymmetry and (2) a group with no visible asymmetry. Before the study sample was selected, the anatomical landmarks described in Table I were marked on the skulls with a pencil by means of consensus of two observers (JD and ZF). Visible deviation was defined as at least 4mm deviation of menton (Me) from the midline [6]. A midline was constructed with a laser beam passing through nasion (N) and the anterior nasal spine (ANS). For inclusion in the symmetric group, deviation of less than 4mm of Me from the constructed laser beam midline was a criterion. Because the growth of cranial base could be affected in subjects with congenital asymmetry, skulls with a cleft palate, hemifacial microsomia, or plagiocephaly were not considered. In both groups, the skulls also had to have a fixed occlusion, with the mandible fixed to the

skull by means of two metal springs. Ultimately, a total of 14 skulls (5 asymmetric and 9 symmetric) were included for this study. Prior to the radiographic examination, metal markers with a diameter of 1.5 mm were glued onto the selected landmarks (Table 1) with cyanoacrylate glue (Pattex, Nieuwegein, Netherlands).

Table I	Landmarks used in this study. ([a], no metal markers used)	
Landmarks and Abbreviation		**Definition**
Unilateral		
Sella	S	Center of the sella turcica (in this case the marker was placed in the center of the floor of sella turcica)
Nasion	N	Most anterior of the frontonasal suture in the median plane
Basion	Ba / MDFM	Middorsal point of the anterior margin of the foramen magnum
Point A	A	Point at the deepest midline concavity on the maxilla between the anterior nasal spine and prosthion
Pogonion	Pog	Most anterior point of the bony chin in the median plane
Menton	Me	Most inferior part of the bony chin in the median plane
Upper incisor contact	UI$_{contact}$	Contact point of the two central upper incisor teeth
Lower incisor contact	LI$_{contact}$	Contact point of the two central lower incisor teeth
Bilateral		
Orbitale	Or	Lowest point in the inferior margin of the orbit
Supra-orbital foramen [a]	SOF	Midpoint of the supraorbital foramen
Medial zygomaticofrontal suture [a]	MZF	Medial point on the orbital rim of the zygomaticofrontal suture
Frontonasomaxillare [a]	FNM	Intersection of the nasomaxillary, frontomaxillary and frontonasal sutures
Fontorbitomaxillare [a]	FOM	Lateral point of the frontomaxillary suture on the medial margin of the orbit
Foramen spinosum	FSp	Center of the foramen spinosum
Porion	Po / SLEAM	Superior lateral point of the external auditory meatus
Jugulare	J	Intersection of the outline of the maxillary tuberosity and the zygomatic buttress
First upper molar	U6	Tip of the mesiobuccal cusp of the maxillary first permanent molar
First lower molar	L6	Tip of the mesiobuccal cusp of the mandibular first permanent molar
Gonion	Go	Constructed point of intersection of the plane tangent to the posterior border of the ramus and a plane tangent to the inferior border of the mandible
Zygomatic arch point	Za	Most lateral border of the zygomatic arch
Anterior clinoid process	ACP	Tip of the anterior clinoid process
Lateral foramen magnum	LFM	Most lateral point of the foramen magnum
Generated by computer software for cephalometric analysis		
Anterior clinoid midpoint	ACP$_{midpoint}$	Midpoint between the left and right ACP
Foramen spinosum midpoint	ELSA	Midpoint between the left and right FSp
Foramen magnum midpoint	LFM$_{midpoint}$	Midpoint between the left and right LFM
Porion midpoint	Po$_{midpoint}$	Midpoint between the left and right Po

The cone-beam computed tomography (CBCT) images were acquired with the KaVo 3D eXam scanner (KaVo Dental GmbH, Bismarckring, Germany). The skulls were placed in the CBCT scanner with the Frankfort horizontal (FH) plane parallel to the floor and the midline laser beam of the CBCT scanner passing through N. The skulls were scanned with a 0.30-voxel size resolution (120 kV, 37.07mA s and 26.9 s). The CBCT datasets were exported from the eXamVisionQ (Imaging Sciences International LCC, Hatfield, PA, USA) software in DICOM multi-file format and imported into SimPlant®Ortho Pro 2.1 software (Materialise Dental, Leuven, Belgium). Surface models for suitable visualization of the hard tissues were created, and the landmarks described in Table I were digitized using the middle of the metal markers as reference.

After the landmarks were digitized, the software automatically constructed the cephalometric 3D midsagittal planes (Table II) commonly used for 3D cephalometric assessment of craniofacial asymmetry in maxillofacial surgery planning [4-7, 10, 11]. These planes were divided into two groups according to the method of construction, i.e., by connection of three midline structures (1, 2 and 3) or by connection of two midline structures perpendicular to a horizontal plane (4, 5 and 6). The software measured the distances illustrated in Fig. 1A by means of preprogrammed analyses. The distances were measured three times for each skull and the mean used as the reference value.

Table II	The cephalometric midsagittal planes used for this study

Definition of the cephalometric 3D midsagittal planes

A. Midsagittal plane through 3 midline structures

1   Vertical plane passing through points S, N, and ANS

2   Vertical plan passing through S, N, and Me

3   Vertical plane passing through the midpoint between the most lateral points on the foramen magnum, the midpoint between the anterior clinoid processes and N

B. Midsagittal plane through 2 midline structures and perpendicular to a horizontal plane

4   Vertical plane passing through points S, N and perpendicular to the Frankfort horizontal plane (FH)[a]

5   Vertical plane passing through the superior point of the Cg, a midpoint between the two anterior clinoid processes and perpendicular to the FH plane

6   Vertical plane passing through points ELSA, MDFM and perpendicular to an alternative horizontal plane (XY)[b]

[a] = FH: The Frankfort horizontal plane, a plane passing through the bilateral landmarks of Or and Po$_{midpoint}$

[b] = XY: An alternative horizontal plane passing through the bilateral points of SLEAM and point ELSA

Morphometric method to determine the midsagittal plane

To determine the true midsagittal plane, the original and mirrored surface models were matched using partial Ordinary Procrustes Analysis (OPA) [16, 21]. After the hard-tissue surface models were segmented with the SimPlant®Ortho software, digital markers with

an Ø of 2.4 mm were imported as STL files and placed in the landmark configuration position, which serves as reference for the OPA. Visible facial anatomical landmarks were used in the supraorbital and nasal bridge region (Table I) that can be accurately identified by using the volume renderings and the cross-sectional slices in all three planes of the CBCT images. The infraorbital landmarks and zygomatic bones were not considered because they could be affected by midface deficiencies [22]. In addition, since most mandibular asymmetry and mild maxillary asymmetry are corrected with bilateral sagittal split osteotomies, genioplasty or Le Fort I surgery, the selected landmark configuration can be considered as stable reference marks for surgical planning [23] (Fig. 1B).

Figure 1 A: Linear measurements to the midsagittal plane. 1: Maxillary rotation (Point A – MSP); 2: Maxillary dental midline deviation (UI$_{contact}$ – MSP); 3: Facial width (Zy – MSP); 4: Maxillary width (J – MSP); 5: Maxillary dental width (U6 – MSP); 6: Mandibular rotation (Pog – MSP); 7: Mandibular dental midline deviation (LI$_{contact}$ – MSP); 8: Mandibular width (Go – MSP). B: Frontal view of a 3D volume rendering of a skull used for this study. The positions landmark configuration (green markers) is illustrated (also see Table I)
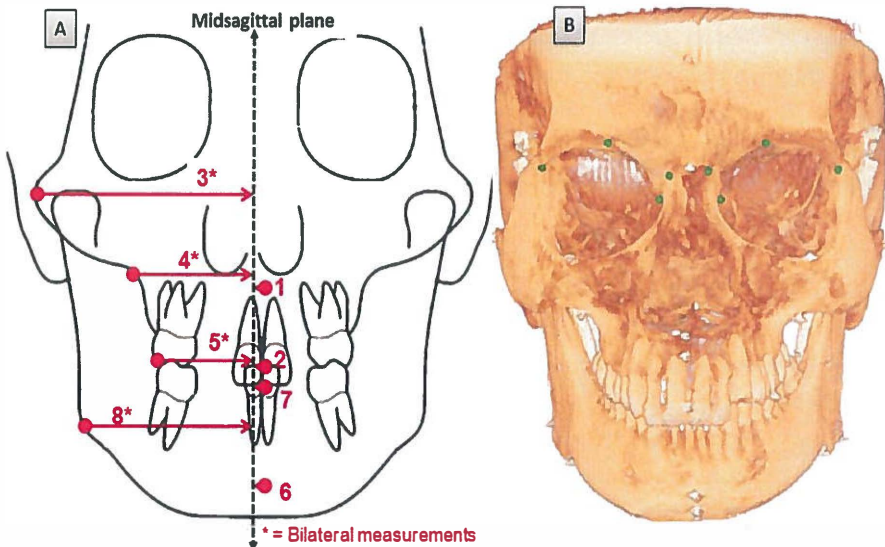
The centroid positions were calculated with the software using the coordinate values of the landmark configuration. Mirror images of the original surface models, digital landmark configurations, and centroids were created around an arbitrary plane with the mirror tool of the software (Fig. 2). Shape alignment by means of partial OPA involves two steps: translation and rotation [21]. First, the centroid markers of the original and mirrored surface models were superimposed using the translation function of the software.

Rotation of the mirrored landmark configuration around the geometric midpoint of the superimposed centroid markers followed until the best fit between all homologous landmarks were achieved by means of the least squared point distance whist preserving the shape and size of each configuration [16] (Fig. 2). The individual symmetrical configuration of point ANS, pogonion and sella (S) was calculated as the mean of the original and mirrored landmarks. The software program created the midsagittal plane by constructing plane through the middle of these individual symmetrical configurations. Subsequently, the 12 linear distances illustrated in Fig. 1A were measured three times for each skull and the mean used as the reference value. In addition, the deviation from point N to the morphometric plane was also measured. An error study was performed after a 3-week interval to validate the morphometric method. Wilcoxon signed-rank sum test was used to detect differences between the two morphometric midsagittal values. Agreement between the measurements was tested by the Pearson correlation coefficient. The standard error of measurement (SEM) of the repeated measurements was calculated as the square root of the variance of the random error from a two-way random effect ANOVA. The smallest detectable difference (SDD) was then calculated as $1.96 \times \sqrt{2} \times$ SEM [24].

Comparison of the cephalometric midsagittal planes

The mean values and standard deviations were calculated for the 12 linear measurements of all the cephalometric 3D midsagittal planes. The mean of the repeated morphometric values of the error study was used as the reference values for comparison. The clinical accuracy of the cephalometric midsagittal planes was compared by means of the absolute error (AE). The AE was defined as the reference (morphometric) midsagittal plane values subtracted by the cephalometric midsagittal plane value. Additionally, Mann-Whitney tests were used to detect possible differences between the asymmetric and symmetric groups. P values of less than 0.05 were

considered significant. All statistics were performed with a standard statistical software package (SPSS version 16, Chicago, IL).

4.3.3 Results

The results of the error study (Table III) validated the morphometric midsagittal plane and confirmed its accuracy and reliability previously reported [15, 18-20]. There were no statistical differences between the measurements (P = 0.25-0.97) and the agreement was high (r = 0.845-0.999). The small method error (mean = 0.39 mm; 95% CI = 0.31-0.47 mm) is more than clinically acceptable for cephalometric measurements and confirmed the accuracy of the method [25]. The mean and standard deviation of all the midsagittal planes are illustrated in Table IV. When comparing the cephalometric values to the morphometric values by means of the AE, a large variation was seen in both symmetrical and asymmetrical groups (Table V). As expected, the midsagittal planes constructed by connecting midline structures (1-3) resembled the morphometric plane more closely in the symmetric group; however, the mean differences were still more than 1.00 mm. In both groups, the values of the midsagittal planes (4 and 5) constructed as perpendiculars to the FH plane were clinically the most accurate in resembling the morphometric values. For most of the measurements of these planes, the mean absolute errors were less than 1.00 mm.

The differences between the values of midsagittal planes 1-3 and 6 can be considered clinically relevant (>1.00 mm) compared to the morphological values in both groups. The amount of mandibular rotation in the asymmetric group was 7.22 ± 5.18 mm compared to 1.72 ± 1.11 mm in the symmetric group. This was the only variable significantly different (P = 0.01) between the symmetric and asymmetric skulls. Further analysis of the asymmetric skulls revealed that the main causes of asymmetry were probably due to differences between the bilateral ramus and/or mandibular body lengths. There were clinically significant (> 1.00 mm) differences between the ramus lengths only or the mandibular body lengths only in two skulls. In three skulls, clinically significant differences were found in both the ramus and mandibular body lengths.

Figure 2 *Morphometric method by means of OPA of original and mirrored 3D surface models used to derive the midsagittal plane.*
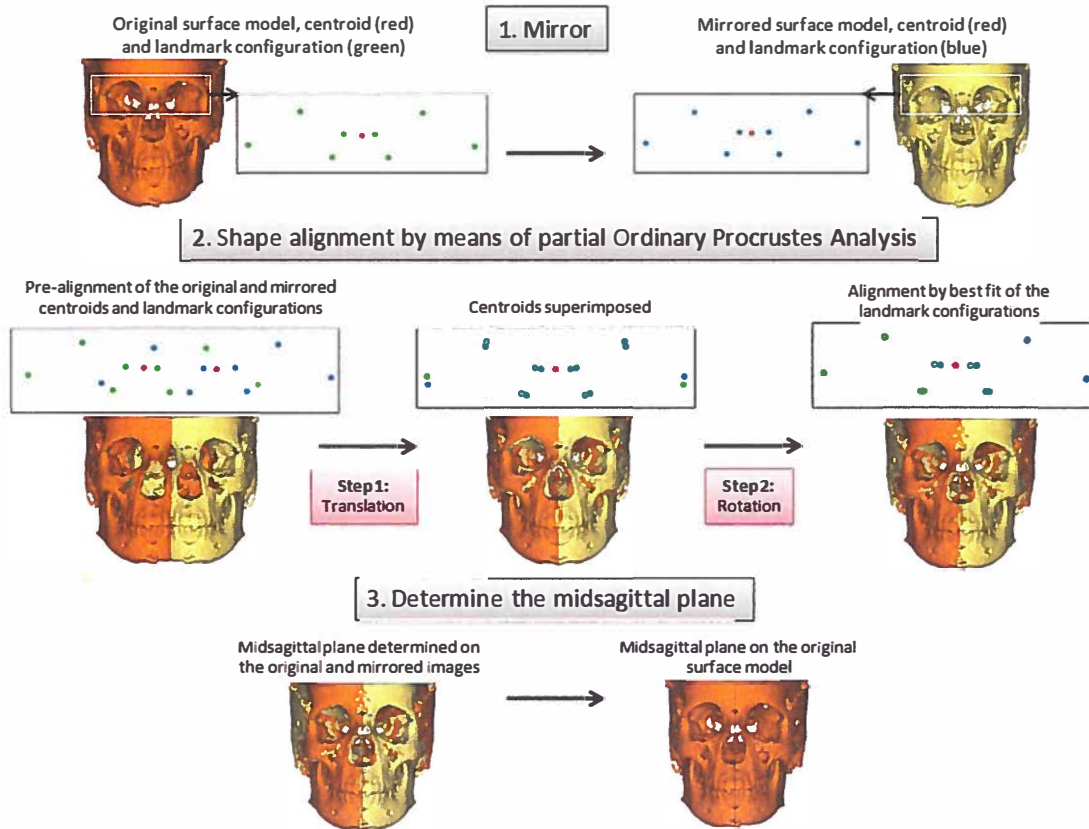
Table III	Validity of the morphometric method used in this study (values in mm)							
	(A) Morphometric 1		(B) Morphometric 2		Method Error		(A) vs. (B)	
Variable	Mean	SD (±)	Mean	SD (±)	SEM	SDD (95%)	r	P
Asymmetric group (n=5)								
Maxillary rotation	1.38	0.73	1.56	0.55	0.07	0.21	0.904	0.60
Maxillary dental rotation	1.25	0.81	1.36	1.05	0.10	0.28	0.930	0.92
Facial width left	60.87	2.32	61.00	1.96	0.08	0.21	0.991	0.92
Facial width right	64.24	1.06	63.83	1.03	0.25	0.70	0.895	0.47
Maxilla width left	34.69	1.22	34.80	1.20	0.06	0.18	0.975	0.75
Maxilla width right	38.21	1.62	38.01	1.89	0.08	0.23	0.988	0.60
Maxilla dental width left	28.26	1.52	28.42	1.65	0.25	0.71	0.938	0.60
Maxilla dental width right	28.51	2.70	28.38	3.08	0.16	0.44	0.989	0.75
Mandibula rotation	7.02	5.32	7.42	5.06	0.16	0.45	0.998	0.92
Mandibula dental rotation	1.89	2.18	2.09	2.61	0.17	0.48	0.984	0.75
Mandibula width left	44.05	3.20	44.08	3.03	0.22	0.63	0.985	0.92
Mandibula width right	44.66	1.53	44.47	1.97	0.24	0.67	0.954	0.75
Nasion deviation	0.27	0.15	0.40	0.30	0.02	0.07	0.845	0.25
Symmetric group (n=9)								
Maxillary rotation	1.12	0.81	1.14	0.54	0.11	0.30	0.850	0.69
Maxillary dental rotation	1.11	0.54	1.08	0.87	0.08	0.23	0.904	0.76
Facial width left	58.12	4.09	58.08	3.85	0.06	0.17	0.998	0.90
Facial width right	59.48	4.21	59.37	4.32	0.03	0.07	0.999	0.76
Maxilla width left	35.50	2.55	35.31	2.49	0.11	0.30	0.984	0.97
Maxilla width right	37.67	3.40	37.53	3.70	0.08	0.23	0.997	0.83
Maxilla dental width left	25.72	2.00	25.73	1.86	0.12	0.32	0.982	0.97
Maxilla dental width right	26.65	2.85	26.59	2.99	0.10	0.28	0.993	0.97
Mandibula rotation	1.70	1.19	1.74	1.09	0.18	0.51	0.914	0.93
Mandibula dental rotation	1.52	1.00	1.62	0.95	0.11	0.31	0.934	0.76
Mandibula width left	43.31	4.46	43.44	4.34	0.25	0.68	0.993	0.97
Mandibula width right	45.07	3.80	44.79	4.05	0.29	0.79	0.991	0.90
Nasion deviation	0.55	0.27	0.33	0.26	0.02	0.06	0.871	0.93

* P values of 0.05 and less considered significant
SEM standard error of measurement
SDD (95%) smallest detectable difference
r intra-observer agreement
SD Standard deviation

| Table IV | The mean and standard deviation of the different midsagittal planes of the asymmetric and symmetric skulls |

	Morphometric midsagittal plane		Cephalometric midsagittal planes											
			A. 3 Midline structures only						B. 2 Midline structures perpendicular to a horizontal plane					
			1		2		3		4		5		6	
Variable	Mean	SD(±)	Mean	SD(±)	Mean	SD(±)	Mean	SD(±)	Mean	SD(±)	Mean	SD(±)	Mean	SD(±)
Asymmetric group (n=5)														
Maxillary rotation	1.47	0.62	0.76	0.31	4.84	2.38	3.41	0.62	1.33	0.85	1.81	1.17	1.03	0.59
Maxillary dental rotation	1.31	0.91	1.86	0.75	5.63	3.10	3.92	1.34	1.20	0.42	1.74	0.87	2.21	0.41
Facial width left	60.94	2.14	62.15	1.57	60.94	3.27	61.26	1.64	61.65	1.87	62.12	1.85	62.13	1.79
Facial width right	64.04	0.99	62.84	1.53	63.56	1.41	63.62	1.39	63.37	1.22	62.85	1.33	62.89	1.92
Maxilla width left	34.75	1.20	36.50	1.11	33.80	3.83	33.71	1.17	35.17	1.13	35.18	1.22	36.15	1.59
Maxilla width right	38.11	1.75	36.35	2.22	38.86	2.67	39.11	1.72	37.73	1.22	37.71	0.97	36.72	2.34
Maxilla dental width left	28.34	1.54	31.06	1.86	26.82	6.68	26.54	2.48	28.89	2.45	28.83	2.77	30.21	2.65
Maxilla dental width right	28.45	2.88	25.73	3.81	30.19	5.21	30.45	2.95	28.06	2.28	28.14	2.03	26.63	4.05
Mandibula rotation	7.22	5.18	10.04	5.55	0.52	0.62	6.65	6.54	6.44	4.64	5.97	4.57	9.23	6.13
Mandibula dental rotation	1.99	2.39	4.24	0.77	3.67	3.39	3.04	3.52	1.52	1.68	1.58	1.52	3.61	1.76
Mandibula width left	44.06	3.09	47.71	3.18	43.62	6.98	43.22	2.78	45.47	2.64	46.26	2.65	46.40	2.92
Mandibula width right	44.57	1.72	40.92	2.27	45.30	5.84	45.36	2.17	43.31	1.71	42.48	1.38	42.22	2.84
Symmetric group (n=9)														
Maxillary rotation	1.13	0.67	0.47	0.34	1.34	1.09	1.98	1.51	1.02	0.62	1.37	1.08	1.01	0.69
Maxillary dental rotation	1.10	0.70	1.65	0.73	0.89	1.00	2.20	1.85	0.79	0.79	0.82	0.78	1.47	1.15
Facial width left	58.10	3.85	59.31	4.35	58.77	4.34	58.56	4.00	58.85	4.37	58.64	4.30	59.11	4.22
Facial width right	59.43	4.14	57.90	3.69	58.50	3.80	58.69	4.02	58.69	4.28	58.86	3.71	58.13	3.82
Maxilla width left	35.41	2.45	36.78	3.34	35.40	3.10	35.13	2.44	35.62	3.36	35.58	2.99	36.36	3.16
Maxilla width right	37.60	3.45	36.18	2.61	37.57	2.87	37.82	3.50	37.39	2.67	37.46	3.24	36.64	2.70
Maxilla dental width left	25.73	1.87	27.72	2.12	25.54	2.00	25.09	1.20	25.73	1.92	25.80	2.30	26.59	1.55
Maxilla dental width right	26.62	2.83	24.62	2.88	26.87	2.64	27.28	4.27	26.34	2.78	26.39	2.76	25.80	3.32
Mandibula rotation	1.72	1.11	2.75	1.81	0.74	0.57	2.76	1.89	2.00	1.16	2.10	1.24	2.31	2.13
Mandibula dental rotation	1.57	0.95	1.53	1.04	1.15	0.90	2.51	1.80	1.51	1.03	1.54	1.31	1.64	1.39
Mandibula width left	43.37	4.27	45.35	4.48	44.43	5.08	43.80	3.64	43.76	4.58	44.28	4.34	44.67	4.39
Mandibula width right	44.93	3.82	42.81	5.24	43.76	3.40	44.36	4.51	44.49	3.90	43.98	4.23	43.60	3.82

SD Standard deviation

Table V	Clinical differences determined by means of the absolute error of the cephalometric midsagittal planes (1-6) when compared to the morphometric reference midsagittal plane

Cephalometric midsagittal planes Vs. Morphometric midsagittal plane

	A. 3 Midline structures only						B. 2 Midline structures perpendicular to a horizontal plane					
	1		2		3		4		5		6	
Variable	Mean	SD(±)	Mean	SD(±)	Mean	SD(±)	Mean	SD(±)	Mean	SD(±)	Mean	SD(±)
Asymmetric group (n=5)												
Maxillary rotation	0.82	0.39	3.37	1.94	1.94	0.90	0.40	0.36	0.71	0.46	0.89	0.16
Maxillary dental rotation	0.98	0.62	4.33	2.99	2.62	1.07	0.53	0.59	1.02	0.45	1.18	0.45
Facial width left	1.21	0.63	1.06	1.02	0.73	0.26	0.87	0.28	1.28	0.70	1.20	0.93
Facial width right	1.20	0.60	0.87	1.35	0.62	0.24	0.73	0.38	1.19	0.72	1.15	1.03
Maxilla width left	1.75	0.77	2.89	1.84	1.11	0.69	0.53	0.36	0.69	0.53	1.62	1.05
Maxilla width right	1.76	0.87	2.85	1.85	1.07	0.70	0.50	0.44	0.66	0.61	1.70	1.01
Maxilla dental width left	2.72	1.22	4.76	3.09	1.80	1.33	0.84	0.73	1.00	0.95	2.25	1.48
Maxilla dental width right	2.72	1.39	4.97	3.25	2.00	1.07	0.58	0.67	0.70	0.84	2.20	1.48
Mandibula rotation	3.85	1.62	6.70	5.38	2.44	1.06	0.85	1.30	1.30	1.14	3.03	1.80
Mandibula dental rotation	2.76	1.39	3.36	3.47	1.38	1.22	0.54	0.69	0.62	0.72	2.42	1.55
Mandibula width left	3.65	1.06	4.71	4.74	0.98	1.19	1.47	1.12	2.20	1.41	2.34	1.36
Mandibula width right	3.65	1.17	4.63	4.19	0.83	1.06	1.31	1.07	2.09	1.36	2.34	1.47
Symmetric group (n=9)												
Maxillary rotation	0.75	0.65	1.11	0.67	1.23	1.19	0.70	0.40	0.72	0.50	0.78	0.62
Maxillary dental rotation	1.27	0.37	0.98	0.76	1.48	1.42	0.56	0.49	0.69	0.36	1.11	0.83
Facial width left	1.38	0.93	0.99	0.89	0.69	0.68	0.99	0.90	0.96	0.88	1.41	1.21
Facial width right	1.52	1.15	1.07	1.02	0.81	0.88	0.92	0.68	0.93	0.83	1.49	1.26
Maxilla width left	1.52	0.81	0.95	0.55	1.00	0.73	0.85	0.69	0.78	0.60	1.13	0.94
Maxilla width right	1.65	0.79	0.96	0.56	0.99	0.71	0.82	0.75	0.63	0.65	1.15	0.90
Maxilla dental width left	2.17	1.03	1.22	0.73	1.64	1.13	0.80	0.71	0.72	0.32	1.21	0.85
Maxilla dental width right	2.60	0.83	1.38	1.05	1.97	1.39	0.65	0.49	0.71	0.37	1.58	0.86
Mandibula rotation	1.77	1.13	1.09	0.88	2.02	1.61	1.00	0.62	0.88	0.57	2.03	1.11
Mandibula dental rotation	1.48	0.75	0.99	0.65	1.29	1.15	0.73	0.55	0.76	0.35	1.49	0.93
Mandibula width left	2.42	1.17	1.88	1.48	1.32	0.97	0.91	0.50	1.24	0.82	1.30	0.91
Mandibula width right	2.48	1.34	1.96	1.63	1.41	0.99	0.90	0.45	1.22	0.78	1.33	0.87

SD Standard deviation

4.3.4 Discussion

The results of this study show that there were clinically relevant differences between cephalometric midsagittal planes and the true plane of symmetry on CBCT images. Therefore, the additional cost of extra software to extract a morphometric midsagittal plane might outweigh the risk of misdiagnosis or inaccurate treatment planning of craniofacial asymmetry. In addition, other advantages of a morphometric midsagittal plane further justify its use. A major advantage is that it can compute the midsagittal plane using intact regions unaffected by the asymmetry [16, 19, 20], and therefore can be used to determine the midsagittal plane in severe and congenital asymmetries. This is not always possible when using cephalometric planes based on anatomical landmarks, i.e. the auditory meatus might be affected in congenital malformations which would make the Frankfort horizontal plane unreliable. Other advantages of a midsagittal plane computed with morphometric methods are: it is very reliable, it can be simple and quick (newer software can automatically extract the midsagittal plane), it can be applied to 3D datasets from laser surface scanners and stereophotogrammetry, and all to computerized tomography imaging [15, 16, 18-20].

We used dry skulls and metal markers aiming to reduce the measurement error. Although the asymmetric sample size can be regarded as small, it can be justified because the method error was very small and able to detect true clinical differences between the different midsagittal planes. In addition, it must be noted that the sample is unique and that asymmetric dry skulls are difficult to acquire for comparative study. Jacobsen et al. [26] defined the 3D midsagittal plane as a midline plane bisecting the head sagittally through point N when viewing the patient in natural head position (NHP) from the frontal view. Therefore, the midsagittal plane derived from the NHP is based on the visual perception and does not rely on internal structures. In the present study 3D reference planes based on the NHP could not be investigated because dry skulls were used. However, we found that the mean deviation of point N from the morphometric midsagittal plane was less than 0.50 mm in both groups suggesting its suitability as reference point in both groups. Future research may investigate if the NHP is more suitable and reliable than the anatomical landmarks for the construction of standardized planes for cephalometric analysis with CBCT imaging.

Trpkova et al. [27] studied two-dimensional radiographs of various asymmetries and concluded that vertical lines constructed as perpendiculars through midpoints between bilateral pairs of orbital landmarks are more accurate and valid than those constructed between two midpoints. Although we studied 3D images, the results of the present

study are in agreement with this conclusion. The values from midsagittal planes constructed as perpendiculars to the FH plane showed the least differences from the morphometric values. The midsagittal plane constructed as a perpendicular to the FH plane passing through N and S mimicked the morphometric plane the best in both groups. However, care should be taken to apply these data for clinical use. Although the mean differences between this plane and the morphometric plane were less than 1.00 mm for most measurements, the standard deviation was often large and significant [25]. In addition, our sample did not include congenital asymmetries or asymmetries of the midface. This is important as the FH plane might be invalid as reference plane for congenital asymmetries and asymmetries associated with midface deficiencies.

Recently, a standardized plane orientation for 3D cephalometric analysis was used to describe asymmetry [4, 28]. When using these planes, the effect of the positioning of the patients head during image acquisition is eliminated. The landmarks used to construct the planes were shown to be very reproducible, and all points are located on sutures that are not significantly affected by growth after 5 years of age [4, 28]. Yàñez-Vico et al. [4] reported an intraobserver error of 1.36 mm for linear measurements and 0.91° for angular measurements using this plane orientation. However, it must be noted that their measurements were not made to the midsagittal plane but derived from the subtraction of left and right side measurements. Importantly, we found that a geometric principal described by Nagasaka et al. [29] has a significant effect on the measurements to the midsagittal plane. This principal illustrated that the distances between landmarks also have an influence on the magnitude of measuring error of the linear and angular measurements and that the more close two landmarks are, the greater the angular measurement error tends to be. This geometric principal has a significant 3D effect on the construction of the midsagittal plane because the landmarks of foramen spinosum midpoint (ELSA) and MDFM are very close to each other. Therefore, a 0.40 mm deviation of MDFM could result in 6.15 mm difference of the variable used to measure mandibular deviation in one of the skulls (Fig. 3). Although the landmarks are situated on sutures and not affected by growth after 5 years of age, differences in remodeling occur which may result in small asymmetries [30]. Therefore, the midsagittal plane of this "standardized" plane orientation might not be valid for asymmetry analysis.

The large variations of the cephalometric midsagittal planes in the symmetric group were somewhat surprising but can possibly be explained by the fact that a perfect "symmetric" face does not really exist and a degree of facial asymmetry is inherent for every individual [1, 12, 13]. Therefore, midline landmarks used to construct 3D

midsagittal planes are also likely to deviate from the true plane of symmetry. Moreover, the combined 3D effect when connecting two or more of the off-center midline points resulting from small regional remodeling could produce a significant deviation from the actual plane of symmetry. This supports the suggestion that internal structures of the skull may be irrelevant to the visible facial symmetry, even in symmetric skulls. Therefore, determining an absolute midsagittal plane based on midline cephalometric points will vary among individuals and remains questionable.

Figure 3 A: Midsagittal plane constructed connecting landmarks MDFM and ELSA perpendicular to the horizontal plane XY. B: A small lateral deviation (0.40 mm) in MDFM results in significantly greater the linear measurement error when measuring Pog to the midsagittal plane (6.15 mm difference)
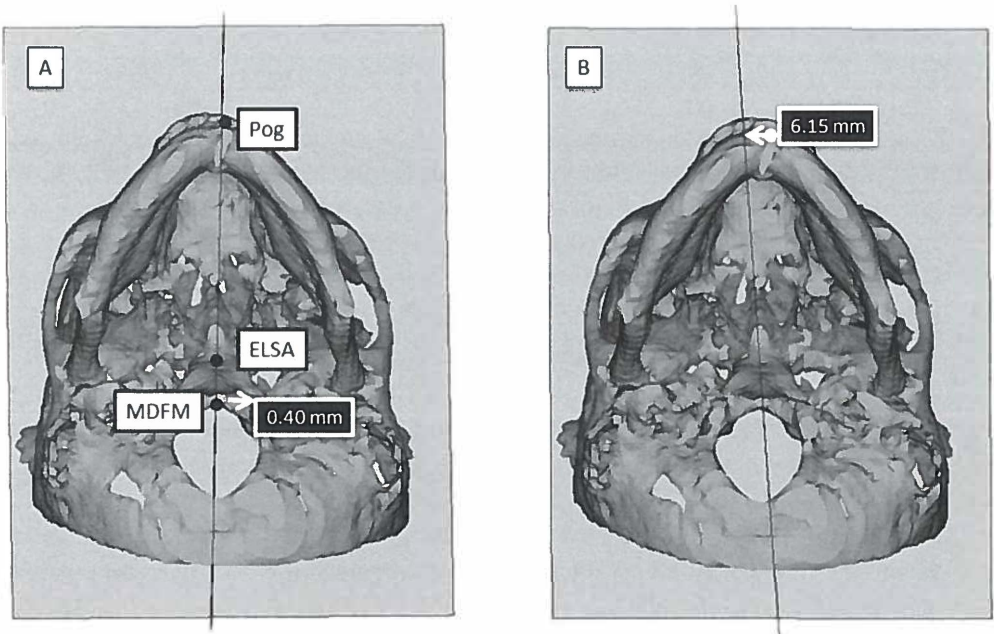
4.3.5 Conclusion

Clinical relevant differences exist between the different 3D cephalometric midsagittal planes and the true plane of symmetry determined by the visible facial features. When

using the cephalometric planes based on midline structures for clinical diagnosis and treatment planning of craniofacial asymmetry, care has to be taken as they might differ from the true plane of symmetry. A morphometric approach to determine the midsagittal plane using visually intact regions of the skull not affected by the asymmetry as the reference might be more valuable for diagnosis and treatment planning of craniofacial asymmetry.

4.3.6 References

1. Klingenberg CP, Barluenga M, Meyer A (2002) Shape analysis of symmetric structures: Quantifying variation among individuals and asymmetry. Evolution 56: 1909-1920
2. Profitt WR, Turvey TA (1991) Dentofacial asymmetry. In Profitt WR, White Jr RP (eds). Surgical orthodontic treatment. Mosby, St Louis, pp 483-549
3. Hwang H-S, Hwang CH, Lee K-H, Kang B-C (2006). Maxillofacial 3-dimensional analysis for the diagnosis of facial asymmetry. Am J Orthod Dentofacial Orthop 130: 779-785
4. Yàñez-Vico RM, Iglesias-Linares A, Torres-Lagares D, Gurierrez-Perez JL, Solano-Reina E (2010) Three- dimensional evaluation of craniofacial asymmetry: an analysis using computed tomography. Clin Oral Invest. doi: 10.1007/s00784-010-0441-7
5. Tuncer BB, Atac MS, Yuksel S (2009) A case report comparing 3-D evaluation in the diagnosis and treatment planning of hemimandibular hyperplasia with conventional radiography. J Craniomaxillofac Surg. doi: 10.1016/j.jcms.2009.01.004
6. Baek S-K, Cho I-S, Chang Y-I, Kim M-J (2007) Skeletodental factors affecting chin point deviation in female patients with class III malocclusion and facial asymmetry: a three dimensional analysis using computed tomography. Oral Surg Oral Med Oral Pathol Oral Radiol Endod 104: 628-39
7. Kwon T-G, Park H-S, Ryoo H-M, Lee S-H (2006) A comparison of craniofacial morphology in patients with and without facial asymmetry – a three-dimensional analysis with computed tomography. Int J Oral Maxillofacial Surg 35: 43-48
8. Junck L, Moen JG, Hutchins GD, Brown MB, Kuhl DE (1990) Correlation methods for the centering, rotation and alignment of functional brain images. J Nuclear Med 31: 1220-1226
9. Lui Y, Collins RT, Rothfus WE (2001) Robust midsagittal plane extraction from normal and pathological 3-D neuroradiology images. IEEE Trans Med Imaging 20: 175-192
10. Swennen GJR, Schutyser F, Hausamne JE (2005) Three-dimensional cephalometry. A color atlas and manual. Heidelberg Springer, Berlin, pp 183 – 226
11. Damstra J, Oosterkamp BCM, Jansma J, Ren Y (2010) Combined 3-dimensional and mirror-image analysis for the diagnosis for asymmetry. Accepted for publication, Am J Orthod Dentofacial Orthop
12. Gawilkowska A, Szczurwski J, Czerwinski F, Miklaszwenska D, Adamiec A, Dzieciolowska E (2007) The fluctuating asymmetry of mediaeval and modern human skulls. Homo 58: 159-172
13. Haraguchi S, Iguchil Y, Takada K (2008) Asymmetry of the face in orthodontic patients. Angle Orthod 78: 421-426

14. Ferrario VF, Sforsa C, Poggio CE, Tartaglia G (1994) Distance from symmetry: A three-dimensional evaluation of facial asymmetry. J Oral Maxillofac Surg 52: 1126 – 1132

15. De Momi E, Chapuis J, Pappas I, Ferrigno G, Hallerman W, Schramm A, Caversaccio M (2006) Automatic extraction of the mid-facial plane for craniomaxillofacial surgery planning. Int J Oral Maxillofac Surg 35: 636 – 642

16. Hajeer MY, Ayoub AF, Millet DT (2004) Three-dimensional assessment of facial soft-tissue asymmetry before and after orthognathic surgery. Br J Oral Maxillofac Surg 42: 396-404

17. McIntyre GT, Mossey PA (2003). Size and shape measurement in contemporary cephalometrics. Eur J Orthod 25: 231-242

18. Hartman J, Meyer-Marcotty P, Hausler G, Stellzig-Eisenhauer A (2007) Reliability of a method for computing facial symmetry plane and degree of asymmetry based on 3D-data. J Orofac Orthop 68: 477-490

19. Benz M, Laboureux X, Maier T, Nkenke E, Seeger S, Neukam FW et al (2002) The symmetry of faces. In: Greiner G, Niemann H, Ertl T, Girod B, Seidel HP (eds) Vision, modelling and visualization. IOS, Amsterdam, pp 332-339

20. Meyer-Marcotty P, Alpers GW, Gerdes ABM, Stellzig-Eisenhauer A (2010) Impact of facial asymmetry in visual perception: a 3-dimensional data analysis. Am J Orthod Dentofacial Orthop 137: 168.e-168.e8

21. Dryden IL, Mardia KV (1998) Statistical shape analysis. Wiley, Chichester, pp 45-47

22. Moro A, Correra P, Boniello R, Gaspari G, Pelo S (2009) Three-dimensional analysis in facial asymmetry: comparison with model analysis and conventional two-dimensional analysis. J Craniofac Surg 20: 417-422

23. Reyneke JP (2003) Basic guidelines for the diagnosis and treatment of specific dentofacial deformities. In: Reyneke JP (ed) Essentials of orthognathic surgery. Quintessence Publishing Co Inc , Hanover Park, pp 230-245.

24. Damstra J, Fourie Z, Huddleston Slater JJ, Ren Y (2010) Accuracy of linear measurements from cone-beam computed tomography-derived surface models of different voxel sizes. Am J Orthod Dentofacial Orthop 137: 16.e.1 – 16.e.6

25. Richardson A (1981) A comparison of traditional and computerized methods of cephalometric analysis. Eur J Orthod 3: 15-20

26. Jacobson RL (2006) Three-Dimensional Cephalometry. In: Jacobson A, Jacobson RL (eds) Radiographic Cephalometry: From Basics to 3-D Imaging, 2nd edn. Quintessence Publishing Co Inc, Hanover Park, pp 233-47

27. Trpkova B, Prasad NG, Lam EWN, Raboud D, Glover KE, Major PW (2003) Assessment of facial asymmetries from posterior cephalograms: Validity of reference lines. Am J Orthod Dentofacial Orthop 123: 512-520

28. Lagravere MO, Hansen L, Harzer W, Major PW (2006) Plane orientation for standardization in 3-dimensional cephalometric analysis with computerized tomography imaging. Am J Orthod Dentofacial Orthop 129: 601-604

29. Nagasaka S, Fujimora T, Segoshi K (2003) Development of a non-radiographic cephalometric system. Eur J Orthod 25: 77-85

30. Kim YH, Sato K, Mitani H, Shimizu Y, Kikuchi M (2003) Asymmetry of the sphenoid bone and its suitability as a reference for analysing craniofacial asymmetry. Am J Orthod Dentofacial Orthop 124: 656-66

Chapter 5

General discussion

5. 1. Introduction

The 3D CBCT images offer a unique and new appreciation of the anatomical structures and underlying anomalies not possible with conventional radiographs.[1-4] However, in almost all aspects of CBCT imaging, from utilization to application, inherent limitations and pitfalls exist. Indications and guidelines for the use of CBCT imaging for orthodontics are currently controversial because CBCT imaging exposes the patient to a higher radiation dose than conventional cephalograms.[5-11] Technical difficulties that start with acquisition of the scan by positioning the patient in the natural head position (NHP) could be problematic.[12,13] Determining the correct scanning parameters for each indication is also essential in order to keep radiation exposure as low as possible.[7] Moreover, beam inhomogeneity of CBCT imaging causes difficulties and inaccuracies of the volume rendering and segmentation processes.[14-17] The addition of the third dimension has also brought about new challenges regarding interpretation of the 3D data.[18] This is certainly true for orthodontists trained exclusively in 2D cephalometry. A transition from 2D to 3D cephalometry requires additional training for the clinician to enable correct interpretation of the 3D data and full appreciation of the new possibilities of CBCT imaging.[2]

Since correct and accurate application of CBCT imaging in orthodontics and orthognathic surgery depends largely on the user's appreciation of the limitations inherent in the method, the general aim of this research project was to explore some of the potential limitations and pitfalls of CBCT in cephalometry and to investigate possible solutions. In the following discussion, the general aims and specific research aims described in Chapter 1 will be addressed in relation to the main results. In addition, the clinical relevance of the findings and future perspectives regarding CBCT imaging and 3D cephalometry will be explored.

5.2. Validity of 2D and 3D cephalometric measurements

Orthodontists are very attentive to detail and therefore tend to be very fussy about precision in cephalometrics.[19] However, to make valid conclusions from cephalometric measurements, the smallest detectable difference (SDD) should be determined in order to detect significant ($\alpha = 0.05$) change. The SDD describes the 95% confidence limit of the measurement error as recommend by the International Organization of Standardization.[19-27] Previous literature has argued that these limits might be too strict

to apply to cephalometric measurements.[28] This is perhaps why Dahlberg's formula has always been the accepted method of determining the measurement error in orthodontics.[28,29] However, Dahlberg's formula is not able to detect change at a level of $\alpha = 0.05$ which limits its application in clinical related studies.

The results of the studies in this manuscript confirm that the presumed sub millimeter precision of cephalometric measurements, whether 2D or 3D, is a myth. [19-21] Our results also confirm the need to quantify the measurement error in addition to reporting the reliability of measurements by means of correlation coefficients.[22] In the literature, the magnitude of the clinical significance for cephalometric measurements varies, but is usually regarded as a difference of less than 1 measuring unit.[30] The SDD of almost all 2D and 3D measurements in our studies are more than one measuring unit and can therefore be regarded as clinically relevant.[19,20] However, it is questionable whether one measuring unit really determines actual clinical significance. Alternatively it might be suggested that clinical relevance should be related to the index considered e.g., an error of 1° of the SNA or SNB angle could be considered less pronounced than a 1mm error for the WITS appraisal. However, a very high degree of accuracy is required if the goal is to assess growth changes or to perform surgical planning. Therefore, future research might investigate and address specific values to determine clinical relevance for specific measurements. Nevertheless, the measured difference between two observations must be at least equal or larger than the SDD for any specific measurement in order to be regarded as real change.[19,20]

The measurement error of cephalometric measurements, whether 2D or 3D, cannot be attributed only to variability in landmark identification but is also the result of certain geometric principles.[19,20] An important factor in the interpretation of landmark identification data is that each landmark shows a distinct pattern of distribution (envelope of error).[31-34] This is unique for each landmark and it varies between 2D and 3D identification of the same landmark. Research has shown that due to better visualization in all three planes of space, landmarks like Orbitale (Or) and Porion (Po) can be more accurately located on 3D than 2D images.[34] However, the addition of the third dimension means that the envelope of error of point Po varies more along the medio-lateral direction compared to the more vertical variation in the 2D location of this point.[34, 35] Therefore, it could also have a significant influence on the resulting measurement error depending on the geometry of the specific measurement e.g., a significant variation of point B in the vertical direction has a minor influence of the measurement error of SNB. In addition, the sources of measurement error can be

accumulative e.g. the large variation of the landmarks of Co, point A and Gn in 2D explains the larger measurement error of measurements incorporating in these landmarks.[19,25] The third dimension introduces an additional source of error in the mediolateral direction, which offers an explanation why certain angular measurements (e.g. SNA and SNB) show greater measurement error in 3D than 2D.[18-20,34]

3D cephalometry relies on reference planes constructed by connection of bilateral landmarks.[2-4] This is in contrast to 2D cephalometry which relies on lines for reference. The human face is inherently asymmetric which results in different orientations of the horizontal planes when assessing the patient from the frontal view.[19,36-38] This introduces also a new source of error because the measurements between planes could vary depending on where measurement was made on the planes (Figure 1, Chapter 2.2). Most 3D cephalometric software solves this problem by automatically determining the smallest angular value between two planes. However, this may introduce another measurement error and makes comparison between studies difficult. A possible yet simple solution for this problem is to use the same reference for measurements between horizontal planes e.g., the intersection of the midsagittal plane and the horizontal plane as we proposed in Chapter 3.3.[39]

Nagasaka et al.[40] illustrated that the more closely two landmarks are, the greater the linear and angular measurement error tends to be which explains the increased measurement error of the dental angular measurements. Due to the short distances between the tip and apex used to construct the axis of the incisors, the resulting angular measurement error is magnified when a small variation in one of the landmarks occurs (Figure 1, Chapter 2.1). This effect also becomes more apparent in 3D when two landmarks in close proximity are used to construct a reference plane e.g., left and right posterior maxillary points (PMP) to construct the palatal plane.[20] If one of the landmarks varies by a minor amount, the resulting change in the orientation of the plane could be significant (Figure 2, Chapter 2.2). It can therefore be recommended that 3D planes constructed through two landmarks in close relation to each other should be avoided in 3D cephalometry.[20]

Measurement error in 2D and 3D cephalometry can be reduced by means of repeated measurements, additional training, using more experienced operators and improving the definition of the landmarks.[19] However, it can never be eliminated because random error of individual interpretation of the landmark data will always occur.[22] Therefore, determining the measurement error in cephalometrics is important, without which valuable and reliable conclusions can not be reached.

5.3 Acquisition of CBCT 3D images

One of the basic principles of CBCT imaging is to always use the light beam markers to guarantee correct positioning of the patient.[6,7] This is critical when preforming a CBCT scan with a reduced field of view in order to image the region of interest only.[7] In addition, the light beams may also be helpful to position the patient in the NHP for maxillofacial imaging.

The NHP has become an indispensible method to appraise the head due to its stability.[42-46] Alternative reference planes e.g., the Frankfort horizontal plane may not be reliable as considerable variation exists.[46] Due to the longer scanning times of CBCT imaging, the patients head has to be fixed in the machine to avoid movement artifacts, therefore capturing the NHP in the CBCT device is difficult. A recent study described a complicated method to register the NHP by means of customized bite jigs and a facebow/gyroscope combination.[13] Although the method was accurate, practical application seems difficult since it is time consuming. In addition, the facebow/gyroscope construction is quite large and might interfere with the scanning path of most CBCT devices. Our method uses two laser levels and glass markers to determine the NHP before scanning.[12] The advantages are: it is simple, it does not require additional expensive equipment, and it is not labor intensive.[12] Since publication of our method, a slight modification has been made to the laser-level set-up. Morphometric methods are very reliable to determine the midsagittal plane, therefore capturing the yaw of the head in NHP might be of less importance.[47] This makes the set-up even simpler because it eliminates the need for the vertical laser. The horizontal laser level is therefore used in order to register the pitch and roll of the patient in NHP. The horizontal light beam of the CBCT scanner can also be used to align the markers on the face for direct capturing of the head in the NHP.

5.4 Utilization of CBCT in orthodontics

Considering that CBCT imaging still exposes the patient to a higher radiation dose than conventional cephalograms, its added benefits should be carefully weighed against the increased radiation exposure before it can be prescribed.[5] Therefore, a clear need exists for evidence-based selection criteria for CBCT imaging in orthodontics to guarantee responsible use of the modality.[5] The 20 "Basic Principles" of the European Academy of Dentomaxillofacial Radiology (EADMFR) and the provisional guidelines of the

"SEDENTEXCT" project currently act as guidelines for the save and evidence-based use of CBCT for maxillofacial imaging.[6,7]

Since the current evidence does not show that the 3D images results in improved diagnosis and management of routine orthodontic patients,[6-8] the *routine use* of CBCT images for orthodontic treatment is not supported. The current evidence-based indications of CBCT imaging for the orthodontic applications are discussed in Table I.[7]

Table I	Current SEDENTEXCT guidelines for the evidence-based indications of CBCT imaging in Orthodontics.[7]
Indication	**Evidence in the literature**
1. **For localized assessment of impacted canines and determination of possible root resorption due to impacted canines**	- 3D images significantly improved the orthodontist ability to locate the impacted tooth and their roots and their relationship to neighboring teeth and other structures.[50-57] - Intelligent use of CBCT images eliminates the problems associated with traditional radiography when treating impacted maxillary canines[53, 54]. - Acquisition of CBCT images to determine root resorption due to impacted canines or other impactions is supported. But the smallest volume size compatible with the situation should be used if at all possible.[7] - CBCT images are very accurate for assessment of external root resorption at a voxel resolution of 0.25 - 0.40 mm.[57]
2. **For treatment of cleft palate patients**	- CBCT imaging may play a decisive role in the improvement of the ultimate treatment result, especially in cleft patients requiring numerous operations.[7,50] - 3D images provide invaluable information regarding morphology of the bony defects and proximity and localization of the adjacent teeth of the cleft, for which purpose the lower dose of CBCT is preferred.[7] - Adjustable fields of view is a clear advantage of CBCT when the region of interest is a localized part of the jaws, especially in growing children.[7]
3. **For examination of the TMJ (where the existing modality is conventional CT)**	- CBCT should be performed where conventional CT is the existing modality[7] to detect osseous changes. - CBCT is accurate and could be the modality of choice for the imaging of the osseous components of the TMJ.[58,59,60] - CBCT imaging should be considered in addition to MRI imaging TMD if the risk of osseous changes associated with disc displacements is present[59].
4. **For complex skeletal abnormality requiring combined orthodontic and surgical management**	- CBCT imaging can be justified for craniofacial cases where rapid-prototyping and reverse engendering techniques have to be used to restore the skeletal defects.[61-64] The benefits of CBCT imaging clearly outweigh the risk in these extremely complex cases.

One problem with the adopted guidelines and resolutions is unclear definitions, for example: the guideline regarding orthognathic and surgical management of skeletal abnormality can be confusing. The guideline does not recommend routine use of CBCT imaging for the craniofacial skeleton for orthognathic surgery, but suggests that CBCT *may be justified* in the treatment planning of complex cases of skeletal abnormality requiring combined orthodontic and surgical management in patients older than 16 years.[7] The difficulty lies in what defines "complex cases of skeletal abnormality". It can be argued that all cases needing surgical jaw correction is inherently "complex"; therefore justifying CBCT for the planning of all orthognathic cases. Until the criteria and definitions are clearly defined, the guidelines for the clinical use of CBCT imaging will result in different interpretations. [9,49]

Our results help to clarify the indications of CBCT imaging for management of combined orthodontic and surgical management of skeletal abnormality. The results confirm that CBCT imaging is justified for asymmetric patients requiring a combination of orthodontic and surgical treatment.[65] The CBCT images were more accurate in evaluating the underlying cause of the mandibular asymmetry than PA cephalograms and provide more accurate information for diagnosis and surgical treatment planning. This is important since the accuracy of maxillofacial surgery depends not only on the surgical techniques but also on an accurate surgical plan.

Since CBCT technology is fairly new, more applications of CBCT are being discovered which are not always possible with traditional radiography. Improved treatment outcome might be difficult to prove for some applications. When considering new applications it is the responsibility of the clinician to determine if the risk from diagnostic imaging outweighs the benefits. Conversely, the clinician should also consider the potential harm to the patient if the imaging is inadequate or a diagnosis and problem is missed. This is a very important and valid point, yet difficult to address since reports of orthodontic complications diagnosed by means of conventional imaging are rarely published.[66] New applications of CBCT imaging might therefore be considered as an adjunctive tool in the diagnostic purposes. For example, the added value of CBCT for airway analysis in the diagnosis of obstructive sleep apnea (OSA) is the accurate assessment of the airway in the anteroposterior and mediolateral direction, though the gold standard of OSA remains a sleep study. [67,68]

Another very promising application of CBCT in orthodontics is determining the anatomical limitations of tooth movement which is not possible with conventional radiography.[9] Recent studies have shown that alveolar bone thickness can be accurately

detected by means of CBCT.[69] In orthodontic treatment, a non-extraction or camouflage treatment approach often involves expansion of the teeth e.g., lower incisors in the anterior mandibular area or upper molars in the transverse direction. The application of CBCT imaging in these cases is to detect the anatomical boundary and provide orthodontists with invaluable information in treatment planning to avoid dehiscence and fenestration of the roots. Therefore, the orthodontic treatment plan should consider the direction of movement and the anatomical integrity of the alveolar morphology of the planned tooth movements. Other limits to tooth movement not detectable by conventional radiographs are enostosis, condensing osteitis and dense bone islands etc.

5.5 Visualization of CBCT derived surface models

The use of CBCT derived 3D surface models for planning of craniofacial surgery by means of computer-aided surgery simulation (CASS) shows great promise to overcome problems associated with conventional 2D methods.[61-64,70-72] However, the proposed advantages of CBCT imaging and CASS can only be realized and validated if accurate 3D models are made available first. Currently, the major obstacles of CASS are the accuracy of the CBCT derived surface models and the correct visualization of the inter-occlusal relationships in the 3D model. [70-72]

Factors with a significant effect on the accuracy of the surface models are: voxel size, beam inhomogeneity from different CBCT scanners, and differences of threshold based segmentation methods.[2,73] Our results indicated that surface models derived from CBCT images were accurate and no differences of linear measurements were detected between surface models derived from CBCT images with different voxel sizes (0.25 mm and 0.40 mm).[74] A 0.40 mm voxel resolution provides adequate information for quantification and can be used for maxillofacial surgery planning.[74] This is clinically relevant as a smaller voxel scan exposes the patient to a higher radiation dose. Importantly, a smaller voxel resolution scan is more appropriate for diagnostic purposes (e.g., evaluating root resorption) because the diagnosis is made on the axial, coronal and sagittal slices rather than surface models.[7,57] Smaller voxel resolutions usually results in a "smoother" and higher quality images due to less noise artifacts and more detailed anatomic information (Figure 1c and d, Chapter 3.2).

Van Vlijmen et al.[75] found clinically significant differences between surface models from two different CBCT scanners. This beam inhomogeneity between CBCT scanners

explains the differences in accuracy of the derived surface models .[14-17,75] In contrast, the scanning position of the patient does not seem to have an effect.[76] The major factor in determining the accuracy of derived surface models appears to be the user entered threshold value.[41] Because the user determines the threshold value of visible and invisible voxels, the segmentation process is subject to inaccuracies.[2,41] In chapter 3.2, the influence of the segmentation process was eliminated by specifying a single or global threshold value and using glass markers. This differs from the clinical setting where differences in bone densities complicate the threshold settings. It is almost impossible to apply a single threshold value (whether operator or automatically determined) for the whole skull or even for a single jaw. When a single threshold is applied to the maxilla or mandible, it is likely to be inaccurate since the bone density differs significantly from other areas within the structures itself.[41] The results from our team showed that segmented models provided by commercial service are more accurate than those performed by clinician.[41] Therefore, if surface models are needed for high precision e.g., pre-surgical planning, the additional cost of a commercial segmentation seems to be justified. In addition, the time-saving aspect might further justify outsourcing the segmentation process to commercial companies, provided that they produce accurate models.

5.6 Application of CBCT images for cephalometry

There are a few fundamental differences when comparing 2D and 3D cephalometry.[18-20] 3D cephalometry relies on measurements made to reference planes rather than lines. In addition, a CBCT scan permits measurement on derived cephalograms, volume renderings, surface models and slices in all three planes in space of the imaged structures. In contrast, 2D cephalometry relies on one single captured image of the face which has significant limitations.[77] The advantage of 3D images acquired from CBCT is that additional information (not always possible with conventional radiographs) can be extracted which could be very helpful and beneficial for patient management and treatment.

Direct comparison between 2D and 3D cephalometry is difficult because classic cephalometry is a 2D representation of 3D structures and is subject to geometric distortions and systematic errors.[79-81] To overcome this problem, lateral cephalograms can be derived from 3D CBCT images. The resulting measurements from derived lateral cephalograms are comparable with traditional cephalograms and therefore suitable for

longitudinal research.[79-81] However, derived lateral cephalograms does not justify using CBCT as a primary investigation.[7] More importantly, it is time consuming and costly to derive a lateral cephalogram from CBCT because it requires extra steps and specific software for the analysis.[39] Most importantly, the 3D characteristics are lost when a cephalogram is derived from the CBCT images. To overcome these problems, our 3D analysis was modified so that the measurements were based on lines in the midsagittal plane of the 3D image, which are comparable with 2D measurements from conventional cephalograms without losing the 3D characteristics [39,82,83] Another advantage is that the presentation of the 3D measurements is very similar to conventional 2D measurements routinely used by orthodontists.[39] This might be useful in the transition from 2D to 3D cephalometry.

One of the most useful applications of 3D cephalometry may be the use of volume rendering and surface models which introduced new assessment methodologies. The ability of the software to create a mirror-image of the surface model around an arbitrary plane and its usefulness to reproduce severe unilateral skeletal defects by means of rapid-prototyping have been discussed previously in the manuscript.[62-64] The added value of mirror-imaging and superimposition to extract additional information may help in management of asymmetric cases and allows for comparisons of surfaces and volumes not possible with other radiographic techniques. [84] There are a number of advantages of the mirror-image analysis described in Chapter 4.2. It confirms the existing quantitive measurements, it helps reduce diagnostic errors, it does not rely on normative values for diagnosis, it creates new appreciation of the abnormality because the differences can be depicted as volume rather than numbers, it helps in development of treatment strategies, and it improves communication between orthodontists and maxillofacial surgeons. The most valuable advantage is that it is a visual tool to explain to the patient the extent of the underlying abnormality and the possibilities and limitations of the treatment [84].

CBCT quantifies craniofacial asymmetry by means of subtraction of bilateral measurements and differences of measurements made to a midsagittal plane to laterally positioned landmarks.[3,85,86] Traditionally, midsagittal planes have been constructed using cephalometric points, however recent literature have also suggested the use of morphometric midsagittal planes to quantify assymery.[87-97] Morphometrics is the branch of mathematics which performs shape analysis of geometric objects.[87] In essence; cephalometrics can be described as a subset of morphometrics. Morphometric methods such as Procrustes analysis and Euclidean distance matrix analysis are accepted

in all fields of biology to determine the true plane of symmetry in structures with object symmetry.[87,88] These methods have also been used to study craniofacial asymmetry.[89-97] A major advantage in cephalometry is that a morphometric approach can compute the midsagittal plane using intact regions unaffected by the asymmetry.[47,90,95-97] It is therefore suitable to determine the midsagittal plane in severe and congenital asymmetries. Research has shown that this method is very reliable in determining the midsagittal plane when using 3D datasets.[47,90,95] Conventional midsagittal planes are constructed by means of connecting anatomical landmarks, often in the midline of the face.[98-104] However, the usefulness or validity of these planes has been questioned in the literature.[47,97] In addition, these planes sometimes rely on structures not relevant to the visual perception.[97] Our results illustrate that there are clinical differences between measurements derived from a morphometric midsagittal plane and those from conventional midsagittal planes based on anatomical midline structures.[47] Therefore, the use of conventional midsagittal planes will vary amongst individuals and remain questionable to describe craniofacial asymmetry.

Our results show that the measurement errors of cephalometric variables are often too large to detect true treatment effects. To overcome this, superimposition of pre- and post-treatment radiographs can be performed. However, the accuracy of 2D superimposition remains questionable.[105] Provided that 3D models are accurate, 3D superimposition has been proven to be reliable and may be more accurate than 2D superimposition to determine changes after craniofacial surgery. [106,107]

5.7 Future applications and perspectives

It is hard to imagine, but it happens that new technologies are sometimes applied to adopt old methods. For example, some clinicians use CBCT software to extract 2D images that they are accustomed to. This might be useful during the transition from 2D to 3D cephalometry. However, future cephalometric analyses should focus on 3D measurements in order to take advantage of the full potential of 3D imaging.[108] This might lead not only to the development of new analyses but also to the introduction of new cephalometric landmarks in 3D.[2] In particular, it is expected that morphometrics will play a more important role in 3D cephalometry in the future.[47] Although morphometric methods have been used in 2D cephalometry,[94-96] data from 3D imaging provide new analyses possibilities using surface and shape data not possible with 2D methods.[47,70,90,97]

Future research should continuously examine and redefine the evidence-based indications for the application of CBCT in orthodontics.[108] Specifically, it is hoped that CBCT imaging might cast a brighter light on the prediction of treatment outcomes.[109] However, since the technology is new, it might yet take some time before clinical outcome trails will be published. Justification of new applications of CBCT images (not possible with traditional radiography) is therefore difficult as direct comparison is impossible and perceived benefits could be subject to personal bias. In such cases the clinician has the responsibility to objectively consider of the risk of the higher radiation dose of the CBCT images and to resist the temptation to prescribe this technique for every orthodontic patient. In addition, the clinician should seriously consider the medicolegal and liability issues related to CBCT imaging. From the medicolegal aspect, the clinician is not only responsible for reading the CBCT scan pertaining to their specialty, but also legally responsible for reading the entire image volume.[110] This point becomes even more important since a recent study illustrated a high percentage of incidental maxillary sinus findings not associated with the primary indication of The CBCT images.[111] This study highlights possible underestimation of the potential pathology on CBCT images and the need for the complete scan to be interpreted by a radiologist. Therefore, as the utilization of CBCT images increases, future orthodontic and maxillofacial surgery postgraduate or even undergraduate programs should consider including more extensive training in oral and maxillofacial radiology to enable reading of the entire scanning volumes by the clinician.

The 3D planning of craniofacial surgery by means of computer-aided surgery simulation (CASS) will become more important in the future. However, it is essential that accurate surface models are made available first. New advances and technology will continue to improve the accuracy of CBCT-derived surface models. In particular, it is anticipated that future segmentation procedures of CBCT images might be based on both intensity and gradient magnitude of the signals for a higher accuracy of surface models,[41] which are essential for 3D superimposition. Due to the inherent limitations of cephalometric measurement error, 3D superimposition might help to improve diagnosis, surgical treatment planning and assessment of treatment outcomes.[31,84]

One obstacle in performing 3D planning of craniofacial surgery is the correct and accurate visualization of the inter-occlusal relationships in the total 3D model. Various methods have been described to visualize the inter-occlusal relationships in the 3D craniofacial model.[72,112-114] Although the reliability of these methods seems to be acceptable, the methods are fairly intricate, time-consuming and computer-intensive

and may even expose the patient to an additional CBCT scan.[72] Unfortunately, impressions of presurgical models used to fabricate the surgical splints are subject to inaccuracies due to deformation of the alginate caused by the orthodontic brackets. Kau et al.[115] illustrated that accurate dental models can be derived from CBCT scans alone. However, this necessitates an additional high resolution scan with increased radiation exposure. Moreover, the results may not apply to pre-surgical models because Kau et al.[115] used teeth without orthodontic brackets. Preliminary results from our team show that digital models made with the 3M ESPE Lava™ chairside intra-oral scanner of teeth with orthodontic brackets to be very accurate and reliable. Such a scanner does not expose the patient to radiation and the accuracy is not influenced by scattering caused by metallic restorations or brackets. Though the application of intra-oral scanners in orthodontic is still in its infancy, it shows great promises for the digital set-up. Future research will focus on the implementation of this technology for CASS to possibly improve the accuracy of the inter-occlusal relationships in the 3D model.

Considering that it took 30 years for Broadbent's cephalometric technique to achieve widespread clinical application, the current application and utilization of CBCT in orthodontics as a new imaging modality has been rapid.[1,116,117] Perhaps this is due to the total integration that the 3D images makes possible. Instead of looking at each partial diagnostic record (e.g., the cephalogram, dental casts and photos), we now have a single volume that includes all the information. This allows for unique appreciation of the anatomical structures and anomalies. Current evidence and guidelines do not support the routine CBCT imaging of all orthodontic patient.[6-8] However, considering the rapidly evolving and new advances regarding further radiation reduction and improved image quality, it may be plausible to think that CBCT imaging would eventually be the imaging modality of choice for all orthodontic patients.[2, 118,119]

5.7 Conclusion

Technical advances will no doubt result in an even more important role of CBCT imaging in orthodontics and maxillofacial surgery. The 3D nature of this new technology has led to development of applications never seemed possible before. However, a number of inherent limitations and pitfalls of CBCT imaging (from utilization to application) needs to be addressed before the potential of the technology can be fully realized. The studies in this manuscript addressed some of the limitations and pitfalls and explored some of the potential applications. The results of our specific research aims confirmed that:

1. The SDD of almost all commonly used 2D and 3D cephalometric measurements can be considered clinically significant (more than 1 measuring unit).
2. The accuracy of CBCT-derived surface models was sufficient for orthodontic and craniofacial treatment planning.
3. Increasing the voxel resolution from 0.40 mm to 0.25 mm to construct a 3D surface model did not result in an increased accuracy of the linear measurements.
4. Conventional 2D measurements are comparable to 3D measurements of a modified 3D analysis based on the midsagittal plane.
5. CBCT imaging is more accurate in determining the difference of the mandibular dimensions (ramus length, body length and total length) therefore providing more reliable information regarding the characteristics of the asymmetry than PA cephalometry.
6. There are clinically relevant differences between 3D cephalometric midsagittal planes used to describe craniofacial asymmetry and a symmetry plane derived from a morphometric method based on visible facial features.

Finally it can be concluded that that CBCT remains a valuable tool for patient management, and not a solution. The advantages that it offers also bring added ethical and legal responsibilities for the clinician. Safe utilization and correct interpretation of the CBCT images remains the responsibility of the clinician and should not be taken lightly. Perhaps John Naisbitt[120] sums it up best with the statement: *"In our minds, at least, technology is always on the verge of liberating us from personal discipline and responsibility. Only it never does and never will."*

5.8 References

1. White SC. Cone-beam imaging in dentistry. Health Phys 2008; 95: 628-637
2. Halazonetis DJ. From 2-dimensional cephalograms to 3-dimensional computed tomography scans. Am J Orthod Dentofacial Orthop 2005; 127: 627-637
3. Jacobson RL. Three-Dimensional Cephalometry. In: Jacobson A, Jacobson RL eds. Radiographic Cephalometry: From Basics to 3-D Imaging. 2nd ed. Hanover Park. Quintessence Publishing Co, Inc. 2006:233-247
4. Swennen GJR, Schutyser F, Hausamen JE. Three-dimensional cephalometry. A color atlas and manual. Heidelberg Springer, Berlin 2005
5. Farman AG, Scarfe WC. Development of imaging selection criteria and procedures should precede cephalometric assessment with cone-beam computed tomography. Am J Orthod Dentofacial Orthop 2006; 130: 257-265

6.   EADMFR. Basic principles for the use of dental cone beam CT. www.eadmfr.info 2008

7.   SEDENTEXCT. Provisional guidelines CBCT for dental and maxillofacial radiology. www.sedentexct.eu/guidelines 2009

8.   www.aaomembers.org/Resources/Publications/ebulletin-05-06-10.cfm

9.   Mah JK, Hung JC, Choo H. Practical applications of cone-beam computed tomography in orthodontics. J Am Dent Assoc 2010; 141 suppl 3:7S-13S

10.   Kokich VG. Cone-beam computed tomography: have we identified the orthodontic benefits? Am J Orthod Dentofacial Orthop 2010; 137, S16

11.   Mussig E, Wortche R, Lux CJ. Indications for digital volumetric tomography in orthodontics. J Orofac Orthop 2005; 66: 241-249

12.   Damstra J, Fourie Z, Ren Y. Simple technique to achieve a natural head position of the head for cone beam computed tomography. Br J Oral Maxillofac Surg 2010, 48: 236-238

13.   Schatz EC, Xia JJ, Gateno J, English JD, Teichgraeber JF, Garret FA. Development of a technique for recording and transferring natural head position in 3 dimensions. J Craniofac Surg 2010; 21: 1452-1455

14.   Loubele M, Jacobs R, Maes F, Denis K, White S, Coudyser W et al. Image quality vs radiation dose of four cone-beam computerized scanners. Dentomaxillofac Rad 2008; 37; 309-319

15.   Hassan B, Metska ME, Ozok AR, Van der Stelt PF, Wesselink PR. Comparison of five cone beam computed tomography systems for the detection of vertical root fractures. J Endod 2010; 36: 126-129

16.   Loubele M, Maes F, Schutyser F, Marchal G, Jacobs R et al. Assessment of bone segmentation quality of cone-beam CT versus multislice spiral CT: a pilot study. Oral Surg Oral Med Oral Pathol Oral Radiol Endod 2006; 102: 255-234

17.   Loubele M, Guerrero ME, Jacobs R, Suetens P, van Steenberghe D. A comparison of jaw dimensional and quality assessments of bone caractiristics with cone-beam CT, spiral tomography, and multislice CT. Int J Oral Maxillofac Implants 2007; 22: 446-454

18.   Van Vlijmen OJC, Maal T, Berge SJ, Bronkhorst EM, Katsaros AM, Kuipers-Jagtman. A comparison between 2D and 3D cephalometry on CBCT scans of human skulls. Int J Oral Maxillofac Surg 2010; 39: 156-160

19.   Damstra J, Huddleston Slater JJR, Fourie Z, Ren Y. Reliability and the smallest detectable difference of lateral cephalometric measurements. Am J Orthod Dentofacial Orthop 2010; 138: 546.e1-e8 Discussion 546-547

20.   Fourie Z, Damstra J, Huddleston Slater JJR, Ren Y. Reliability and the smallest detectable difference of three-dimensional cephalometric measurements. Submitted, Am J Orthod Dentofacial Orthop, 2010

21.   Van der Linden FPGM. Sheldon Friel Memorial Lecture 2007. Myth and Legends in orthodontics. Eur J Orthod 2009;30:449-468

22.   Harris EF, Smith RN. Accounting for measurement error: A critical but often overlooked process. Arch of Oral Biol 2009;54 Suppl 1:S107-17

23.   Hopkins WG. Measures of reliability in sports medicine and science. Sports Med 2000;30:1-15

24. International Organization of Standardization. Accuracy (trueness and precision) of measurement methods and results. Part 1. General principles and definitions. Geneva, Switzerland: International Organization of Standardization 1994: ISO 5725-1

25. Kropmans TJ, Dijkstra PU, Stegenga B, Stewart R, de Bont LG. Smallest detectable difference in outcome variables related to painful restriction of the temporomandibular joint. J Dent Res 1999;78-784-89

26. Damstra J, Fourie Z, Huddleston Slater JJR, Ren Y. Accuracy of linear measurements from cone-beam tomography derived surface models of different voxel sizes. Am J Orthod Dentofacial Orthop 2010;137:16.e1-16.e6

27. Smeulders MJ, Van den Berg S, Odeman J, Nederveen AJ, Kreulen M, Maas M. Reliability of in vivo determination of forearm muscle volume using 3.0 T magnetic resonance imaging. J Magn Reson Imaging 2010; 31: 1252-5

28. Battagel JM. A comparative assessment of cephalometric errors. Eur J Orthod 1993; 15: 305-314

29. Houston WJB, Maher RE, McElroy D, Sheriff M. Sources of error in measurements from cephalometric radiographs. Eur J Orthod 1986; 8: 149-151

30. Richardson A. A comparison of traditional and computerized methods of cephalometric analysis. Eur J Orthod 1981;3:15-20

31. Kamoen A Dermaut L, Verbeeck R. The clinical significance of error measurement in the interpretation of treatment results. Eur J Orthod 2001;23:569-578

32. Lou L, Lagravere MO, Compton S, Major PW, Flores-Mir C. Accuracy of measurements and reliability of landmark identification with computed tomography (CT) techniques in the maxillofacial area: a systematic review. Oral Surg Oral Med Oral Pathol Oral Radiol Endod 2007; 104: 402-11

33. De Oliviera AEF, Cevidanes LHS, Phillips C Motta A, Burke B, Tyndall D. Observer reliability of three-dimensional cephalometric identification on cone-beam computerized tomography. Oral Surg Oral Med Oral Pathol Oral Radiol Endod 2009; 107: 256-265.

34. Ludlow JB, Gubler M, Cevidanes LHS, Mol A. Precision of cephalometric landmark identification: cone-beam tomography vs. conventional cephalometric views. Am J Orthod Dentofacial Orthop 2009; 136: 312e1-10; discussion 312-3

35. Marci V, Athanasiou AE. Sources of error in lateral cephalometry. In: Athanasiou AE. Orthodontic cephalometry. London, UK: Mosby-Wolfe: 1995:125-140

36. Gawilkowska A, Szczurwski J, Czerwinski F, Miklaszwenska D, Adamiec A, Dzieciolowska E. The fluctuating asymmetry of mediaeval and modern human skulls. Homo 2007; 58: 159-172

37. Haraguschi S, Iguchil Y, Takada K. Asymmetry of the face in orthodontic patients. Angle Orthod 2008; 78: 421-426

38. Peck S, Peck L, Kataja M. Skeletal asymmetry in esthetically pleasing faces. Angle Orthod 1991; 61: 43-46

39. Damstra J, Fourie Z, Ren Y. Comparison between two-dimensional and midsagittal three-dimensional cephalometric measurements of dry human skulls. Br J Oral Maxillofac Surg 2010, doi:10.1016/j.bjoms.2010.06.006

40. Nagasaka S, Fujimora T, Segoshi K. Development of a non-radiographic cephalometric system. Eur J Orthod 2003;25:77-85

41. Fourie Z, Damstra J, Schepers R, Gerrits PO, Ren Y. Segmentation process significantly influences the accuracy of 3D surface models derived from cone beam computed tomography. Eur J Radiol 2011, Accepted

42. Lundstrom A, Lundstrom F, Lebret LML, Moorrees CFA. Natural head position and natural head position: basic consideration in cephalometric analysis and research. Eur J Orthod 1995; 17:111-120

43. Cooke MS, Wei SHY. The reproducibility of natural head posture: a methodological study. Am J Orthod Dentofacial Orthop 1988; 93: 20-28

44. Cooke MS. Five-year reproducibility of natural head posture: a longitudinal study. Am J Orthod Dentofacial Orthop 1990; 97: 489-494.

45. Peng L, Cooke MS. Fifteen-year reproducibility of natural head posture: a longitudinal study. Am J Orthod Dentofacial Orthop 1999; 116: 82-85.

46. Moorrees CFA. Natural head position: the key to cephalometry. In: Jacobson A, Jacobson RL eds: Radiographic cephalometry, From Basics to 3-D imaging. Hanover Park. Quintessence Publishing Co, Inc. 2006: 153-16

47. Damstra J, Fourie Z, De Wit MF, Ren Y. A three-dimensional comparison of a morphometric midsagittal plane to cephalometric midsagittal planes for craniofacial asymmetry. Clin Oral Investig 2011; doi:10.1007/s00784-011-0512-4

48. Harrell WE, Jacobson RL, Hatcher DC, Mah J. Cephalometric imaging in 3-D. In: Jacobson A, Jacobson RL eds: Radiographic cephalometry, From Basics to 3-D imaging. Hanover Park. Quintessence Publishing Co, Inc. 2006: 233-246

49. White SC, Pae E-K. Patient image selection criteria for cone beam computed tomography imaging. Semi Orthod 2009; 15 : 19-28

50. Korbmacher H, Kahl-Nieke B, Schollchen M, Heiland M. Value of two cone-beam computed tomography systems from an orthodontic pint of view. J Orofac Orthop 2007; 68: 278-289

51. Holberg C, Steinhauser S, Geis P, Rudski-Janson I. Cone-beam computed tomography in orthodontics: Benefits and Limitations. J Orofac Orthop 2005; 66: 434-444

52. Walker L, Enciso R, Mah J. Three-dimensional localization of maxillary canines with cone-beam computed tomography. Am J Orthod Dentofacial Orthop 2005; 128: 418-423

53. Becker A, Chaushu G, Chaushu S. Analysis of failure in the treatment of impacted maxillary canines. Am J Orthod Dentofacial Orthop 2010; 137: 734-754

54. Becker A, Chaushu S, Casap-Caspi N. Cone-beam computed tomography and the orthosurgical management of impacted teeth. J Am Dent Assoc. 2010: 141 suppl 3: 14S-18S

55. Heimisdottir K, Bosshardt D, Ruf S. Can the severity of root resorption be accurately judged by means of radiographs? A case report with histology. Am J Orthod Dentofacial Orthop 2005; 128: 106-109

56. Ericson S, Kurol J. Incisor root resorption due to ectopic maxillary canines imaged by computerized tomography: a comparative study in extracted teeth. Angle Orthod 2000; 70: 276-283

57. Liedke GS, Dias da Silviera HE, Dias da Silviera HL, Duntra V, Poli de Figueiredo A. Influence of voxel size in the diagnostic ability of cone beam tomography to evaluate simulated external root resorption. J Endod 2009, 35: 233-235

58. Honda K, Larheim TA, Maruhashi K, Matsumoto K, Iwai K. Osseous abnormalities of the mandibular condyle: diagnostic reliability of cone-beam computed tomography with helical computed tomography based on autopsy material. Dentomaxillofac Radiol 2006; 35: 152-157

59. Alkhader M, Kuribayashi A, Ohbayashi N, Nakamura S, Kurabayashi T. Usefulness of cone beam computed tomography in temporomandibular joints with soft tissue pathology. Dentomaxillofac Radiol 2010; 39: 343-348

60. Farronato G, Garagiola U, Carletti V, Cressoni P, Mercatali L, Farronato D. Change in condylar and mandibular morphology in juvenile idiopathic arthritis: Cone-beam volumateric imaging. Minerva Stomatol 2010; 10: 519-534

61. Swennen GRJ, Mollemans W, Schutyser F. Three-dimensional treatment planning of orthognathic surgery in the era of virtual imaging. J Oral Maxillofac Surg 2008; 67: 2080-92

62. Gateno J, Xia JJ, Teichgraeber JF, Christensen AM, Lemoine JJ et al. Clinical feasibility of computer-aided surgical stimulation(CASS) in the treatment of complex cranio-maxillofacial deformities. J Oral Maxillofac Surg 2007; 65: 728-734

63. Xia JJ, Gateno J, Teichgraeber JF. Secrets in computer-aided surgical simulation for complex cranio-maxillofacial surgery. In: English JD, Peltomaki T, Pham-Litchel K eds: Mosby's Orthodontic Review. St Loius. Elsevier Inc. 2009: 277-287

64. Zhou L-B, Shang H-T, He L-S, Bo B, Liu G-C, Zhao J-L. Accurate reconstruction of discontinuous mandible using reverse engineering/computer-aided design/rapid prototyping technique: a preliminary clinical study. J Oral Maxillofac Surg 2010; 68: 2115-2121

65. Damstra J, Fourie Z, Ren Y. Evaluation and comparison of postero-anterior cephalograms and cone-beam computed tomography images for the detection of mandibular asymmetry. Eur J Orthod 2011; Accepted

66. Davidovitch Z, Krishan V. Adverse effects of orthodontics: a report of 2 cases. World J Orthod 2008; 9: e64-e77

67. Celenk M, Farrell ML, Eren H, Kumar K, Singh GD, Lozanoff S. Upper airway detection and visualization from cone beam image slices. J Xray Sci Technol 2010; 18: 121-135

68. Kushida C, Littner M, Morgenthaler T et al. Practise parameters for the indications of polysomnography and related procedures: an update for 2005. Sleep 2005; 28: 499-521

69. Evangelista K, Vasconcelos Kde F, Bumann A, Hirsch E Nikta M, Silva MA. Dehiscence and fenestration in patients with Class I and Class II division 1 malocclussions assessed with cone-beam computed tomography. Am J Orthod Dentofacial Orthop 2010; 138: 133.e1-e7

70. Cevidanes LHS, Tucker S, Styner M, Kim H, Chapuis J, Reyes M, Profitt WR, Turvey T, Jaskolka M. Three-dimensional surgical simulation. Am J Orthod Dentofacial Orthop 2010; 138: 361-371

71. Swennen GRJ, Mollemans W, Schutyser F. Three-dimensional treatment planning of orthognathic surgery in the era of virtual imaging. J Oral Maxillofac Surg 2008; 67: 2080-92

72. Swennen GRJ, Mollemans W, De Qlercq C, et al. A cone-beam computed tomography triple scan procedure to obtain a three-dimensional augmented virtual skull model appropriate for orthognathic surgery planning. J Craniofac Surg 2009: 20: 297-307

73. Grauer D, LSH Cevidanes, Profitt WR. Working with DICOM craniofacial images. Am J Orthod Dentofacial Orthop 2009; 136: 460-470

74. Damstra J, Fourie Z, Huddleston Slater JJR, Ren Y. Accuracy of linear measurements from cone-beam tomography derived surface models of different voxel sizes. Am J Orthod Dentofacial Orthop 2010;137:16.e1-16.e6

75. Van Vlijmen OJ, Rangel FA, Berge SJ, Bronkhorst EM, Becking AC, Kuiper-Jagtman AM. Measurements on 3D models of human skulls derived from different cone beam scanners. Clin Oral Investig 2010; doi: 10.1007/s00784-010-0440-8

76. Hassan B, Van der Stelt P, Sanderink G. Accuracy of three-dimensional measurements obtained from cone beam tomography surface-rendered images for cephalometric analysis: influence of patient position. Eur J Orthod 2009; 31: 129-134

77. Marci V, Athanasiou AE. Sources of error in lateral cephalometry. In: Athanasiou AE. Orthodontic cephalometry. London, UK: Mosby-Wolfe; 1995: 125-40.

78. http://oxforddictionaries.com/definition/cephalometry

79. Van Vlijmen OJC, Berge J, Swennen GR, Bronkhorst EM, Katsaros C, Kuipers-Jagtman AM. Comparison of cephalometric radiographs obtained from cone-beam computed tomography scans and conventional radiographs. J Oral Maxillofac Surg 2009; 67: 92-7

80. Kumar V, Ludlow JB, Cevidanes LHS. Comparison of conventional and cone beam CT synthesized cephalograms. Dentomaxillofacial Radiology 2007; 36: 263-9.

81. Kumar V, Ludlow JB, Cevidanes LHS, Mol A. In vivo comparison of conventional and cone beam CT synthesized cephalograms. Angle Orthod 2008; 78: 873-79.

82. Bholsithi W, Tharanon W, Chintakanon K, Komolpis R, Sinthanayothin C. three-dimensional vs. two-dimensional cephalometric analysis with repeated measurements from 20 Thai males and 20 Thai females. Biomed Imaging Interventional J 2009, 5, e21.

83. Nalçaci R, Öztürk F, Sökücü O. A comparison of two-dimension al radiography and three-dimensional computed tomography in angular cephalometric measurements. Dentomaxillofacial Radiology 2010; 39: 100-6.

84. Damstra J, Oosterkamp BCM , Jansma J, Ren Y. Combined 3-dimensional and mirror-image analysis for the diagnosis of asymmetry. Am J Orthod Dentofacial Orthop 2010

85. Hwang H-S, Hwang CH, Lee K-H, Kang B-C. Orthognathic 3-dimensional image analysis for the diagnosis of facial asymmetry. Am J Orthod Dentofacial Orthop 2006; 130: 779-785

86. Baek S-K, Cho I-S, Chang Y-I, Kim M-J. Skeletodental factors affecting chin point deviation in female patients with class III malocclusion and facial asymmetry: a three dimensional analysis using computed tomography. Oral Surg Oral Med Oral Pathol Oral Radiol Endod 2007; 104: 628-639

87. Klingenberg CP, Barluenga M, Meyer A (2002) Shape analysis of symmetric structures: Quantifying variation among individuals and asymmetry. Evolution 56: 1909-1920

88. Zelditch ML, Donald L, Swiderski H, Sheets D, Fink WL (2004) Geometric morphometrics for biologists: a primer. Elsevier, London, pp 1-128

89. Ferrario VF, Sforsa C, Poggio CE, Tartaglia G (1994) Distance from symmetry: A three-dimensional evaluation of facial asymmetry. J Oral Maxillofac Surg 52: 1126 – 1132

90. Hajeer MY, Ayoub AF, Millet DT (2004) Three-dimensional assessment of facial soft-tissue asymmetry before and after orthognathic surgery. Br J Oral Maxillofac Surg 42: 396-404

91. Ferrario VF, Sforsa C, Miani A Jr, Serrao A (1995) A three-dimensional evaluation of facial asymmetry. J Anat 186: 103-110

92. McIntyre GT, Mossey PA (2010) Asymmetry of the craniofacial skeleton in parents of children with a cleft lip, with or without cleft palate, or an isolated cleft palate. Eur J Orthod 32 : 177-185

93. McIntyre GT, Mossey PA (2003). Size and shape measurement in contemporary cephalometrics. Eur J Orthod 25: 231-242

94. Hartman J, Meyer-Marcotty P, Hausler G, Stellzig-Eisenhauer A (2007) Reliability of a method for computing facial symmetry plane and degree of asymmetry based on 3D-data. J Orofac Orthop 68: 477-490

95. Benz M, Laboureux X, Maier T, Nkenke E, Seeger S, Neukam FW et al (2002) The symmetry of faces. In: Greiner G, Niemann H, Ertl T, Girod B, Seidel HP (eds) Vision, modeling and visualization. IOS Press, Amsterdam, pp 332-339

96. Meyer-Marcotty P, Alpers GW, Gerdes ABM, Stellzig-Eisenhauer A (2010) Impact of facial asymmetry in visual perception: a 3-dimensional data analysis. Am J Orthod Dentofacial Orthop 137: 168.e-168.e8

97. De Momi E, Chapuis J, Pappas I, Ferrigno G, Hallerman W, Schramm A, Caversaccio M (2006) Automatic extraction of the midfacial plane for craniomaxillofacial surgery planning. Int J Oral Maxillofac Surg 35: 636 – 642

98. Profitt WR, Turvey TA (1991) Dentofacial asymmetry. In Profitt WR, White Jr RP (eds). Surgical orthodontic treatment. Mosby, St Louis, pp 483-549

99. Ghafari GG (2006) Posteroanterior cephalometry: Craniofacial frontal analysis. In: Jacobson A, Jacobson RL (eds) Radiographic cephalometry, from basics to 3-D imaging, 2nd edn. Quintessence Publishing Co Inc , Hanover Park, pp 267-292.

100. Hwang H-S, Hwang CH, Lee K-H, Kang B-C (2006). Maxillofacial 3-dimensional analysis for the diagnosis of facial asymmetry. Am J Orthod Dentofacial Orthop 130: 779-785

101. Yàñez-Vico RM, Iglesias-Linares A, Torres-Lagares D, Gurierrez-Perez JL, Solano-Reina E (2010) Three-dimensional evaluation of craniofacial asymmetry: an analysis using computed tomography. Clin Oral Invest. doi: 10.1007/s00784-010-0441-7

102. Tuncer BB, Atac MS, Yuksel S (2009) A case report comparing 3-D evaluation in the diagnosis and treatment planning of hemimandibular hyperplasia with conventional radiography. J Craniomaxillofac Surg. doi: 10.1016/j.jcms.2009.01.004

103. Baek S-K, Cho I-S, Chang Y-I, Kim M-J (2007) Skeletodental factors affecting chin point deviation in female patients with class III malocclusion and facial asymmetry: a three dimensional analysis using computed tomography. Oral Surg Oral Med Oral Pathol Oral Radiol Endod 104: 628-39

104. Kwon T-G, Park H-S, Ryoo H-M, Lee S-H (2006) A comparison of craniofacial morphology in patients with and without facial asymmetry – a three-dimensional analysis with computed tomography. Int J Oral Maxillofacial Surg 35: 43-48

105. Gliddon MJ, Xia JJ, Gateno J, Wong HT, Lasky RE, et al. The accuracy of cephalometric tracing superimposition. J Oral Maxillofac Surg 2006; 64: 194-202

106. Cevidanes LHS, Styner M, Profitt WR. Three-dimensional superimposition of the skull base for longitudinal evaluation of the effects of growth and treatment. Orthod Fr 2009; 80: 347-357

107. Cevidanes LHS, Styner M, Profitt WR. Three-dimensional superimposition for quantification of treatment outcomes. In: Nanda R, Kapila S. Current therapy in Orthodontics. London, UK: Mosby-Wolfe: 2010: 36-45

108. Gateno J, Xia JJ, Teichgraeber JF. New 3-dimensional cephalometric analysis for orthodontic surgery. J Oral Maxillofac Surg 2011; 69: 606-622

109. Kau CH, Richmond S, Palamo MJ, Hans MG. Three-dimensional cone beam computerized tomography in orthodontics. J Orthod 2005; 32: 282-293

110. Friedland B. Medicolegal issues related to cone beam CT. Semin Orthod 2009; 15:77-84

111. Pazera P, Bornstein MM, Pazera A , Sendi P, Katsaros C. Incidental maxillary sinus findings in orthodontic patients: a radiographic analysis using cone-beam computed tomography (CBCT). Orthod Craniofac res 2011; 14: 17-24

112. Terai H. Shimahara M, Sakinaka Y, et al. Accuracy of integration of dental casts in three-dimensional models. J Oral Maxillofac Surg 1999; 57: 662-665

113. Gateno J, Xia JJ, Teichgraeber JF, et al. A new technique for the creation n of a computerized composite skull model. J Oral Maxillofac Radiol 2003; 61: 222-227

114. Swennen GJR, Mommaets MY, Abeloos, et al. The use of a wax bite wafer and a double CT scan procedure to obtain a 3D augmented virtual skull model. J Craniofac Surg 2007; 18: 533-539

115. Kau CH, Littlefield J, Rainy N, Nguyen JT, Creed B. Evaluation of CBCT digital dental models and traditional models using Little's index. Angle Orthod 2010, 80: 435-439

116. Johnston LE Jr. A few comments on an elegant answer in search of useful questions. Semin Orthod 2011; 17: 13-14

117. Mah J, Yi L, Huang RC, Choo HR. Advanced applications of cone beam computed tomography in orthodontics. Semin Orthod 2011; 17: 57-71

118. Lu B, Lu H, Palta J. A comprehensive study on decreasing the kilovoltage cone-beam CT dose by reducing the projection number. J Appl Clin Med Phys 2010; 11: 3274

119. Magni A. Cone beam computed tomography and the orthodontic office of the future. Semin Orthod 2009; 15: 29-34

120. Naisbitt, J. Megatrends: Ten new directions transforming our lives. New York: Warner, 1982

Chapter 6

Summaries

6.1 Summary

Chapter 1 Cone beam computed tomography (CBCT) imaging has had a tremendous impact on the practice of orthodontics and craniofacial surgery since its inception almost a decade ago. However, the limitations and pitfalls regarding this imaging method should be addressed in order to fully appreciate and correctly apply the possibilities that CBCT imaging offers. In all aspects of CBCT imaging, from utilization to application, inherent limitations and pitfalls exist. The general and specific research aims of this thesis were formulated to address the following issues regarding the limitations of CBCT as an imaging modality:

In order to make valid conclusions from cephalometric measurements, the measurement error should be determined at a level that can detect significant differences (α = 0.05). Therefore, the smallest detectable difference or SDD (95% confidence interval of the measurement error) should be determined. The clinical relevance of the SDD in cephalometry is that the measured difference between two observations must be at least equal or larger than the SDD in order to be regarded as real change. This importance of the SDD in cephalometry is seldom realized.

CBCT imaging still exposes the patient to more radiation than conventional cephalograms. Therefore, current guidelines do not support CBCT imaging as routine modality for orthodontic practice. However, some differences regarding interpretation of current utilization guidelines of CBCT imaging in orthodontics exist. This is especially true for the new applications of 3D images which are not possible with traditional radiography. Developing clear, yet evidence-based selection criteria for CBCT imaging in orthodontics is therefore needed, not only to guarantee safe use of the technology but to ultimately improve patient management.

Technical difficulties of CBCT start with the positioning of the patient prior to the scanning procedure. To avoid distortion and movement artifacts due to the long scanning times of CBCT, the head of the patient is often fixed which makes capturing the head in the natural head position (NHP) difficult. Because the NHP has become an indispensible method to appraise the head due to its stability, methods and techniques to achieve a NHP of the head for CBCT imaging should be investigated.

To overcome problems associated with 2D methods, 3D planning of craniofacial surgery by means of computer-aided surgery simulation of CBCT-derived surface models has been proposed. However, accurate planning of craniofacial surgery by means of computer-aided surgery simulation can only be achieved if accurate 3D models are

made available first. The differences in voxel size, scanning position, beam inhomogeneity and threshold based segmentation methods are all possible factors which could influence the accuracy CBCT-derived surface models. In particular, the influence of different voxel sizes is clinically very relevant since a smaller voxel scan exposes the patient to higher radiation dose.

The limitations of 2D cephalometry, which relies on one single captured image of the face, have been thoroughly documented in the literature. In contrast, a CBCT scan permits evaluation on derived cephalograms, volume renderings, surface models and slices in all three planes in space of the imaged structures. These new images, not always possible with traditional radiographs, bring about new challenges in the interpretation of data. In addition, they allow for new assessment methodologies and applications which may improve patient management.

In **Chapter 2** the reliability and size of the measurement error (by means of the SDD) of commonly used 2D and 3D variables were determined.

In *Chapter 2.1* the reliability and SDD of 2D cephalometric measurements were investigated. *Chapter 2.2* assessed the reliability and SDD of 3D cephalometric measurements. In both *Chapter 2.1 and 2.2,* the reliability of the measurements was good, but the measuring error was clinically significant (more than one measuring unit) for most of the variables tested. The results question the ability of these variables to detect true treatment effect, especially when a high level of accuracy required. In both studies, the resulting 2D or 3D measurement errors are cumulative due to the variability of the landmark identification. Moreover, certain geometric principles (e.g. envelope of error and distances between the landmarks) have an additional influence on the magnitude of the resulting measurement error which makes the measurement error of each 2D and 3D variable unique.

In **Chapter 3**, aspects regarding acquisition, visualization and interpretation of CBCT images were investigated.

In *Chapter 3.1,* a modified laser level technique was described to record the natural head position (NHP) in all three planes of space. This is a simple method to achieve NHP of 3D images and may be of value for routine craniofacial assessment. Possible advantages of the technique are the simplicity of the method and set-up, it does not require additional expensive equipment, and it is not labour intensive.

In *Chapter 3.2*, the influence of voxel size on surface models derived from CBCT images is investigated. The measurements on 3D surface models were very accurate

when compared to the direct calliper measurements. There was no difference between the accuracy of the measurements between the 0.40 and 0.25 voxel size groups. The results suggest that a 0.40 mm voxel resolution provides adequate information for maxillofacial surgery planning. This is clinically relevant as a larger voxel scan exposes the patient to a lesser radiation dose.

Chapter 3.3 compared 2D and 3D cephalometric values by using a 3D analysis based on the midsagittal plane. The results confirmed that values from the 3D analysis in the midsagittal plane are reliable and comparable with the values from 2D cephalometry. This eliminates the need to derive an additional lateral cephalogram for analysis. Another clinical advantage the described 3D analysis is that the presentation of the 3D measurements is very similar to conventional 2D measurements routinely used by orthodontists and maxillofacial surgeons. This might possibly enable a smoother transition from 2D to 3D cephalometry.

In **Chapter 4** the application of CBCT imaging for the diagnosis and treatment planning of craniofacial asymmetry was investigated.

The aim of *Chapter 4.1* was to evaluate and compare postero-anterior (PA) cephalograms to CBCT images for the detection of mandibular asymmetry. PA cephalograms were not accurate in detection of the characteristics of the mandibular asymmetry. CBCT images are very reliable and accurate for the detection of mandibular asymmetry and should be considered when a visible chin deviation is present which requires surgical correction.

Chapter 4.2 describes a 3D method of a mirror-image analysis technique to visualize the asymmetry in order to assist in diagnosis and treatment planning. Visualizing deformities enables a unique appreciation of the underlying deformity which may not be possible by looking at quantitive numbers alone. Perhaps the most valuable advantage of the mirror-analysis is that it is an excellent visual tool to explain the extent of the underlying abnormality to the patient. Other possible advantages of performing a mirror-image analysis are also discussed.

Morphometric methods are used in biology to study object symmetry in living organisms and to determine the true plane of symmetry. The aim of *Chapter 4.3* was to determine if there are clinical differences between 3D cephalometric midsagittal planes used to describe craniofacial asymmetry and a true symmetry plane derived from a morphometric method based on visible facial features. The results indicate that the differences were clinically relevant. As a result of the human skull being inherently asymmetric, determining the midsagittal plane based on midline cephalometric points

will vary and remains questionable. Therefore, care has to be taken when using cephalometric midsagittal planes for diagnosis and treatment planning of craniofacial asymmetry as they might differ from the true plane of symmetry as determined by morphometrics methods.

In **Chapter 5** the general aim, which was to explore and to investigate some of the potential limitations and pitfalls of CBCT in the field of cephalometry was addressed. In addition, the specific research questions in *Chapter 1.3* were answered and the clinical relevance of the findings and the future perspectives was explored and discussed.
The results from this thesis confirmed that:

1. The SDD of almost all commonly used 2D and 3D cephalometric measurements can be considered clinically significant (more than 1 measuring unit).
2. The accuracy of CBCT-derived surface models was sufficient for orthodontic and craniofacial treatment planning.
3. Increasing the voxel resolution from 0.40 mm to 0.25 mm to construct a 3D surface model did not result in an increased accuracy of the linear measurements.
4. Conventional 2D measurements are comparable to 3D measurements of a modified 3D analysis based on the midsagittal plane.
5. CBCT imaging is more accurate in determining the difference of the mandibular dimensions (ramus length, body length and total length) and therefore provides more reliable information regarding the characteristics of mandibular asymmetry than PA cephalometry.
6. There are clinically relevant differences between 3D cephalometric midsagittal planes used to describe craniofacial asymmetry and a symmetry plane derived from a morphometric method based on visible facial features.

The technical advances regarding further radiation reduction and improved image quality of CBCT imaging is rapidly evolving. Therefore, CBCT imaging will play an even more important role in orthodontics and maxillofacial surgery in the near future. It is expected that future application of CBCT images will take full advantage of the potential of the 3D images, especially in cephalometry and planning of maxillofacial surgery. In addition, future clinical studies will use 3D superimposition which might cast a brighter light on the prediction of treatment outcomes. New applications, not possible with traditional radiography e.g., the use of mirror imaging, will be continually developed and

evaluated to determine if the benefits of the CBCT images outweigh the risks. Finally, it must be kept in mind that the use of CBCT imaging brings added ethical and legal responsibilities for the clinician which should not be taken lightly.

6.2. Samenvatting

Hoofdstuk 1 Beeldvorming d.m.v "cone beam computed tomography" (CBCT) heeft sinds de invoering, ongeveer 10 jaar geleden, een grote invloed gehad op de orthodontie en kaakchirurgie. Het is echter belangrijk om de beperkingen en valkuilen van de CBCT te kennen voordat de mogelijkheden van deze techniek juist en daarmee ten volle benut kunnen worden. In alle aspecten van beeldvorming d.m.v. CBCT zitten namelijk inherente beperkingen en valkuilen. De algemene en specifieke doelstellingen van dit proefschrift zijn om de beperkingen en valkuilen van de CBCT als diagnostisch hulpmiddel in kaart te brengen.

Om valide conclusies uit cephalometrische metingen te kunnen trekken, moet de meetfout worden vastgesteld op een niveau waarop significante verschillen (α = 0.05) kunnen worden gemeten. Daarom moet "the smallest detectable difference" of de SDD (het 95% betrouwbaarheidsinterval van de meetfout) worden vastgesteld. De SDD is in de cephalometrie klinisch relevant. Om namelijk van een echte verandering te kunnen spreken, moet het meetverschil tussen twee metingen op zijn minst gelijk of groter dan de SDD zijn. Dit niveau van de SDD wordt in de uitkomsten van diverse cephalometrische studies zelden bereikt.

De patiënt wordt bij beeldvorming d.m.v. CBCT nog steeds blootgesteld aan een hogere stralingsdosis dan bijvoorbeeld bij een conventionele laterale cephalogram het geval is. Om die reden wordt het gebruik van beeldvorming d.m.v. CBCT als routine onderzoek in de orthodontie niet ondersteund door de huidige richtlijnen. Er zijn echter verschillen van inzicht bij de interpretatie van de huidige richtlijnen in de orthodontie. Dit geldt met name voor de toepassing van driedimensionale beeldvorming, hetgeen niet mogelijk is met de traditionele radiografische technieken. Duidelijke en "evidence-based" criteria voor de toepassing van beeldvorming d.m.v. CBCT zijn nodig, niet alleen om veilig gebruik te garanderen, maar ook om de uiteindelijke behandeling te optimaliseren.

Technische problemen bij beeldvorming d.m.v. CBCT beginnen met de juiste positionering van de patiënt in het apparaat. Het hoofd van de patiënt wordt vaak gefixeerd om vervormings- en bewegingsartefacten ten gevolge van de lange scantijd te beperken. Dit beperkt de mogelijkheden om de patiënt in "natural head position" (NHP) in het CBCT apparaat te plaatsen. Omdat de NHP een onontbeerlijke methode is om metingen aan het craniofaciale complex te verrichten, dienen methoden en technieken te worden ontwikkeld om de NHP bij beeldvorming d.m.v. CBCT mogelijk te maken.

Craniofaciale chirurgie met behulp van gipsmodellen en 2-dimensionale methoden kent beperkingen. Om deze reden wordt chirurgische planning door middel van computer gesimuleerde chirurgie op "CBCT-derived surface model" als alternatief onderzocht. Echter voor een accurate driedimensionale planning van craniofaciale chirurgie met behulp van computer simulaties zijn nauwkeurige driedimensionale modellen noodzakelijk. De verschillen in voxel grootte, scanpositie, bundel heterogeniteit en segmentatietechnieken zijn echter allemaal factoren die van invloed zijn op de nauwkeurigheid van met CBCT beeldvorming verkregen driedimensionale modellen. De voxel grootte is met name een klinisch relevant parameter, aangezien een kleinere voxel grootte de patiënt blootstelt aan een hogere stralingsdosis.

De beperkingen van tweedimensionale cephalometrie, welke gebruik maakt van een opname van het hoofd in het sagittale vlak, zijn uitvoerig beschreven in de literatuur. CBCT beeldvorming biedt daarentegen de mogelijkheid om naast een verkregen cephalogram, volumetrische parameters, oppervlakte modellen en coupes in drie dimensies te beoordelen. Deze nieuwe mogelijkheden brengen nieuwe uitdagingen in de interpretatie van data met zich mee. Uiteindelijk kunnen de nieuwe beoordelingsmethoden en toepassingen resulteren in een verbetering van de patiëntenzorg.

In **Hoofdstuk 2** wordt de betrouwbaarheid en grootte van de meetfout (met behulp van de SDD) van veel gebruikte tweedimensionale en driedimensionale beeldvormende technieken onderzocht.

In *hoofdstuk 2.1* wordt de betrouwbaarheid en SDD van tweedimensionale metingen in de cephalometrie onderzocht. In *hoofdstuk 2.2* wordt dit gedaan voor driedimensionale metingen. Zowel bij tweedimensionale als driedimensionale beeldvormende technieken is de betrouwbaarheid van de metingen goed. De meetfout is echter klinisch significant voor veel van de gemeten variabelen (d.w.z. meer dan een meeteenheid). Dit geeft aan dat met behulp van de in *hoofdstuk 2.1 en 2.2* bestudeerde variabelen een daadwerkelijk behandeleffect niet betrouwbaar kan worden aangetoond. Vooral indien er een hoog niveau van nauwkeurigheid vereist is. In beide studies zijn de tweedimensionale of driedimensionale meetfouten cumulatief als gevolg van de variaties bij het bepalen van de cephalometrische punten. Daarbij hebben bepaalde meetkundige beginsels (b.v. marge van de meetfout en de afstand tussen de meetpunten) een belangrijke bijkomende invloed op de grootte van de meetfout. Dit maakt elke tweedimensionale en driedimensionale variabele uniek.

In **Hoofdstuk 3** worden de vervaardiging, de beeldkwaliteit en de interpretatie van CBCT beeldvorming onderzocht.

In *hoofdstuk 3.1* wordt een gemodificeerde lasertechniek beschreven om de "natural head position" in alle drie dimensies te bereiken. Deze eenvoudige methode om de NHP bij driedimensionale beeldvorming te bereiken is van meerwaarde voor de klinische praktijk. De techniek is eenvoudig, weinig arbeidsintensief en vraagt geen hoge investeringskosten.

In *hoofdstuk 3.2* wordt de invloed van verschillende voxelgroottes op de nauwkeurigheid van driedimensionale oppervlaktemodellen, verkregen uit CBCT beeldvorming, bestudeerd. De metingen gedaan op de driedimensionale oppervlakte modellen blijken zeer nauwkeurig te zijn ten opzichte van directe metingen met een schuifmaat. Er is geen verschil in nauwkeurigheid tussen de 0.40 mm en 0.25 mm voxelgrootte. De resultaten geven aan dat een 0.40 mm voxelgrootte voldoende informatie geeft voor een goede driedimensionale chirurgische planning. Dit is van klinisch belang aangezien CBCT beeldvorming met een grotere voxelgrootte de patiënt aan minder straling blootstelt.

Hoofdstuk 3.3 vergelijkt tweedimensionale en driedimensionale chephalometrische waarden met elkaar door gebruik te maken van een driedimensionale analyse gebaseerd op het midsaggitale vlak. De resultaten bevestigen dat de waarden van deze driedimensionale analyse betrouwbaar en vergelijkbaar zijn met de tweedimensionale analyse. Op deze manier is er naast de CBCT beeldvorming geen aanvullende laterale schedelfoto nodig. Een bijkomend voordeel is dat de in deze studie toegepaste driedimensionale analyse veel overeenkomsten kent met de conventionele tweedimensionale analyse die meestal door orthodontisten en kaakchirurgen wordt toegepast. Dit zou kunnen bijdragen aan een soepele overstap van de tweedimensionale naar een driedimensionale cephalometrische analyse.

In **Hoofdstuk 4** wordt het gebruik van CBCT beelden voor de diagnose en behandelplanning van craniofaciale asymmetrieën onderzocht.

In *hoofdstuk 4.1* worden voor-achterwaardse (PA) cephalogrammen en beeldvorming d.m.v. CBCT met elkaar vergeleken voor de diagnose van mandibulaire asymmetrieën. PA cephalogrammen bleken niet accuraat in de vaststelling van een mandibulaire asymmetrie. Beeldvorming d.m.v. CBCT was daarentegen zeer betrouwbaar en accuraat in het opsporen van mandibulaire asymmetrieën. Op basis van de bevindingen in deze studie kan worden gesteld dat beeldvorming d.m.v. CBCT moet

worden overwogen wanneer er een zichtbare kindeviatie is die een chirurgische correctie gewenst.

Hoofdstuk 4.2 beschrijft een driedimensionale analyse waarbij gebruik wordt gemaakt van een spiegelbeeld om de asymmetrie te diagnosticeren en bij de behandelplanning te ondersteunen. Het visualiseren van een asymmetrie maakt de afwijking vaak veel duidelijker dan het vaststellen een afwijking alleen op basis van getallen. De meeste toegevoegde waarde van de spiegelbeeld-analyse is waarschijnlijk het feit dat het een uitstekende manier is om de afwijking aan de patiënt te laten zien en uit te leggen. Andere mogelijke voordelen van de spiegelbeeld-analyse worden eveneens besproken in dit hoofdstuk.

In de biologie worden morphometrische methoden toegepast om symmetrie van levende organismen te bestuderen en het ware vlak van symmetrie te bepalen. In *Hoofdstuk 4.3* wordt gekeken of er klinische verschillen zijn tussen het driedimensionale cephalometrische midsagittale vlak en het daadwerkelijke symmetrie vlak verkregen met behulp van de morphometrische methode. De resultaten geven aan dat de verschillen klinisch relevant zijn. Omdat de menselijke schedel asymmetrisch is, zal de vaststelling van het midsagittale vlak op basis van cephalometrische punten in het midden verschillen en is om die reden niet zeker. Achtzaamheid is daarom nodig als er gebruik wordt gemaakt van het cephalometrische midsagittale vlak bij de diagnose en behandelplanning van craniofaciale asymmetrieën. Dit vlak kan verschillen van het echte vlak van symmetrie volgens de morphometrische methode.

In **Hoofdstuk 5** wordt het algemene doel van dit proefschrift, namelijk de potentiële beperkingen en valkuilen van beeldvorming d.m.v. CBCT ten aanzien van de cephalometrie, besproken. Verder worden de specifieke vraagstellingen uit hoofdstuk 1.3 beantwoord. Daarbij wordt de klinische waarde van de bevindingen en het toekomstperspectief onderzocht en beschreven.

Uit de resultaten van dit proefschrift kan worden afgeleid dat:

1. De SDD kan, van bijna alle veel gebruikte metingen in de tweedimensionale en driedimensionale cephalometrie, als klinisch significant worden beschouwd (d.w.z. meer dan een meeteenheid).
2. De nauwkeurigheid van de met behulp van de CBCT verkregen oppervlakte modellen is toereikend voor orthodontische en orthognatische behandelplanning.

3. Het vergroten van de voxel resolutie van 0.40 mm naar 0.25 mm om een 3-dimensionaal oppervlakte model te construeren heeft niet een grotere nauwkeurigheid van de lineaire metingen tot gevolg.

4. Conventionele tweedimensionale metingen zijn vergelijkbaar met driedimensionale metingen volgens een gemodificeerde driedimensionale analyse in het midsagittale vlak.

5. Beeldvorming d.m.v. CBCT is meer nauwkeurig in het vaststellen van verschillen in mandibulaire dimensies (ramus lengte, corpus lengte en totale lengte) en geeft daarom meer betrouwbare informatie in het geval van een mandibulaire asymmetrie dan een PA cephalogram.

6. Er zijn klinisch relevante verschillen tussen driedimensionale cephalometrische midsagittale vlakken en het vlak van symmetrie verkregen met de morphometrische methode om craniofaciale asymmetrieën vast te stellen.

Bij beeldvorming d.m.v. CBCT gaan de technische ontwikkelingen op het gebied van stralingsreductie en de verbetering van beeldkwaliteit snel. Om die reden zal beeldvorming d.m.v. CBCT in de nabije toekomst een steeds belangrijkere rol gaan spelen in de orthodontie en kaakchirurgie. Het is te verwachten dat het gebruik van beeldvorming d.m.v. CBCT in de toekomst het volle potentieel van driedimensionale mogelijkheden zal benutten, vooral in relatie tot de cephalometie en chirurgische planningen. Omdat toekomstige studies vermoedelijk driedimensionale superimpositie zullen gaan toepassen, zal er mogelijk een betere voorspelling gedaan kunnen worden van het behandelresultaat. De nieuwe mogelijkheden die beeldvorming d.m.v. CBCT biedt, waaronder spiegelbeeldanalyse, zullen steeds verder worden ontwikkeld en geëvalueerd om te bepalen of de voordelen ervan opwegen tegen de risico's. Ten slotte moet goed in gedachten worden gehouden dat het gebruik van beeldvorming d.m.v. CBCT grote ethische en juridische verantwoordelijkheden voor de clinicus met zich meebrengt. Dit moet vooral niet lichtvaardig worden genomen.

6.3. Opsomming

Hoofstuk 1 Konusbundel rekenaar tomografie (KBRT) het 'n geweldig impak op die gebied van Ortodonsie sowel as Kaak-Gesig en Mondchirurgie sedert sy onstaan 'n dekade gelede gemaak. Dit is egter belangrik om eers die beperkinge en struikelblokke van die radiologiese tegniek te begryp en aan te spreek voordat die moontlikhede van KBRT ten volle gerealiseer kan word. Inherente beperkinge and struikelblokke bestaan in alle aspekte van die beeldvorming tegniek – ook t.o.v. die gebruike en toepassing van die beelde. Die algemene en spesifieke navorsingsdoelwitte van die proefskrif is geformuleer ten einde die beperkinge en struikelblokke van KBRT as radiologiese beelvorming modaliteit aan te spreek.

Om geldige gevolgtrekkings moontlik te maak uit Kefalometriese metings, moet die metingsfoute eers bepaal word op 'n vlak wat betekenisvolle verskille (α = 0.05) kan opspoor. Die kleinste waarneembare verskil (KWV) bepaal die 95% vertrouensinterval van die metingsfout en kan dus gebruik word. Die KWV het 'n belangrike kliniese rol in Kefalometrie. Die gemete verkil tussen twee Kefalometriese waarnemings moet ten minste gelyk, of groter as, die KWV wees ten einde as 'n ware of beduidende verandering beskou te kan word. Die belang van die KWV t.o.v. Kefalometriese metings word selde besef.

KBRT stel die pasiënt aan meer straling bloot as konvensionele laterale Kefalogramme. Dit is een van die hoofredes waarom huidige riglyne tans nie KBRT ondersteun as roetiene beeldvorming modaliteit vir die algemene Ortodontiese praktyk nie. Tog is daar 'n paar meningsverskille rakende die interpretasie van die huidige riglyne in Ortodonsie. Dit kom veral voor by nuwe toepassings van die 3-D beelde wat nie altyd moontlik is met tradisionle radiografie tegnieke nie. Die ontwikkeling van duidelike, maar ook wetenskaplik bewese, indikasies vir KBRT is dus nodig. Dit sal nie net veilige gebruik van die tegnologie veseker nie, maar ook verbeterde pasiënt behandeling waarborg.

Tegniese probleme van KBRT begin met die posisionering van die pasiënt vóór die skanderingsproses. Om distorsie en bewegingsartefakte as gevolg van die lang skanderingstye van KBRT te beperk, moet die kop van die pasiënt dikwels aan die apparaat vasgemaak word. Die gevolg daarvan is dat die kop nie altyd in die natuurlike hoof-posisie (NHP) geskandeer kan word nie. Omdat die NHP 'n onontbeerlike metode is om die pasiënt se kop in Ortodonsie te ondersoek, moet metodes en tegnieke ontwikkel word om stabilisering van die NHP vir KBRT beeldvorming moontlik te maak.

Om die probleme m.b.t. die beplanning van kaakchirurgie met 2-D metodes op te los, word beplanning deur middel van rekenaargesteunde chirurgiese simulasie van KBRT-afgeleide modelle as alternatief voorgestel. Akkurate beplanning van kaakchirurgie deur rekenaargesteunde simulasie kan slegs bereik word indien akkurate 3-D modelle beskikbaar gestel word. Verskille in Voxel grootte, skandering posisie, die straling homogeniteit of heterogeniteit, asook die segmenteringsmetodes word genoem as moontlike faktore wat 'n invloed op die akkuraatheid van KBRT-afgeleide modelle kan uitoefen. Veral die invloed van verskillende Voxel grootes is van kliniese belang aangesien 'n kleiner Voxel skandering die pasiënt aan 'n beduidende hoër stralingsdosis sal blootstel.

Die beperkinge van 2-D Kefalometrie wat staatmaak op een enkele beeld van die gesigsarea, is deeglik in die literatuur gedokumenteer. In teenstelling daarmee maak KBRT beelde evaluasies moontlik t.ov. volumetriese evaluasies, oppervlaksmodelle, afgeleide Kefalogramme asook die 3-D snyvlakke van die geskandeerde strukture. Hierdie nuwe beelde, wat nie altyd haalbaar is met tradisionele radiografie nie, sorg vir nuwe uitdagings t.ov. die interpretasie van hierdie data. Dit laat ook nuwe evalueringsmetodes en toepassings toe wat mootlik kan lei tot verbetering t.ov die pasiënt se behandeling.

In **Hoofstuk 2** word die betroubaarheid en metingsfout (KWV) van algemene 2-D en 3-D Kefalometriese metings ondersoek.

In *Hoofstuk 2.1* word die betroubaarheid en KWV van 2-D Kefalometriese metings en in *Hoofstuk 2.2* van 3-D Kefalometriese metings ondersoek. In beide *Hoofstuk 2.1 en 2.2* is gevind dat die betroubaarheid van die Kefalometriese metings goed was, maar die metingsfoute was klinies betekenisvol (meer as een metingseenheid) vir die meeste metings wat getoets is. Die resultate bevraagteken dus die vemoë van Kefalometriese metings om ware verskille te kan opspoor, veral wanneer 'n hoë vlak van akkuraatheid vereis word. In beide studies is die metingsfoute kumulatief as gevolg van variasies t.ov. die identifikasie van die landmerke. Sekere geometriese beginsels (bv. die omvang van die metingsfout sowel as die afstand tussen landmerke) het 'n belangrike bykomende invloed op die grootte van die metingsfout. Dit is aspekte wat die metingsfout van elke 2-D en 3-D meting uniek maak.

In **Hoofstuk 3** is aspekte rakende die verkryging, visualisering en interpretasie van KBRT beelde ondersoek.

In *Hoofstuk 3.1* word 'n gemodifiseerde laservlak-stabiliseringstegniek beskryf om die NHP in al drie ruimtelike vlakke te registreer. Dit is n redelike eenvoudige metode om die NHP van 3-D beelde te bepaal en mag van waarde wees om die gesig van die pasiënt in 3-D te beoordeel. Moontlike voordele van die tegniek is die eenvoud van die metode en die opstelling daarvan. Verder is ook geen duur bykomende apparatuur nodig nie en die tegniek is nie arbeidsintensief nie.

In *Hoofstuk 3.2* word die invloed van verskillende Voxel groottes op die akkuraatheid van 3-D KBRT-afgeleide oppervlaksmodelle ondersoek. Die metings van die 3-D modelle was baie akkuraat as dit vergelyk word met metings wat direk met 'n passer gedoen is. Daar was geen verskil tussen die akkuraatheid van die metings tussen die 0.40 mm en 0.25 mm Voxel grootte groepe nie. Die resultate dui daarop dat 'n 0.40 mm gootte voldoende inligting vir kaakchirurgie (beplanning deur middel van rekenaargesteunde simulasie) sal verskaf. Hierdie bevinding is klinies relevant omdat 'n groter Voxel grootte die pasiënt aan 'n beduidende kleiner stralingdosis sal blootstel.

Hoofstuk 3.3 vergelyk 2-D and 3-D Kefalometriese waardes deur gebruik te maak van 'n gemodifiseerde 3-D ontleding wat op die midsagittale vlak gebaseer is. Die resultate bevestig dat die gemodifiseerde 3-D ontleding betroubaar is en vergelykbaar is met die 2-D Kefalometriese waardes. Dit elimineer die noodsaaklikheid om 'n bykomende ontleding uit te voer op 'n ekstra 2-D Kefalogram, wat afgelei moet word uit die 3-D beelde. Nog 'n kliniese voordeel van die gemodifiseerde 3-D ontleding is dat die voorstelling van die 3-D metings soorgelyk is aan die 2-D metings waaraan Ortodontiste en Mondchirurge gewoond is. Dit kan moontlik help vir n gladde oorskakeling van 2-D na 3-D Kefalometrie.

In **Hoofstuk 4** word die toepassing van KBRT beelde vir die diagnose en behandelingsbeplanning van kraniofasiale asimmetrie ondersoek.

Die doel van die ondersoek in *Hoofstuk 4.1* was om postero-anterior (PA) Kefalogramme en KBRT beelde te evalueer en te vergelyk vir die opsporing van mandibulêre asimmetrie. PA Kefalogramme is bewys as onakkuraat t.o.v. die opsporing van die eienskappe van asimmetrie in die onderkaak. Die KBRT beelde, in teenstelling, was baie akkuraat en betroubaar vir die opsporing van asimmetrie van die onderkaak. Die resultate bevestig dat KBRT oorweeg moet word indien 'n chirurgiese ingreep nodig is om 'n sigbare afwyking van die ken te herstel.

Hoofstuk 4.2 beskryf n 3-D ontledingsmetode waar 'n spieël-beeld gebruik word om skeletale asimmetrie te diagnoseer en om te help met die beplanning van die behandeling. Visualisering met die spieël-beeld metode vergemaklik beter observasie

van die afwykings, iets wat nie moontlik is as daar slegs na die waardes van die Kefalometriese metings gekyk word nie. Hierdie spieël-beeld tipe ontleding is ook 'n uitstekende hulpmiddel om die omvang van die onderliggende afwyking aan die pasiënt te verduidelik. Ander voordele van die spieël-beeld ontleding word ook in hierdie hoofstuk bespreek.

Morfometriese metodes word in Biologie gebruik om simmetrie in lewende organismes te bestudeer en om die ware vlak van simmetrie te bepaal. Die doel van *Hoofstuk 4.3* was om te bepaal of daar kliniese verskille tussen 3-D Kefalometriese midsagittale vlakke en 'n morfometriese midsagittale vlak is. Die resultate dui daarop dat die verskille wel klinies relevant is. As gevolg van die inherente asimmetrie van die menslike skedel, sal midsagittale vlakke wat op Kefalometriese punte in die midlyn gebaseer is, mootlik onbetroubaar wees, wat die gebruik daarvan kan bevraagteken. Hierdie feit moet in gedagte gehou word want 'n Kefalometriese midsagittale vlak mag verskil van die ware midsagittale vlak. Dit kan diagnose en behandeling van pasiënte met kraniofasiale asimmetrie beinvloed..

Die algemene doel van hierdie proefskrif, naamlik om sommige van die potensiële beperkinge en struikelblokke van KBRT te ondersoek, word in **Hoofstuk 5** bepreek. Verder word die spesifieke navorsingsvrae wat in *Hoofstuk 1.3* genoem is, beantwoord en die kliniese belang van die bevindinge, asook toekomsperspektiewe, word verder ondersoek en bespreek.

Die bevindinge van die proefskroef het bevestig dat:
1. Die metingsfout (KWV) van byna alle algemene 2-D en 3-D Kefalometriese metings klinies betekenisvol is (meer as een metings eenheid).
2. Die akkuraatheid van KBRT-afgeleide oppervlaksmodelle voldoende was en gebruik kan word vir die beplanning van Ortodontiese en Kaakchirurgiese behandelings.
3. Die verhoging van die Voxel resolusie van 0.40 mm na 0.25 mm nie tot n verbeterde akkuraatheid van die afgeleide oppervlaksmodelle lei nie.
4. Konvensionele 2-D evaluasie en metings van die gemodifiseerde midsagittale 3-D ontleding vergelykbaar is .
5. KBRT beelde meer akkuraat as PA Kefalometrie is t.o.v. bepaling van die verskille van die onderkaak dimensies. Dit verskaf dus meer betroubare inligting oor die eienskappe van die onderliggende asimmetrie.

6. Daar kliniese verskille tussen 3-D Kefalometriese midsagittale vlakke en morfometriese midsagittale vlakke is.

Die tegniese vooruitgang met betrekking tot verdere vermindering van straling en die verbetering van beeldkwaliteit van KBRT is bemoedigend. Daarom sal KBRT in die nabye toekoms 'n belangriker rol in Ortodonsie en Kaakchirurgie speel. Daar word verwag dat die toekomstige toepassinge van die beeldingstegniek die volle potensiaal van die 3-D beelde sal ontgin, veral in Ortodonsie en Kaakchirurgie. Daarbenewens sal toekomstige kliniese studies van 3-D superponering gebruik maak, wat moontlik 'n nuwe lig op die voorspelling van behandelingsuitkomste sal werp. Nuwe toepassings, veral dié wat nie moontlik is nie met tradisionele radiografie nie bv. die gebruik van spieël-beeld tegnieke, sal voordurend ontwikkel en geëvalueer word om te bepaal of die voordele van hiedie tegnieke swaarder weeg as die risiko's. Ten slotte moet in gedagte gehou word dat die gebruik van KBRT beelde baie etiese en wetlike verantwoordelikhede vir die klinikus byvoeg, iets wat beslis nie ligtelik opgeneem moet word nie.

Appendices

I. List of publications

1. **Damstra J**, Mistry D, Cruz C, Ren Y. Anteroposterior and transverse changes in the positions of palatal rugae after rapid maxillary expansion. Eur J Orthod 2009; 31: 327-332

2. **Damstra J**, Huddleston Slater JJR, Fourie Z, Ren Y. Reliability and the smallest detectable difference of lateral cephalometric measurements. Am J Orthod Dentofacial Orthop 2010; 138: 546.e1-e8

3. **Damstra J**, Fourie Z, Huddleston Slater JJR, Ren Y. Reliability and the smallest detectable difference of three-dimensional cephalometric measurements. Am J Orthod Dentofacial Orthop 2011, Accepted

4. **Damstra J**, Fourie Z, Ren Y. Simple technique to achieve natural head position for cone beam CT scans. Br J Oral Maxillofac Surg 2010; 48: 236-238

5. **Damstra J**, Fourie Z, Huddleston-Slater JJR, Ren Y. Accuracy of linear measurements of cone beam CT derived surface models of different voxel sizes. Am J Orthod Dentofacial Orthop 2010; 137: 16.w1-16.e6

6. Fourie Z, **Damstra J**, Gerrits PO, Ren Y. Accuracy and reliability of facial soft tissue thickness measurements of cone beam CT scans. Forensic Sci Int 2010; 199: 9-14.

7. Oosterkamp BCM, **Damstra J**, Jansma J. Facial asymmetry: the benefits of cone beam computerized tomography. Ned Tijdschr Tandheelk 2010; 117: 269-273

8. **Damstra J**, Fourie Z, Ren Y. A comparison between two-dimensional and midsagittal three-dimensional cephalometric measurements of dry human skulls. Br J Oral Maxillofacial Surg 2010, doi: 10.1016/j.boms.2010.06.006

9. Fourie Z, **Damstra J**, Gerrits PO, Ren Y. Linear accuracy and repeatability of anthropometric facial measurements using cone-beam computed tomography. Cleft-Palate Craniofac J 2010; doi: 10.1597/10-076

10. Fourie Z, **Damstra J**, Gerrits PO, Ren Y. Evaluation of anthropometric accuracy and reliability using different three-dimensional scanning systems. Forensic Sci Int 2011; 207: 127-134.

11. **Damstra J**, Fourie Z, Ren Y. Evaluation and comparison of postero-anterior cephalograms and cone-beam computed tomography images for the detection of mandibular asymmetry. Eur J Orthod 2011; doi: 10.1093/ejo/cjr045

12. **Damstra J**, Oosterkamp BCM , Jansma J, Ren Y. Combined 3-dimensional and mirror-image analysis for the diagnosis of asymmetry. Am J Orthod Dentofacial Orthop 2010; Accepted

13. **Damstra J**, Fourie Z, De Wit MF, Ren Y. A three-dimensional comparison of a morphometric midsagittal plane to cephalometric midsagittal planes for craniofacial asymmetry. Clin Oral Investig 2011; doi:10.1007/s00784-011-0512-4

14. Fourie Z, **Damstra J**, Ren Y. Application of cone beam computed tomography in facial imaging science. Shanghai J Stomatol 2011; Accepted

15. **Damstra J**, Fourie Z, Ren Y. Practical limitations of cone-beam computed tomography in 3D cephalometry. Shanghai J Stomatol 2011; Accepted

16. Fourie Z, **Damstra J**, Schepers R, Gerrits PO, Ren Y. Segmentation process significantly influences the accuracy of 3D surface models derived from cone beam computed tomography. Eur J Radiol 2011, Accepted

17. Fourie Z, Engelbrecht WP, **Damstra J**, Gerrits PO, Ren Y. The influence of the segmentation process on 3D measurement from cone beam computer tomography-derived models Clin Oral Investig 2011; Submitted

II. Acknowledgements

My sincerest thanks to the following people who directly or indirectly contributed to this manuscript:

Prof. Dr. Yijin Ren, my promoter - for your time, support, wisdom, patience and expert mentorship of my research projects and preparation of this thesis.

Drs. Zachie Fourie, research comrade and true friend - it was truly a joy and privilege to work with you. May your future be worthy of your dreams.

The members of the beoordelingscommissie: **Prof. dr. R.R.M. Bos, Prof. dr. A.M. Kuijpers-Jagtman** and **Prof. dr. P.E. Rossouw** - for their time and effort in judging and reviewing this thesis.

Special thanks to **Prof. dr. Andrew Sandham** for giving me a postgraduate position in 2007.

Special thanks to the **contributors** - without their generous sponsorship this thesis would not have been possible.

The **Prof. K.G. Bijlstra Stichting** - for acquisition of the skulls used in this thesis.

My fellow post-graduates and good friends, **Katrina Finnema, Zachie Fourie, Floris Pelser and Alianne Renkema** - for being such an excellent and special group. I will look back at the past 4 years with such fond memories. Special thanks to **Katrina and Floris,** for being the paranymfs and for your extra effort and help.

Mrs. Gea van der Bijl - for all your work regarding the arrangements for the promotion. Please take note that all your effort did not go unnoticed. All your input was much appreciated.

Dr. James Huddleston Slater - for your excellent thoughts and advice regarding statistics.

Prof. dr. Peter Gerrits and the **Department of Anatomy at the UMCG** - for your excellent help and enthusiasm with the research projects.

Prof. dr. FA de Wet - for your excellent help with the translation of the summary into Afrikaans.

Drs. Katrina Finnema and **Drs. Henk Rouwé** - for your perfect translation of the summary into Dutch.

Drs. Henk Rouwé - for your excellent clinical teaching, insights and guidance during my study in Groningen. You proved that it is possible to teach an old dog some new tricks. It has been such a pleasure to learn from you.

III. Curriculum Vitae

Janalt Damstra was born on the 22nd of September, 1973 in Pretoria, South Africa. He matriculated from the Afrikaans High school for Boys (AHS/Affies), Pretoria, in 1991. The following year he started his dental education at the University of Pretoria. After graduating as a dentist in July 1998, he entered private practice, initially in the UK and later in the Netherlands. Whilst in private practice, the author completed a Postgraduate Diploma in Dentistry *(Cum laude)* in 2002 and an Honours Degree in Dental Science *(Cum laude)* in 2003 at the Dental School of Stellenbosch University. Between July 2004 and July 2005, the author spent one year at the College of Dentistry of New York University (NYU), completing the full-time Advance Study Program in Orthodontics for international dentists. After three years of part-time study, the author completed the degree of Master of Science in Odontology at the Department of Orthodontics, University of Pretoria, in December 2006. The author entered the four year full-time orthodontic specialty training program at the Department of Orthodontics, University Medical Center Groningen (UMCG) in September 2007. The years of his residency were spent combining his specialty training and completing the research in this thesis. The author qualified as an orthodontist on the 21st of July, 2011. Janalt is married to Liesl Damstra (Brierley). They have 3 children: Lauren (2002), Megan (2007) and Joshua (2010).